REPUBLIQUE ALGERIENNE DEMOCRATIQUE ET POPULAIRE

MINISTERE DE L'ENSEIGNEMENT SUPERIEUR ET DE LA RECHERCHE SCIENTIFIQUE

UNIVERSITE DR. YAHIA FARES DE MEDEA

FACULTE DE TECHNOLOGIE

Département du Génie Électrique

THÈSE

EN VUE DE L'OBTENTION DU DIPLOME DE DOCTOREUR EN SCIENCES

UNIVERSITE DR. YAHIA FARES DE MEDEA (ALGERIE)

Laboratoire de recherche sur les systèmes électroniques avancés (LSEA), Université de Médéa, Médéa, Algérie

Filière : Électrotechnique **Option : Électrotechnique**

Présentée par Sahnoune Chaouche Rachid

Thème

Elaboration d'une plateforme d'essai dédiée au diagnostic des défaillances dans les enroulements des transformateurs de puissance.

Soutenue le : 25-09-2024 **Devant le Jury composé de :**

Nom et Prénom	Grade		
1. M. SEBAA Karim	Prof	Univ. De Médéa	Président
2. M. MOUALDIA Abelhafid	Prof	Univ. De Médéa	Examinateur
3. Mr. ZAOUI Abdelhalim	Prof	ENSTA DE Algerie	Examinateur
4. M. GRICHE Issam	MCA	Univ. De Bouira	Examinateur
5. Mr. HOUASSINE Hamza	Prof	Univ. De Bouira	Rapporteur
6. Mr. MOULAHOUM Samir	Prof	Univ. De Médéa	Co- Rapporteur
7. Mr. BENSAID Samir	Prof	Univ. De Bouira	Inviter

Année univsitaire: 2023/2024

PEOPLE'S DEMOCRATIC REPUBLIC OF ALGERIA

MINISTRY OF HIGHER EDUCATION AND SCIENTIFIC RESEARCH

UNIVERSITY DR. YAHIA FARES OF MEDEA

FACULTY OF TECHNOLOGY

Department of Electrical Engineering

THESIS

TO OBTAIN THE DOCTOR IN SCIENCE DIPLOMA

UNIVERSITY DR. YAHIA FARES FROM MEDEA (ALGERIA)

Advanced Electronic Systems Research Laboratory

(LSEA), University of Medea, Medea, Algeria

Sector: electrical engineering

Option: electrical engineering

Theme

Development of a Test Platform Dedicated to Diagnosing Faults in Power Transformer Windings

Presented by **Rachid Sahnoune Chaouche**

Supported on: 26-09-2024 **In front of the following jury:**

Name and First name	Grade		
1. M. SEBAA Karim	Prof	University of Medea	President
2. M. MOUALDIA Abelhafid	Prof	University of Medea	Examinator
3. Mr. ZAOUI Abdelhalim	Prof	ENSTA of Algeria	Examinator
4. M. GRICHE Issam	MCA	University of Bouira	Examinator
5. Mr. HOUASSINE Hamza	Prof	University of Bouira	Thesis director
6. Mr. MOULAHOUM Samir	Prof	University of Medea	Co- Director
7. Mr. BENSAID Samir	Prof	University of Bouira	Invited

University year: 2023/2024

Abstract

Based on the fact that the electrical power transformer is one of the most important elements of the electrical network. Truly is a critical equipment that ensures the transmission of electrical energy with minimal losses in energy. Faults in the electrical power transformer system are anything that causes an abnormal change in current or voltage values. The most common cause of this is a breakdown in the insulation on the conductors due to electrical or mechanical pressures, due to the aging of the transformer, or due to external factors such as electromagnetic forces. Among the most critical aspects of a transformer that need to be monitored is the mechanical condition of the windings. The frequency response analysis (FRA) test is a reliable test to evaluate the mechanical integrity of the power transformer winding, and to detect other types failures that infect the core. Frequency Response Analysis (FRA) is a non-invasive, non-destructive and crucial diagnostic tool for assessing mechanical and electrical issues, allowing for proactive maintenance and preventing unexpected failures. A sinusoidal signal is injected into the winding input, so that the same signal is measured at the same time at the winding output, or in other words, the transfer function response is measured. In the healthy condition of the power transformer winding, it maintains the same signal. However, in the event of losses in the winding as a result of aging or electromagnetic forces, the exit signal is different from the reference signal. Electrical and mechanical faults in the winding of an electrical transformer are treated separately, and on the other hand, by considering that they occur together at the same time. Initially, a state-space model is developed with dedicated consideration a turn short-circuits faults in disks. The first step concerns the redefinition of the resistance, inductance and capacitance matrices to introduce the coefficients relating to defects. Simulating the frequency response by considering a short circuit fault at different rates and in different disks, to determine the extent of the effect of the short circuit on the behavior of the power transformer. This modeling makes it possible to propose new models adapted to the needs of power transformer diagnosis. Then, this thesis studies several winding deformations, which include axial displacement, radial displacement, and axial displacement with SC consideration. Conducting an investigation into frequency response analysis can be a powerful tool to study the impact of such faults on the behavior of a power transformer.

Finally, In the final chapter of this thesis, a test platform was presented that provides the service of building an equivalent model of a power transformer. Also, one of the features of this platform is that it is a powerful tool that helps in conducting routine tests and safety tests to

detect mechanical faults of the power transformer windings. In addition, a program was presented that automatically connects the LCR meter to the computer for the purpose of providing the necessary data obtained through tests, whether in design tests or startup tests.

Keywords: Power transformer, state space model, Winding, a test platform, axial displacement, radial displacement, short-circuit, FRA.

خلاصة

انطلاقاً من أن محول الطاقة الكهربائية يعد من أهم عناصر الشبكة الكهربائية. إنها حقًا معدات مهمة تضمن نقل الطاقة الكهربائية بأقل قدر من الخسائر في الطاقة. الأعطال في نظام محولات الطاقة الكهربائية هي كل ما يؤدي إلى تغير غير طبيعي في قيم التيار أو الجهد. السبب الأكثر شيوعًا لذلك هو انهيار العزل على الموصلات بسبب الضغوط الكهربائية أو الميكانيكية، بسبب تقادم المحول، أو بسبب عوامل خارجية مثل القوى الكهرومغناطيسية. من بين الجوانب الأكثر أهمية اختبارًا موثوقًا لتقييم (FRA) للمحول التي تحتاج إلى مراقبة هي الحالة الميكانيكية للفات. يعد اختبار تحليل استجابة التردد السلامة الميكانيكية لملف محول الطاقة واكتشاف أنواع أخرى من الأعطال التي تصيب القلب. يعد تحليل استجابة التردد أداة تشخيصية غير جراحية وغير مدمرة وحاسمة لتقييم المشكلات الميكانيكية والكهربائية، مما يسمح بالصيانة (FRA) الاستباقية ومنع الأعطال غير المتوقعة. يتم حقن إشارة جيبية في دخل الملف، بحيث يتم قياس نفس الإشارة في نفس الوقت عند خرج الملف، أو بمعنى آخر، يتم قياس استجابة وظيفة النقل. في الحالة الصحية لملف محول الطاقة، فإنه يحافظ على نفس الإشارة. ومع ذلك، في حالة حدوث خسائر في اللف نتيجة للتقادم أو القوى الكهرومغناطيسية، فإن إشارة الخروج تختلف عن الإشارة المرجعية. يتم التعامل مع الأعطال الكهربائية والميكانيكية في ملف المحول الكهربائي بشكل منفصل، ومن ناحية أخرى، على اعتبار أنها تحدث معا في نفس الوقت..

في البداية، تم تطوير نموذج مساحة الحالة مع الأخذ في الاعتبار معالجة أعطال الدوائر القصيرة في الأقراص. تتعلق الخطوة الأولى بإعادة تعريف مصفوفات المقاومة والحث والسعة لإدخال المعاملات المتعلقة بالعيوب. محاكاة الاستجابة الترددية من خلال دراسة عطل دائرة كهربائية قصيرة بمعدلات مختلفة وفي أقراص مختلفة، لتحديد مدى تأثير دائرة القصر على سلوك محول الطاقة. تتيح هذه النمذجة إمكانية اقتراح نماذج جديدة تتكيف مع احتياجات تشخيص محولات الطاقة. بعد ذلك، تدرس هذه الأطروحة العديد من التشوهات المتعرجة، والتي تشمل الإزاحة المحورية، والإزاحة الشعاعية، والإزاحة المحورية مع مراعاة SC. يمكن أن يكون إجراء تحقيق في تحليل استجابة التردد أداة قوية لدراسة تأثير مثل هذه الأخطاء على سلوك محولات الطاقة. وأخيرا، في الفصل الأخير من هذه الأطروحة، تم تقديم منصة اختبار توفر خدمة بناء نموذج مكافئ لمحولات الطاقة. كما أن من مميزات هذه المنصة أنها أداة قوية تساعد في إجراء الاختبارات الروتينية واختبارات السلامة للكشف عن الأخطاء الميكانيكية في ملفات محولات الطاقة. بالإضافة إلى ذلك تم تقديم برنامج بالكمبيوتر تلقائيا لغرض توفير البيانات اللازمة التي يتم الحصول عليها من خلال LCR يقوم بربط جهاز قياس الاختبارات سواء في اختبارات التصميم أو اختبارات بدء التشغيل.

الكلمات المفتاحية: محول القدرة، نموذج فضاء الحالة، اللف، منصة اختبار، الإزاحة المحورية، الإزاحة الشعاعية، FRA. ماس كهربائي،

Acknowledgements

Praise be to God, the Most Gracious, the Most Merciful, who guided me and facilitated the path to success for me in completing this research, which I hope will be a useful tool and means for students of knowledge in this field. I am really grateful to many people for their support in my studies and for finally completing this thesis. At the beginning, I would like to extend my sincere thanks to my main advisor, Professor Hamza Houassine, and also all thanks to my brother, Dr. Sahnoune chaouche Moustafa, whose experience I benefited from in this field, and to the assistant advisor, Professor Samir Moulahoum, and also all thanks and appreciation to Professor Samir bin Said for his support. Once again, all thanks and appreciation to all professors for their guidance, advice and support. Which were countless during my PhD candidacy. Once again, all thanks and appreciation to all professors for their guidance, advice and support. Which were countless during my PhD candidacy. I learned a lot from them, especially the culture of research, professionalism and work ethics. Their professionalism always inspires me. Their expertise always impresses me. Their enthusiasm always motivates me. I also extend my appreciation to all my colleagues in the maintenance group at the Algeria Refinery. To those who have been a strong support for me from near or far to complete my research, thank you for your help and being wonderful friends.

Also, I would like to express my deep gratitude to all my family members for their endless support, love and prayers, especially my mother for her encouragement, and my wife for her great patience and support throughout my studies.

Finally, words of gratitude and appreciation are the simplest expressions that every student can offer to every teacher from whom he learned to thank him for his main role and working with students to push them towards a better future. Distinguished teachers who are always keen to deal with students kindly and encourage them.

Table of Contents

Abstract i
Acknowledgements.....iii
Table of Contents I
List of figures IV
List of tables V
List of abbreviations IIV
General Introduction 1

Chapter 1: Power Transformer Components and Most Reliable Method to Detect Their Faults

1.1.Introduction 4
1.2.Electrical power transformer.....5
1.3.Construction.....6
1.3.1. Bushings.....6
1.3.2. Tap changer.....7
1.3.3. Core 8
1.3.4. Insulation 8
1.3.5. Windings 9
1.4.The objective of transposition in power transformer winding 9
1.5.Types of Transformer Windings 10
1.5.1. Pancake Windings 11
1.5.2. Layer (Barrel) Windings 12
1.5.3. Helical Windings 13
1.5.4. Disk Windings 14
1.6. Causes of transformer failures and diagnostic methods 14
1.7.Causes of transformer Failure 15
1.8.Winding deformations of power transformer 18
1.8.1. Axial Electromagnetic force 19
1.8.2. Inter-turn Fault 20
1.9.Most common routine transformer testing 20
1.10. The sweep frequency response analysis 26
1.10.1. The method for FRA Test Connections 27
10. Conclusion 30

Chapter 2: State-Space Equations of The Equivalent Lumped Model for Transformer Winding.

2.1.Introduction ……31
2.2. The simplified meaning of optimization ……32
2.3.Particle swarm optimization used to determine the equivalent model……34
2.3.1. Standard PSO Structure……...……...……35
2.4.Equivalent model of an isolated electrical transformer winding ……36
2.5. Identification of model parameters by the FRA-SMI method……38
2.5.1. Low frequency response (LFR sub-band) ……39
2.5.2. Mid-frequency response (sub-band MFR) ……39
2.5.3. High frequency response (HFR sub-band) ……40
2.6.Estimation of the parameters of the isolated winding using the method by the "FRA-SMI"……40
2.6.1. Parameters can be measure ……41
2.6.2. Inductance matrix estimation……....43
2.7. State-space equations of the equivalent lumped model for winding defects simulation...44
2.7.1. State-space equation for the coupled ladder network……...44
2.7.2. Determination of the percentage of the short-circuited turn's number in each winding disk……...45
2.8. Conclusion……...49

Chapter 3: The Effect of Power Transformer Impedance on Short Circuit Failures.

3.1. Introduction ……50
3.2. Percentage Impedance written in nameplates ……51
3.3. Transformer impedance in case of short circuit fault……52
3.4. Short-circuit failure in one disk in isolated winding……53
3.5. Simulation of isolated model winding……53
3.6. Influence of short circuit for winding frequency characteristics……56
3.6.1. Short circuit fault simulation results in disk 6……57
3.6.2. Case of multiple faults of short circuit in isolated winding……..…58
3.6.3. Short circuit faults on disks 5 and 6 by 5% ($f_5 = f_6$ 0.95 and $n_5 = n_6 = 95$) ……58
3.6.4. Short circuit in disk 2 with 20%, 25% in disk 3 and 40 in disk 4……59

3.6.5. Short circuit in disk 2 with 20%, 25% in disk 3 and 40 in disk 4……60
3.7. Short circuit faults in isolated transformer winding in case experimental……61
3.7.1. short-circuit failure in multiple disks in isolated winding…….……...62
3.8. Estimation of the severity of short-circuit faults in disks……. …...63
3.9. The salient features extract……...64
3.10. Conclusion…….....65

Chapter 4: Deformations Instigated by AD, AD with SC and Radial.

4.1. Introduction ……66
4.2. Deformations Instigated by Axial displacement ……...67
4.2.1. Failure mode caused by axial forces ……...…68
4.3. Deformations Instigated by Axial displacement with SC ……70
4.3.1. Axial displacement (5mm) with SC (40%) in disk 5 ……73
4.3.2. Axial displacement (20mm) with SC (40%) in disk 5 ……...74
4.5.An illustrative example of AD with SC consideration in disk 5……...76
4.6.Deformation instigated by radial……....77
4.7.Failure mode caused by radial forces……...78
4.7.1. Radial displacement in disk 2 by change Cg2 with 20%.....79
4.8.Conclusion…….....81

Chapter 5: Test Platform Dedicated to Power Transformer Winding Diagnostics.

5.1.Introduction ……..83
5.2.Software design and instrumentation……84
5.2.1. Data acquisition……...84
5.3.Design of the platform……...84
5.4. LCR meter via PC connection……...86
5.5. Particle optimization algorithm (PSO)……..87
1.10.2. The process of estimates of self and mutual inductances l_s and M_{ij}……87
1.10.3. The process of estimates of the series capacitance $C_s$and the ground capacitance C_g...88
1.11. Qualitative evaluation of short-circuit condition in power transformer windings …...90
1.12. Qualitative evaluation of radial displacement condition in power transformer windings...92
1.13. localization of AD escorted by SC ……93

1.14. Study of the change of the equivalent inductance as a function of the percentage of SC ……94
1.15. Conclusion ……...……96
Conclusions ……..…97

1 List of figures

Figure 1.1: Circuit diagram of a transformer…….05
Figure 1.2: The 400kV autotransformer ……...06
Figure 1.3: Schematic Construction of OIP Condenser Bushings for power transformer……07
Figure 1.4: OLTC arrangements……07
Figure 1. 5: phase core-form (a) and shell-form (b) transformers contrasted……08
Figure 1.6: Continuously transposed cable (CTC)…… ……..…...09
Figure 1.7: Types of transformer windings……..…...11
Figure 1.8: Format of Stacked pancake windings…….....12
Figure 1.9: Format of Layer windings……12
Figure 1.10: Helical winding during assembly…….13
Figure 1.11: Disk winding type…….……14
Figure 1.12: Disk winding inner and outer crossovers…….14
Figure 1.13: Defective components of power transformers according to a CIGRE international survey….....15
Figure 1.14: Flux lines and force directions on HV and LV windings……18
Figure 1.15: Illustrative diagram before and after the occurrence of an axial displacement…20
Figure 1.16: Dissipation factor (tan delta) / power factor of insulating oils……..21
Figure 1.17: Polarity test diagram……22
Figure 1.18: Oil insulation test device……23
Figure 1.19: Resistance DC measurement test for windings in the first and third transformers……24

Figure 1.20: The end-to-end open-circuit test…….....25

Figure 1.21: The open-circuit test…….27

Figure 1.22: The open-circuit test……....28

Figure 1. 23: Method of the capacitive inter-winding test……....28

Figure 1.24: Method of the inductive inter-winding test……29

Figure 2.1: Example of the possible solutions to the optimization problems……32

Figure 2.2: The method to get optimal solution in greedy approach…….33

Figure 2.3: The method to get global solution in greedy approach…….33

Figure 2.4: Example of brute force approach…….34

Figure 2.5: The hill climb algorithm…….34

Figure 2.6: Framework of the IDE-PSO algorithm……36

Figure 2.7 Decomposition of the frequency response FRA. …….38

Figure 2. 8: Conceptual model for the basic elements in the experiment…….41

Figure 2.9: The FRA fingerprint corresponding to the healthy winding and the impedance estimation in the health condition…….43

Figure 2.10: The lumped model scheme of transformer winding…….45

Figure 3.1: Percentage Impedance written in nameplates…….52

Figure 3.2: Equivalent circuit of a transformer winding in MATLAB Simulink……...53

Figure 3.3: Frequency response analysis in disk 4 with SC excite…….56

Figure 3.4: The impedance estimation with different faults of SC by (ohm)in disk 6……...57

Figure 3.5: Impedance estimation with 20% fault in disks 5, 5% fault in disk 6…….58

Figure 3.6: Impedance estimation with 20% fault in disk 2, 25% fault in disk 3 and 40% in disk 4…….59

Figure 3.7: Impedance estimation with 10% fault in disk 1, 20% fault in disk 2 and 25% in disk 4…….61

Figure 3.8: Short-circuit faults in disk 5 with different levels, (a) reel faults……62

Figure 3.9: Short-circuit faults in disk 5 with different levels, (b) simulation faults…….62
Figure 3.10: Rates of short-circuits in disk 2…….63
Figure 4.1: Illustration schematic for axial displacement before and after……67
Figure 4.2: Conductors tilting in power transformer winding……68
Figure 4.3: Schematic of axial bending failure of conductors……69
Figure 4.4: Axial collapse due to conductor ‘telescoping……..….69
Figure 4.5: Collapse of winding in power transformer……
Figure 4.6: A graphical representation of the impedance in the event of an axial displacement between disk 5 and 6…….70
Figure 4.7: A graphical representation of the impedance in the event of an axial displacement between disk 5 and 6 with SC……74
Figure 4.8: Axial displacement (20mm) with SC (40%) in disk 5…….74
Figure 4.9: Measured of FRA for isolated winding with AD between D5 and D6…….75
Figure 4.10: Example of AD with cc consideration in disk 5…….76
Figure 4.11: Leakage flux in two windings……77
Figure 4.12: Deformation by buckling (a. Shape after free buckling. b. Shape after forced buckling) ……...78
Figure 4.13: Spiraling Failure……....79
Figure 4.14: Radial displacement in disk 2 by change Cg2 with 20%.....80
Figure 4.15: Radial displacement by change Cg3 and Cg 4 with 50%.....80
Figure 5.1 : Block diagram explain the main steps of the platform. ……..85
Figure 5. 2: Table for control LCR meter through LabVIEW.…….86
Figure 5.3: program for control LCR meter through LabVIEW……87
Figure 5.4: Initialize parameters……...……88
Figure 5.5: Update best solution, with calculate self-inductance and mutual inductances…...89
Figure 5.6: Update best solution, with calculate series and shunt capacitance…….90
Figure 5.7: Test platform to diagnosis short circuit fault……. ….91

Figure 5.8: Measured FRA of the winding before and after RD……..…….92

Figure 5.9**:** platform for Localization process of radial displacement……...93

Figure 5.10: Plotted the change of $\Delta\psi_{scnf}$ in terms of x (number of disks) ……94

Figure 5.10 The change of the equivalent induction in terms of the displacement range in the case of different ratios of SC ……95

2 List of tables

Table 1.1: Value of Core Ground Resistance according to the Standards……...25

Table 2.1: Recommendations before measure parameters……42

Table 2.2: Parameters measured using LCR meter, each according to its range of frequency in which to measure it……43

Table 2.3: Various M_{0i} that have been estimate……43

Table 3.1: Short-circuit on disks of isolated winding……55

Table 3.2: short-circuit 5% in disk 5 and 6……59

Table 3.3: Case of multiple faults of short circuit in different disks……60

Table 3.4: Case of multiple faults of short circuit in different disks……60

Table 3.5: In the case of failure of CC in one disk of insulated winding……62

Table 3.6: Occurrence of a short circuit fault in several disks of insulated winding……63

Table 4.1: Results of axial displacement with short-circuit consideration for different disks winding……76

Table 4.2: Radial displacement in disk D3 and D4……81

List of Abbreviations

FRA: **F**requency **R**esponse **A**nalysis

SC: **S**hort **C**ircuit

FRSL: **F**requency **R**esponse of **S**tray **L**osses

SFRA: **S**weep **F**requency **R**esponse **A**nalysis

CIGRE: International Council on Large Electric Systems

AD: **A**xial **D**isplacement

RD: **R**adial **D**isplacement

M.M.F: **M**agneto**m**otive **f**orce

E.M.F: **E**lectromotive **F**orce

OLTC: **O**n-**L**oad **T**ap **C**hanger DETC

DB: The decibel (symbol: dB) is a relative unit of measurement equal to one-tenth of a bel

ANSI: **A**merican **N**ational **S**tandards **I**nstitute RVM

DGA: **D**issolved **G**as **A**nalysis IEC 60076-18

TTR: **T**urns **R**atio **T**est

PSO: **P**article **S**warm **O**ptimization

LFR: **L**ow-**F**requency **R**esponse

MFR: **M**edium **F**requency **R**esponse

HFR: **H**igh-**F**requency **R**esponse

General Introduction

General Introduction

The electrical power transformer has been considered a durable cornerstone in the power network system. Nowadays, this equipment is the pulsating heart in the substation. The electrical transformer is the most widespread and diverse element in its shapes, sizes and functions in electrical networks. only cables and overhead lines compete with it in this widespread within the electric power system. However, the diversity in the size, shape and function of transformers makes the study of electrical transformers the most important among the elements of the electrical system. Special attention needs to be taken to monitor this expensive asset. Among the most critical aspect of a transformer mechanical failures, or mechanical damages that affect its windings during their life. According to statistics, mechanical stresses represent the highest percentage of faults affecting electrical transformers, at a rate of 37 percent among all the faults, depending on to an American study conducted on a group of transformers [23,66]. The removal process of the winding power transformer to investigate, costs dearly from all sides; removal winding from the tank for detailed inspection is not warranted, as moisture from the atmosphere could contaminate the transformer oil–paper insulation. In recent decades, the invention of the power-sensitive method of frequency response analysis (FRA) made possible the early detection of mechanical deformations and electrical integrity of the power transformer. This useful tool for the interpretation of basic operations for power transformers during their service life.

- The acceptance test, is a process that evaluates the equipment during and after the assembly process by verifying that it is built and operating in accordance with design specifications.
- manufacturing testing of power transformers, include winding insulation resistance test, winding resistance test, vector group test, tan delta test, no-load test or iron losses, load test or copper losses, temperature rise test, partial discharge test, frequency response analysis test, and transformer oil breakdown test.
- commissioning, is the process of ensuring that all systems and components of a building are designed, installed, tested, operated, and maintained according to the operational requirements of the owner and tenants.

In this thesis, the overall aim is a development of a test platform allowing the evaluation of the different mechanical failure windings of power transformers by taking into account more varied and equally important criteria such as the validity of the model, fault location and its severity.

Initially, the Transfer function and state-space model are two powerful complementary tools used to monitor the physical system. These two ways can be very successful in comprehensively analysing electrical power transformer malfunctions. A mathematical model is established to simulate the frequency response of a power transformer in chapter one. The developed model takes into account the occurrence of two failures at the same time to examine the sensitivity of the winding response. As mentioned, FRA is widely recognized as the best tool. FRA is a non-intrusive test, which measures the transfer function response of a transformer winding electrically over a wide frequency range. This thesis studies several winding deformations, which include short-circuiting phenomena, axial displacement without SC, axial displacement with SC consideration, radial displacement without SC, and radial displacement by accompanying SC. These five faults are examined in terms of their severity of damage and the location of the fault for isolated transformer winding. Development of a test platform dedicated to the diagnosis of the windings of the power transformer is the cornerstone of this thesis. This platform is an attempt to find a new method to assess the severity of the mechanical faults of the transformer and give it a clear explanation through the results obtained in a simplified and concise manner. The short-circuit forces mostly lead to the radial component and axial component separately instead of on the total force. The radial force is generated by the axial component of leakage flux, while the axial force is generated by the radial component of leakage flux [Power Transformer Design Practices]. In order to understand how these faults, damage the winding and how could change the frequency response, many investigations have been performed by simulating the response of axial and radial displacement winding with SC fault and without and analysing its. As mentioned before a suitable approach have been submitted to analyse the response could be developed. Elaboration a native autonomously tool to control the LCR meters through computing systems. This is done by adjusting the inputs of the system and using output measurements. This platform will control the impedance measurement (the FRA signal) by the instrument of the LCR meter through MATLAB software. Achieving estimation autonomously to all the parameters of the lumped equivalent model of the winding accurately using frequency response analysis signal morphology interpretation (FRASMI) proposed by Amara et.al [66]. This approach is a powerful tool that has been given addition to this search in appreciation of the parameters.

Obtaining a new representation of the state-space model of the lumped equivalent model of an isolated winding with SC fault between its turns. Where these faults are simulated autonomously (are manifested in a multiplicative manner by fault coefficients on the parameters

changed by the fault). This approach motivates the use of state-space representation in the autonomous simulation of winding failures (eg. SC with AD) to locate and assess its severity.

This thesis is focused on the recognition and interpretation aspect of some electrical and mechanical faults in the transformer winding. The completed process of interpreting the failures Data, the diagnostic tests performed, and the test results are interpreted in general lead to the nature of the defect.

Chapter 1: *The most reliable method to detect faults in power transformer components.*

Chapter 1: ***The most reliable method to detect faults in power transformer components.***

1.1. Introduction

Failures of power transformers can be devastating and costly on all sides. However, the electrical, mechanical and thermal factors combination could potentially cause damage to the power transformer during its lifetime. One or all of these factors may cause the power transformer malfunction, which infects one of the active parts of the power transformer [1].

In the foreground, with transformer failures that have occurred, no obvious external damage is to be seen. than requires in-depth investigations more accurate and more effective methods depending on the type of weaknesses or faults and to give some indication of possibilities for repair [2]. Among the most reliable methods for detecting faults in an electrical power transformer, the feasibility methods include, but are not limited to, the following: Partial discharge analysis, Capacitance and power factor, the Frequency response of stray losses (FRSL) measurement, and Sweep frequency response analysis (SFRA).

SFRA is used to identify and analyses the integrity of a power transformer from mechanical or electrical problems in windings, contacts or cores. To ensure the integrity of the transformer from all defects without having to prior dismantling [3]. SFRA is a non-destructive method. It allows the reliable assessment of a power transformer's integrity by applying low tension to the winding. This process is for obtaining the fingerprint of the reference or comparing it with the previous one. Changes in geometric configuration clearly reflect changes in the impedance of the winding which is being detected by comparing it to the test of reference.

A reliable and very important study conducted by a group A2.37 of CIGRE (International Council on Large Electric Systems) showed that the faults in the transformer windings exceed 30 percent of the total transformer faults. Forecasting mechanical failures, knowing the appropriate corrective measures to ensure reliable operation and extend the life expectancy of the transformer.

1.2. Electrical power transformer

A power transformer in most frequently consists of a pair of windings, they linked together magnetically or by core. There are three basic elements that define the principle of the transformer: the first coil, the second coil, which are connected to each other by the magnetic flux in the third element, which is the core. As shown in the following figure1.1.

When an alternating voltage is applied to one of these windings, generally by definition the primary, a current will flow which sets up an alternating M.M.F and hence an alternating flux in the core. This alternating flux in linking both windings induces an E.M.F in each of them. In the primary winding this is the 'back -E.M. F and, if the transformer were perfect, it would oppose the primary applied voltage to the extent that no current would flow. In reality, the current which flows is the transformer magnetizing current. In the secondary winding the induced E.M.F is the secondary open-circuit voltage [4, 17].

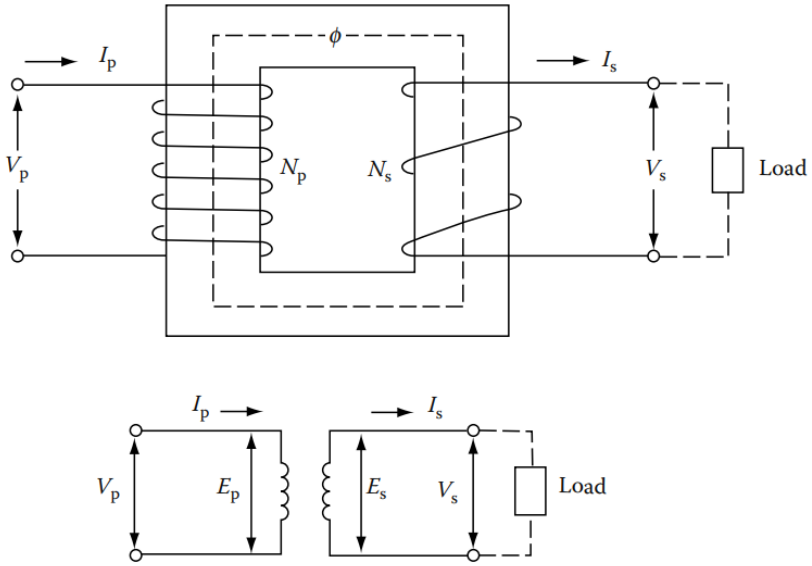


Figure 1.1: Circuit diagram of a transformer.

Primary section:

V_p is the primary voltage

E_p is primary Electromotive Force

I_p is the primary current

Secondary section:

V_S is the secondary voltage

E_s is secondary Electromotive Force

I_s is the secondary current

Power transformers in general are divided into two types the dry type and the immersed in liquid each separately. The first type is intended explicitly for indoor use. For external use, transformers are usually immersed in liquid. This thesis focuses on external liquid-immersed transformers, such as those described in figure1.2. [5, 6].



Figure 1.2: The 400kV autotransformer

1.3. Construction

1. Bushings

Bushings are among the most critical components of a power transformer, which provide highly effective isolation between active line conductor and the tank of transformer. It is an insulating structure that facilitates the passage of an energized, current-carrying conductor through the grounded tank of the transformer. The two principal types of bushing construction are solid or bulk type and capacitance-graded (sometimes called condenser type). In low voltage transformer the solid type with porcelain type insulator is used, while in high voltage mostly the type of capacitance graded bushings is used [7]. The oil-impregnated paper type saturated is the most widespread type around the world. Figure 1.3 shows us the schematic diagram of this type.

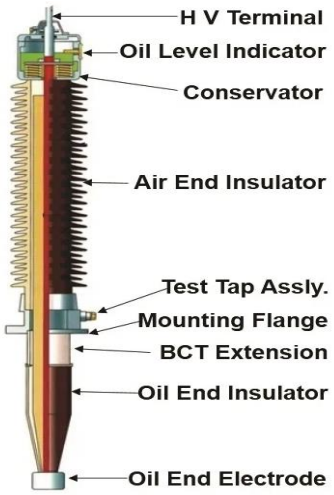


Figure 1.3: Schematic Construction of OIP Condenser Bushings for power transformer.

2. Tap changer

The power transformer equipped with on-load tap changers (OLTCs) has been the main component of electrical networks for nearly ten decades, which has fitted with a tap changer to regulate the output voltage to the required levels. This is typically achieved by changing the ratios of the transformers on the system by altering the number of turns in one winding of the appropriate transformer/s [8]. However, failures of the tap changer can cause costly power breakdowns, as an aid to many investigations when the tap changer failure has been reported the most common malfunctions that occur are the following: Contact problems in the tap selector and at the diverter switch, Open circuit shorted turns or high-resistance connections in the OLTC preventative autotransformer, and Contact problems in the DETC [9]. Three effective methods are recommended and used in the early detection of the type of malfunctions that infect the tap changer and that are: DC winding resistance measurement and OLTC verification, Exciting current measurement, and Sweep frequency response analysis (SFRA).

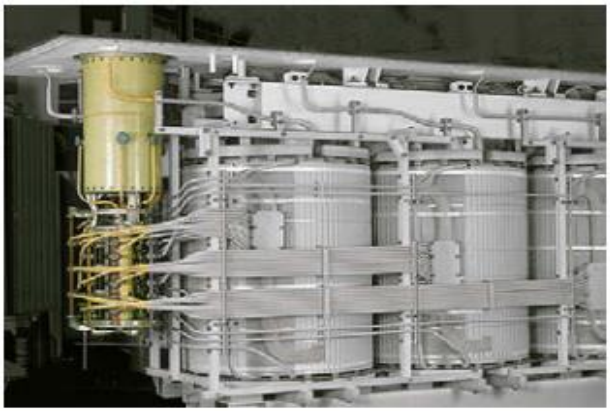


Figure 1.4: OLTC arrangements.

3. Core

Two types of transformer core design, a core-form and a shell-form. In a core-form design, the coils are wrapped or stacked around the core. Whereas, the opposite in the shell-form design, the core is wrapped or stacked around the coils. In distribution transformers, the shell-form design is trendy because the core can be economically wrapped around the coils. The core-form design is more common for moderate to large power transformers, possibly because short-circuit forces can be better managed with cylindrically shaped windings. Figure 1.5 illustrated the general shape and the prominent differences between each of the cores [10, 11].

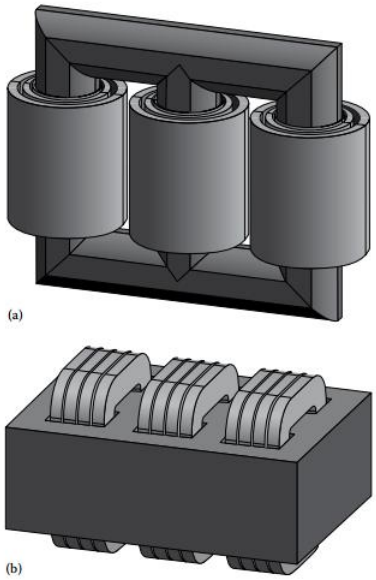


Figure 1. 5: phase core-form (a) and shell-form (b) transformers contrasted.

4. Insulation

While performing the primary function of a power transformer, it is being generated two types of losses. No-load losses (iron losses) and load losses. Losses to iron losses occur within the ferromagnetic core. They are constant regardless of the transformer load. Load losses or "copper" losses are due to the Joule effect. They vary with the square of the current or the power output (if the voltage remains constant), which generate heat. The function of the cooling system (insulating system) is to remove this heat at a steady and controlled rate in order to maintain an acceptable temperature differential between the active part and its surrounding medium. Mineral oil, as well as other types of liquids, have excellent dielectric insulating properties. Mineral oil provides a great insulation medium when used to impregnate the Kraft paper typically used to wrap winding conductors and other elements of the windings. The

capacity to remove heat from the active part is also improved by using a liquid instead of a gas (such as air) as the medium that surrounds the active part [12].

5. Windings

The windings of power transformers are designed to be supported operational and test conditions. Copper and aluminum are the primary materials used in the manufacture of power transformer windings. While we found that aluminum is lighter and generally less expensive than copper. however, copper has higher mechanical strength [13]. The windings of power transformers are made of insulated wires of pure red copper, and all their coils are electrically isolated from each other and the core. Copper occupies the first place in the materials used in the manufacture of windings because it has several advantages, including its high electrical conductivity, knowing that this feature depends mainly on the percentage of impurities present in it, copper that contains, for example, 2% phosphorus or 7% arsenic, its conductivity decreases by 30%. Among the advantages of copper is that it is slow to oxidize, tolerates moist air, has a high degree of flexibility, and is accessible to weld. It is also easy to draw and form [14]

1.4. The objective of transposition in power transformer winding

The purpose of the transposition process in the power transformer windings is to prevent the eddy currents that can arise within the large section of the conductor itself as a result of the exposure of its parts to different levels of flux because of their relative position, whereby a difference in voltage between the layers generated as a result of internal eddy currents in the conductor. whereas the transposition process ensures the disappearance of these currents because they cancel each other out. The windings processed in this way are called CTC (Continuous Transposed Conductor) as presented in the figure bellow [15,16].

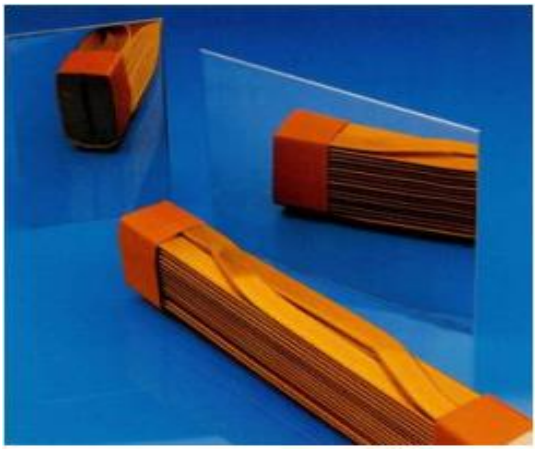


Figure 1.6: Continuously transposed cable (CTC).

1.5. Types of Transformer Windings

There are four most well-known types of electrical transformer windings, and the choice often falls on one of these four types, based on the number of windings required and the value of the current that is carried throughout it. There are two types of coil sections in the electric transformer, either circular or rectangular. The circular section is characterized by rigidity and mechanical durability, while the rectangular section is characterized by the lack of materials used in its manufacture and its weak mechanical strength, especially during the occurrence of a short circuit, but it is limited in use except for small transformers because of the aforementioned. In general, any voids between the coils and the core are filled by wooden spacers or other insulating materials to improve mechanical durability [17].

The concentric windings used for core types of transformers can further be classified into many groups. The most important transformer windings are:

- Pancake windings
- Layer (Barrel) windings
- Helical windings
- Disk windings

In the following figure 1.7 the types of transformer windings are presented, and the next section explains the types of windings, with exposure to the most important features of each winding.



Figure 1.7: Types of transformer windings.

1.5.1. Pancake Windings

This type of winding is known as a 'pancake' because of the distribution of conductors in the disks. This type is used exclusively in transformers, where it is first wrapped in a rectangular shape on wooden models to be placed on an iron core as shown in the figure 1.8 [18].

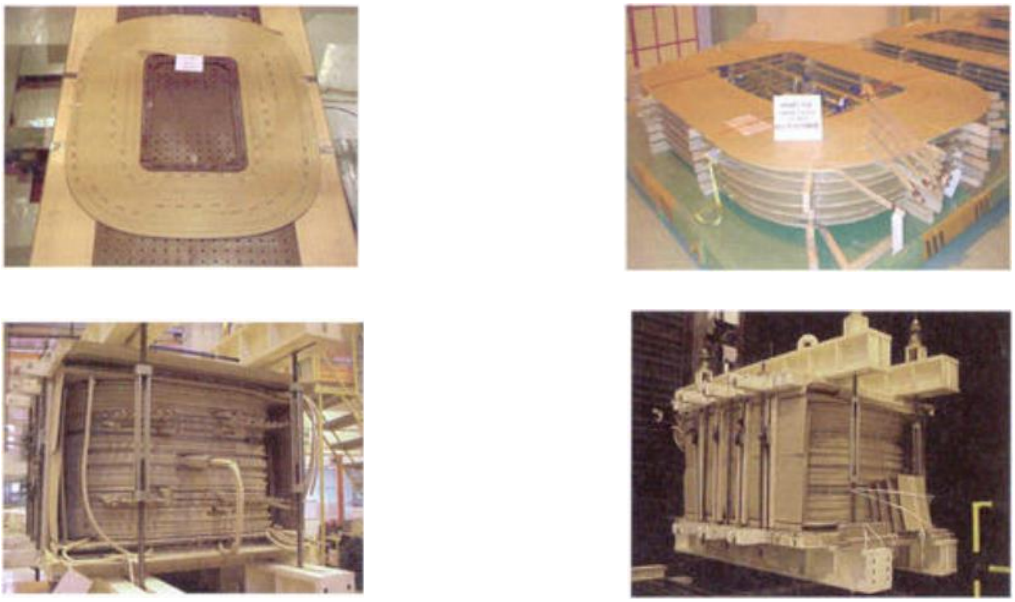


Figure 1.8: Format of Stacked pancake windings.

1.5.2. Layer (Barrel) Windings

Layer or barrel windings are among the simplest types of windings used in power transformers winding in that the insulated conductors are wound directly next to each other around the cylinder and spacers. This method is used with transformers that are equipped with a load tap changer, in which the ends of the winding parts can be taken out to connect them with the tap changer. Figure 1.9 shows a layer winding during assembly that will be used as a regulating winding in an LTC transformer [19].

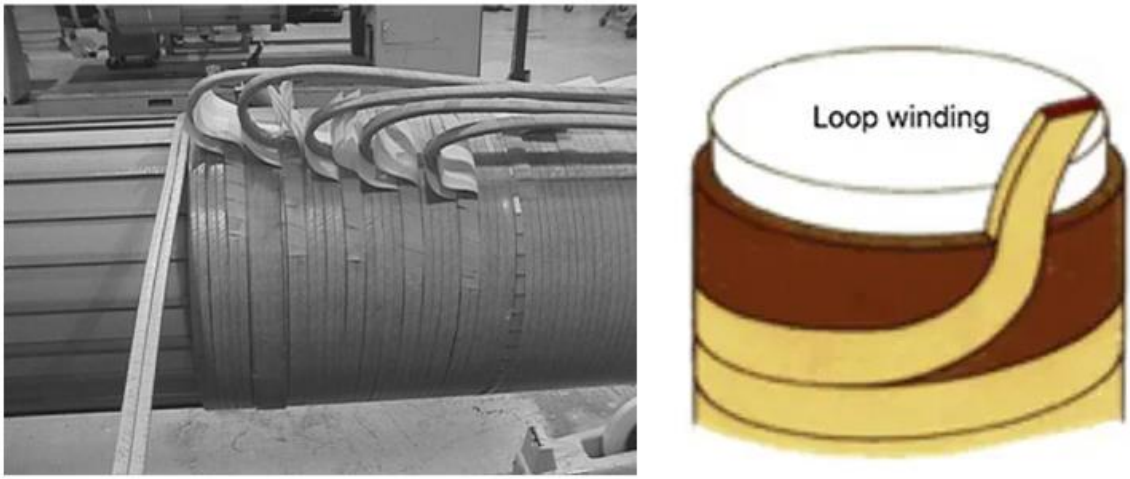


Figure 1.9: Format of Layer windings.

1.5.3. Helical Windings

Helical windings, screw windings or spiral windings are types of windings using for LV coils in medium and high-capacity transformers, with smaller number of turns but in higher current. A helical winding consists of a few to more than 100 insulated strands wound in parallel continuously along the length of the cylinder, with spacers inserted between adjacent turns or disks and suitable transpositions included to minimize circulating currents between parallel strands. One of the most notable features of this type of winding is the improved cooling oil circulation in an easier and better way, and this is the result due to the nature of its design. where a helical winding usually varies from 6 to 20 conductors. In essence, there are axial spacers provided between adjacent turns in helical windings, which helps in the process of permeating the cooling oil well in the winding rolls [20]. This type of winding is mechanically more stable and durable, but it is easy to manufacture as shown in the figure 1.10. Helical windings are used for higher-current applications frequently encountered in the lower-voltage classes [21].

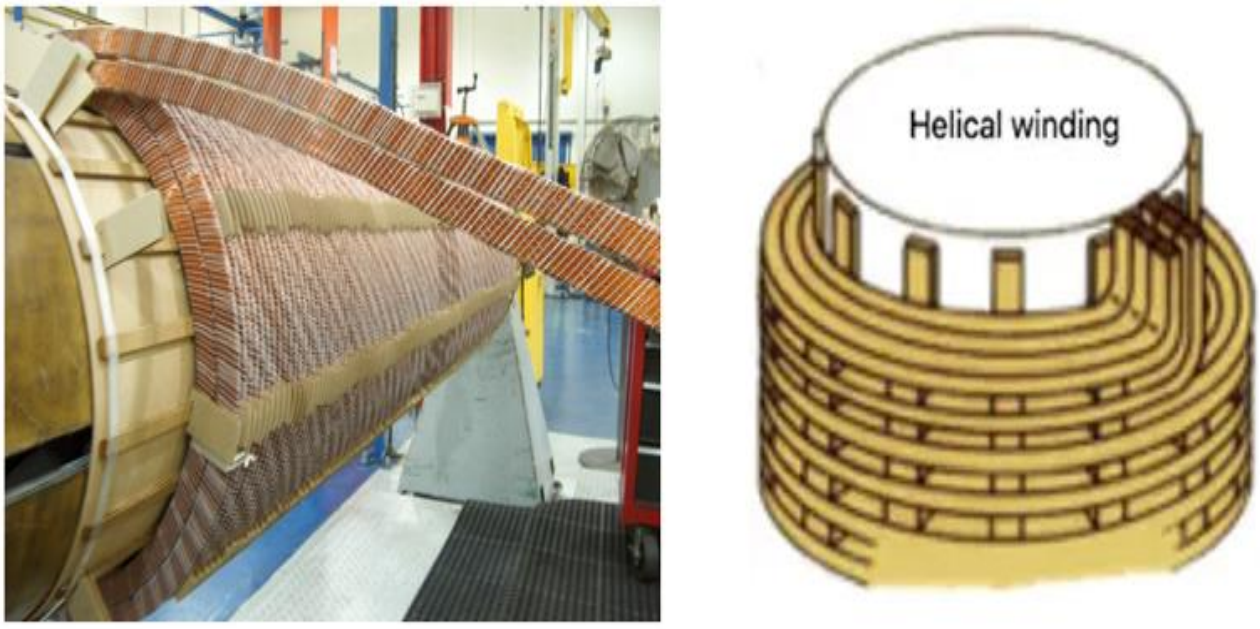


Figure 1.10: Helical winding during assembly.

1.5.4. Disk Windings

This type of winding is used in transformers with the aforementioned characteristics, which contain a huge number of high-voltage windings with low currents. A disc winding can involve consisting of a number of flat coils or disks connected in series or parallel. The coils are formed with rectangular strips wound spirally from the center outwards in the radial direction, as illustrated in the figure below [22].

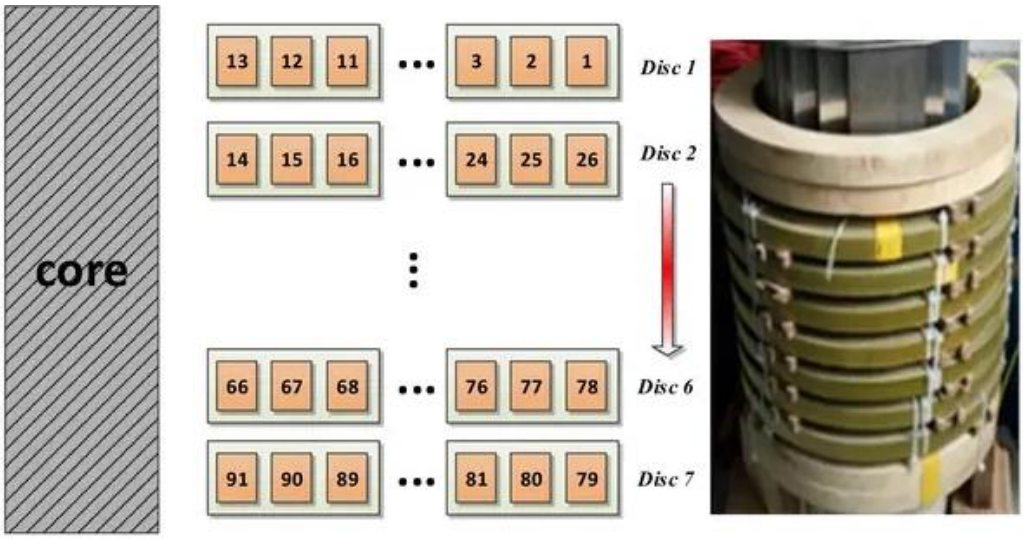


Figure 1.11: Disk winding type.

Figure.1.12. shows typical crossovers during the winding process. Most windings of 25-kV class and above used in core form transformers are disk type. Given the high voltages involved in the test and operation, particular attention is required to avoid high stresses between discs and turns near the end of the winding when subjected to transient voltage surges. Numerous techniques have been developed to ensure an acceptable voltage distribution along the winding under these conditions [7].

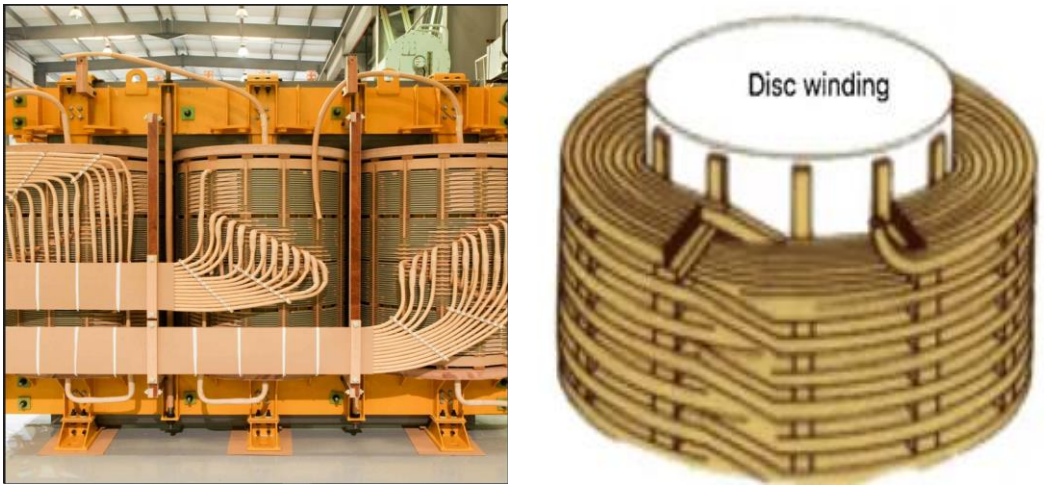


Figure 1.12: Disk winding inner and outer crossovers.

1.6. Causes of transformer failures and diagnostic methods

The International Council on Large Electric Systems (CIGRE / Conseil International des Grands Reseaux Electriques) revealed that has been 44% of forced outages of large transformers related to bushings and windings. The highest failure rates occur at power

transformers in Tap changer, where it tops the list with the highest value of 40%. where these three defective components represent about 84% of the failure statistics of these transformers. While the rest of the faults represent 16 percent, as shown in the following figure.1.13. [23,24]

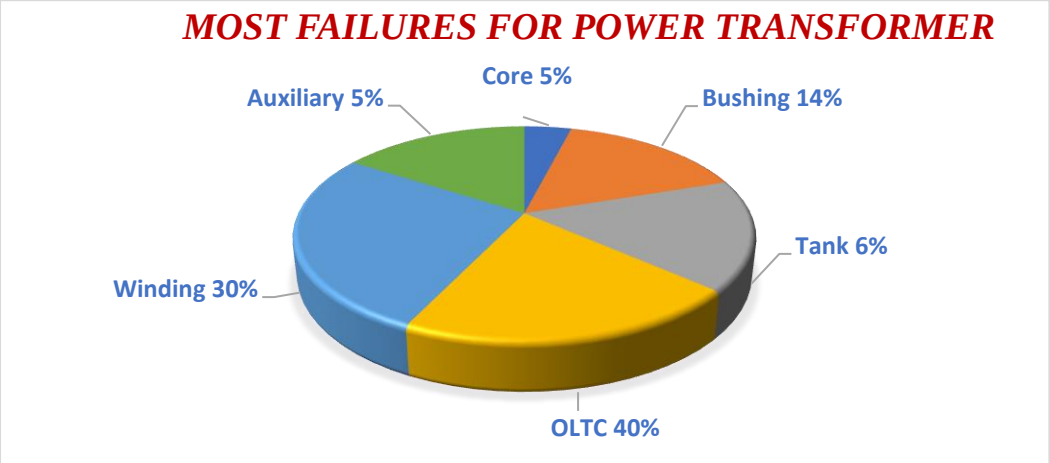


Figure 1.13: Defective components of power transformers according to a CIGRE international survey.

1.7. Causes of transformer Failure

After addressing the most important parts of the electrical power transformer, while expressing some of the causes of failure for each component, in this part we also discuss the most important electrical faults that affect the power transformer. Catastrophic failures of power transformers lead to catastrophic consequences and cause emergency power outages. In general, there are approximately to fitting types of conditions that will cause trouble in power transformers:

- ***Overtemperature:*** Overtemperature can be caused by an overcurrent, overvoltage, insufficient cooling, low liquid level, sludge in the transformer liquid, high ambient, or short-circuited core. In dry-type transformers, this condition can be due to clogged ducts.
- ***Winding insulation failure:*** This type of malfunction comes in many different forms where it can involve phase-to-ground, phase-to-phase, three-phase and/or ground, or turn-to-turn-type short circuits. The causes for this type of failure may be due to a short-circuit fault, lightning, overload or overcurrent condition, or transformer liquid containing moisture and contaminants. This type of failure has been given a great deal of attention in this research. where it represents approximately 34% of the total faults that affect the power transformer.

- ***Incorrect secondary voltage:*** They are three most important cases that cause the incorrect second voltage to malfunctioning which is divided between: Incorrect turn ratio, abnormal primary voltage and shorted turns in the transformer [1].
- ***Bushing failure:*** The combined factors of thermal, and electrical stresses and environmental conditions are one of the main reasons for failure bushings. The high levels of electrical stress in bushings, and failures in oil-impregnated paper (OIP) bushings with porcelain insulators tend to result in sudden and catastrophic failures as the partial breakdown between capacitive graded layers, cracks in resin-bonded insulation, ageing and moisture ingress, open or compromised measuring tap connection, and partial discharges in the insulation [25,26]. The element more accurately reflects the authenticity of bushings is the tan δ. Which is remained low at the forefront of the service, with the bushing is in good condition. an increase in power factor is evidence of a change in the characteristics of the dielectric [9] [27].
- ***Internal arcing:*** This type of fault does not have many causes but severe consequences. It can occur due to low levels of fluid exposing live parts of the transformer, loose connections, or failure of the insulating transformer. High-energy bending faults in power transformers can cause overpressure that leads to open tanks, causing oil to spill out and even catch fire [28].
- ***Core failure:*** The core of the transformer carries magnetic flux and provides mechanical strength to the transformer. failure of the core in general is due to the failure of core laminations, core, bolts, clamps, and so on [29]. Mechanical deformation and floating core ground, they are detected by capacitance and power factor/ dissipation factor measurement: at 50 Hz or 60 Hz, as tip-up test with variable frequency method. Shorted core laminates and disclose it by exciting current measurement, and residual magnetism which detect one of the following effective methods exciting current measurement or demagnetization method. While one of the best and most effective ways to detect all the previously mentioned faults is Sweep frequency response analysis (SFRA).
- ***High exciting current:*** loss of the flux in the core and open core joints are the main reason drawing to high exciting currents [30].
- ***Low dielectric strength:*** There are main reasons and conditions for low dielectric can be caused by condensation and penetration of moisture due to improper ventilation and broken relief diaphragm.

- ***Oxidation of oil:*** Oxidation is cancer for oil in all transformers and it attacks the transformer's paper insulation usually results in the formation of acids and sludge in the transformer liquid. It is mainly due to exposure to air and high operating temperatures [31].
- ***Pressure-relief diaphragm broken:*** The occurrence of a short circuit inside the power transformer creates an arc with a high-temperature degree, which leads to the decomposition and evaporation of the liquid inside the surroundings. This in turn leads to a sudden increase in volume inside the transformer tanks, as this also creates an increase in the tank pressure. This pressure must be relieved before a potential rupture of the tank occurs by releasing pressure from the PRDs [32].
- ***Discoloration of transformer liquid:*** the heat factor that affects the cooling system in the electrical transformer due to its active parts, it is exposed to a group of malfunctions such as moisture in solid insulation, ageing of insulation, moisture, contamination of insulation fluids, and partial discharges. The partial discharge analysis method, power factor/dissipation factor measurement procedure and Partial discharge localization process are undoubtedly the most sensitive means used for detecting malfunctions affecting the isolation system in the power transformer [33].
- ***Leakage of transformer liquid:*** Transformer longevity and wear are two of the main common culprits of leakage in transformers. There are some other causative factors such as the improper assembly of mechanical parts, improper filters, poor joints, improper finishing of surfaces, defects in the material used, or insufficient tightness of mechanical parts [34].
- ***Moisture condensation:*** Moisture condensation is one of the most important enemies of the transformer, and this is because of its negative effects and consequences on the role and life of transformers, especially in the type of open transformers or transformers that are aged and have cracked septa or oil leakage gaskets [35].
- ***Transformer switching Equipment troubles:*** Power transformers are equipped with relays for protection, such as tap chargers. Among the main reasons that hinder the work of such equipment’s are contact corrosion and moisture is also a permanent enemy for them, and this impedes in some way the work of these parts as required such as weak contacts or delays when opening or closing between contacts [36].

1.8. Winding deformations of power transformer

The mechanical integrity of a power transformer is one of the highlighted aspects indicating the health of the power transformer. It serves as is the lifeline of its. The most common power transformer winding faults, which are detected through routine maintenance are short-circuits between windings or between turns, strand-to-strand short-circuits, open circuits in parallel strands, short-circuit to ground, mechanical deformation, and contact problems, open circuits [37,38]. The High electromagnetic forces resulting from a very high current is the main cause damage to the winding in power transformer. Since the force can also be proportional to the square of the winding current, this force is studied on two separate components rather than the total force. The first one is the radial force which, generated by the axial component of the leakage flow, and the reverse is true for the axial force is generated by the radial component of the leakage flow. When a current-carrying conductor is located within a magnetic field, a force is created and applied on the conductor. The magnitude of this force, F, is given by equation (1). Here, B is the flux density vector (T), I is the current intensity vector (A), and L is the conductor length (m). The equation shows that the electromagnetic forces experienced by the winding are proportional to the winding current and the flux density. In addition, the force can also be proportional to the square of the winding current, since the leakage field can be expressed in terms of winding current.

$$F = LI \times B \qquad (1)$$

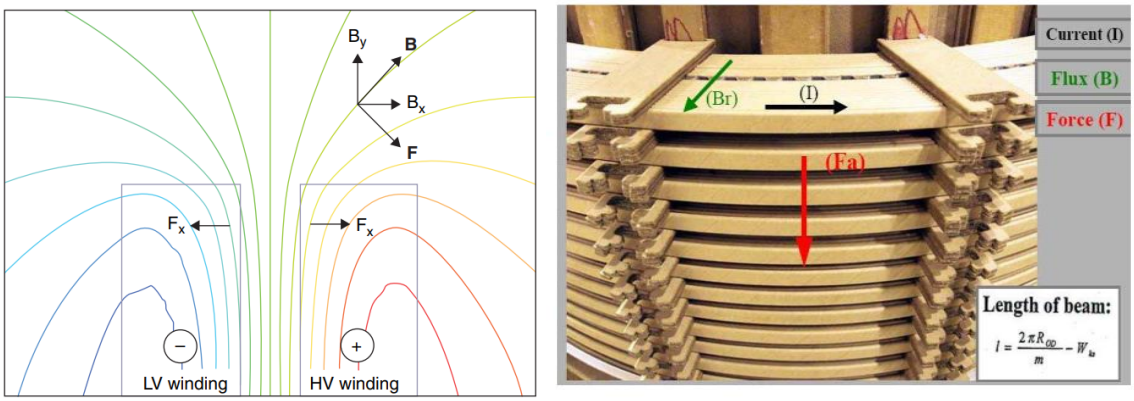


Figure 1.14: Flux lines and force directions on HV and LV windings.

The force direction can easily be determined via Fleming's left-hand rule. As shown in Figure 1, the force direction is always perpendicular to the flux direction. While still referring to Figure 1, the leakage flux density is composed of two components the radial component Bx and the axial component By. Therefore, based on the left-hand rule, Bx creates an axial component force F_y and B_y creates a radial component force F_x. With this understanding, the radial forces

as shown in figure1.11 demonstrate that the internal winding (LV) is constantly being pushed inward (compressive stress) while the external winding (HV) is being pushed outward (tensile stress). Damages due to forces can normally be restricted by appropriate pre-loading of a transformer winding during the assembly process. Very often, the windings are preloaded to a pressure value a minimum of five times the calculated axial short-circuit force. Nevertheless, the pre-loaded clamping pressure decreases gradually throughout a transformer's lifetime. This is mainly due to the cellulose insulation material, which reduces in terms of thickness and elasticity from the effects of moisture, temperature, and ageing. If the clamping pressure decreases to a level which short-circuit forces can overcome, this may cause damage to the winding. The axial and radial components of the forces can cause various forms of structural damage on a transformer winding, which is commonly referred to as the failure mode [27,28].

1.8.1. Axial Electromagnetic force

Axial forces may trigger different failure modes, according to the mechanisms, that will be explained in detail in the following sections. When the axial strength of the winding is insufficient to cope with the axial components of the electromagnetic forces, axial displacement will occur. The AD considered here is in its infancy and so can be assumed confined to a small portion of the winding, which expresses it with δ. figure 1.15 illustrates a single, isolated transformer winding involving six disks, before and after the occurrence of an AD. in power transformer winding, axial displacement can occur in four forms to name of few, and each of them has varying effects on winding parameters, viz, L and C. AD is considered in this example represented as an increase or decrease in axial spacing in between two disks, as illustrated depicted in figure 1.15. To facilitate the study and application of theory among the rules assumed when conducting the experiments was that the spacing between the disks on either side of the AD remained essentially unaffected. Also, AD may practically be present in several other spaces between the disks, but its effects are considered to be minimal. In other words, the mechanistic effect of AD is localized. This simplification reduces the complexity of the model and makes the analytical approach possible. [29]

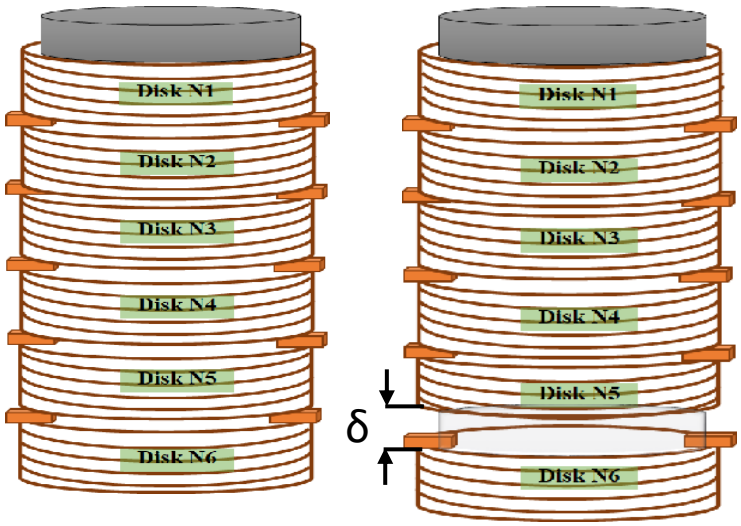


Figure 1.15: Illustrative diagram before and after the occurrence of an axial displacement.

1.8.2. Inter-turn Fault

Inter-turn fault in the windings is one of the internal faults that was studied by several researchers in the last decades [39,40,41]. Changes in the transfer function(V2/V1in) will reveal a wide range of these failure modes. The changes that occur in the frequency response consist of decreasing and increasing magnitudes (in dB) at the level of different resonances (maximum) and entire resonances (minimum) reflect the changes that occur in the winding characteristics, in other words, the changes that occur on the winding parameters.

1.9. Most common routine transformer testing

The aging of the electrical equipment and external factors are one of the reasons for the deterioration of the equipment, and this process may begin as soon as the equipment is installed. maintain the efficiency of equipment operation, and guarantee continuity of service, a maintenance plan must be in place. The foundation of this plan is information, this information can only be obtained from tests. Hence, the importance of tests and their role in maintaining equipment becomes clear. Routine tests and organized programs for maintenance are a way out of failures that impede the life of the equipment and that extend the life of the device. In addition, the cost of repairs is lower, equipment downtime is reduced, and employee and property safety are improved. The alternating current voltage test is better than the direct current voltage in transformer test because it simulates the internal pressure of the device, which it is exposed to during service. However, it does not mean that direct current voltage can be used in

some tests. The following are the most important tests that are routinely performed in the field on the transformer:

IR test: The transformer insulation resistance test is important to determine the insulation resistance between the windings and the ground and between the windings themselves [42,43].

AC or DC hi-pot test (optional): The hi-pot test is a non-destructive, or dielectric voltage withstand (DWV) test used to ensure the insulator's ability to withstand the specified voltage or transient overvoltage during service. Hi-pot tests are useful for finding false or broken insulation in transformers. They are often performed before a transformer enters service [44,45].

Capacitance and power factor or dissipation factor measurement: The importance of this test is that it gives a clear indication of the extent of energy loss through the insulation, by measuring the angle between the voltage and the current passing through the insulation. $\tan\delta$ is defined as the dissipation factor approximately equal to the power factor. Its value practically ranges from 0-0.08, if the insulation system of power transformers or bushings is lower the loss will be larger, and then the $\tan\delta$ will be a higher value [46].

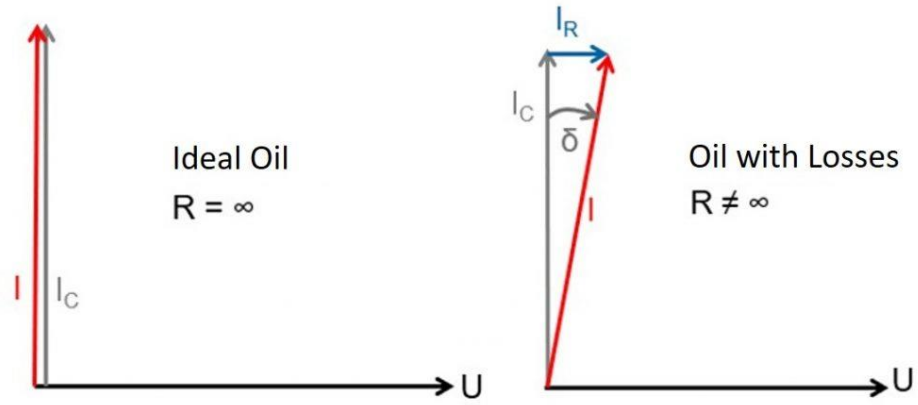


Figure 1.16: Dissipation factor (tan delta) / power factor of insulating oils.

Transformer turns ratio (TTR) measurement: The TTR test is used to detect the presence of open circuits and shorted turns in one winding. This test is performed only in the case of the transformer being out of service. TTR measurements can also be triggered by a tripped relay and other diagnostic tests like power factor measurements. ANSI specifications specify the maximum limit between the measured value and the value written on the nameplate that is not to exceed 0.5%. To find out the test result is used the following relationship [26].

$$\frac{measured\ value - rated\ value}{rated\ value} \times 100 \leq \mp 0.5\% \qquad (2)$$

Polarity test: This test is pivotal, especially when connecting two transformers in parallel, where the polarity can be obtained using the same instrument that measures the TTR. The test can be performed in a simple way as shown in the following figure 1.17.

A low voltage is connected to the primary winding and the values of the three voltages are read respectively as V1, V2, and V3. When the value of the first voltage V1 and the second V2 is reached, the TTR can be calculated, then we see if it is (V1-V2) = V3, this means that the dot on the drawing is intact, meaning that the voltage rises from A2 to A1 in the primary winding, and this will lead to a rise in the voltage of a 2 relative to a1 in the secondary, meaning that it is additive polarity [].

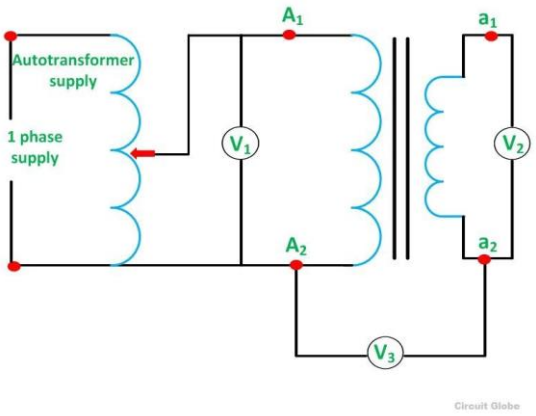


Figure 1.17: Polarity test diagram.

Excitation current test: exciting field current testing has been an old task born with the presence of the transformer in the system network. it is performed to assess t the following transformer failure modes [47]:

- detection if excite an insulator breakdown in the turn-to-turn, interwinding, and/or winding-to-ground insulation.
- Core Defects, the physical movement of the core laminations and severe damage to the core can influence the reluctance and, thus, will result in a change in the exciting current.
- Tap-Changer Component Faults
- Severe Discontinuities, Poor Connections, and/or Open-Circuits

Transformer oil tests: Transformer Oil tests are also among the important tests, and they are in the routine tests section, to detect any failure in the oil at an early stage. the wrong process in taking the oil from the transformer will inevitably affect the test results that are being conducted in the laboratory. two types of oils in the transformer excite, the first type is called Askarels, which is less common, and in the event that there are water bubbles in the oil, it floats on top of the oil, where the density of water is less than the density of oil in this case. In this part of the process, the oil is taken from the top of the transformer. The second type of transformer oil, which is the most widespread around the world, which was mineral oil, whose density is less than the density of water, as it floats above the water, for this reason, The samples are taken from the bottom as shown in the figure 1.18 [48,49].



Figure 1.18: The process of how to take a sample of power electrical transformer oil.

1. ***Insulating fluid dielectric tests:*** This test aims to examine the oil tolerance for high voltages. The process of this test is as follows. A sample of the oil is taken and placed inside a measuring cup between the two electrodes located inside the test device, as shown in figure 1.19. When the movement of the oil in the container is stationary, a voltage is applied to the two electrodes. The process applies a gradual voltage, at a rate of 2 to 5 KV/s. The voltage continues to rise until the insulation collapses. Then the electrical circuit is automatically separated and the so-called breakdown voltage is recorded. The test is repeated five times, with the oil changed each time, and between periods from 10 to 15 minutes, between one examination and another, then we calculate the average value of the measured values. For voltage 11 at less than 30 by 2.5 mm, the results are considered satisfactory. For voltage 66, the result is satisfactory if its dielectric strength does not break it in the test device at less than 50 by 2.5 mm. In the

case that it is lower than that, this is evidence of the presence of impurities, moisture in the oil, or acids, and there is no need for an expensive chemical examination [50, 17].



Figure 1.19: Oil insulation test device.

2. ***Dissolved gas analysis (DGA) tests:*** one of the most important tests that can be determined through it is the condition of transformer oil, which is known as DGA. Through it, it is possible to detect many phases whose effect appears directly on the state of the oil. For example, through this examination, it is possible to know whether or not an internal spark has occurred, the fact that there is a bad contact, the presence of a hot spot, or the occurrence of partial discharge or limits of excessive heat from the contacts. The quality of the oil tells the quality of the transformer in general [51,52].

Polarization recovery voltage test: The presence of water in each of the solid or insulating part is harmful to the life of the transformer. As it reduces both the life of the winding and the insulating paper, and thus reduces the life of the transformer. To detect the presence of moisture we use a robust method which is the RVM method, the voltmeter determines the recovery voltage (RV) after charging the insulation with a DC voltage. Through subsequent relaxation and repeated charging for different times, a so-called polarization spectrum can be generated. The RV range provides an indication of the state in which transformer insulation is present [53].

Transformer core ground test: The transformer core ground test or the core frame tank test. It is among the routine and important tests. It is performed when the transformer is first installed at the side or removed from one location to another or if a problem is indicated by a dissolved

gas analysis (DGA). The following table show the acceptable result values of transformer core ground test and possible recommendation based on the test results [54].

Value of Core Ground Resistance (R in MΩ)	Recommandation
R > 200	**Acceptable.**
100 ≤ R ≤ 200	**Probable Core Ground, Additional investigation advised.**
10 < R < 100	**Definite additional Core Ground. Timely intervention is required.**
0 ≤ R ≤ 10	**Severe core-ground issue. Immediate intervention is required.**

Table 1.1 Value of Core Ground Resistance according to the Standards.

DC winding resistance: This test is sometimes resorted to ensure the presence or absence of loose connections, loss connection on bushings or on the tap changer, because these loose connections create high contact resistance, and this test confirms or denies the existence of this defect, especially if it is proven through the DGA that there is etherine, ethane, or methane gas, then this test is like confirmation. Coil and measure the current as shown in figure1.20 then divide the voltage by the current to calculate the resistance [55].

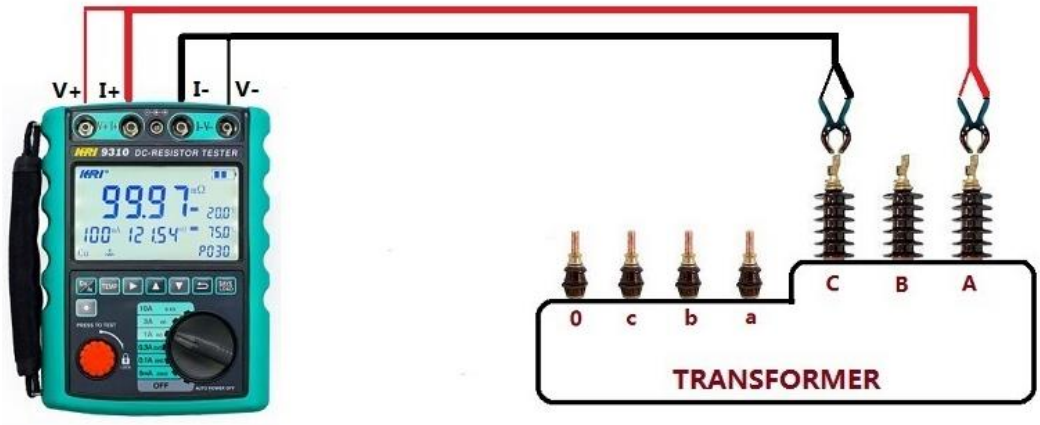


Figure 1.20: Resistance DC measurement test for windings in the first and third transformers.

Induced potential test (optional): In this case, feeding the primary winding with high voltage, while the secondary is open, then put the high voltage on the low one to test the turn-to-turn isolation quality. In order to ensure that saturation of the core does not occur during the test due to the high excitation, we use a higher frequency than normal, usually 200 Hz. The importance

of this test is due to the fact that the transformer in working condition may be exposed to a cut in one of the electrical supply lines, and this leads to the occurrence of an effect resonant phenomenon, which causes the appearance of high voltage waves with a high frequency that may destroy the transformer if there is a weakness in the insulation, hence the importance of this test [25,17]. This test is pivotal in detecting air gaps between the spires, which are detected by the high-voltage. the presence of insulators, which leads to sparking in the air-gap area, leads to a high current in the test devices, and in this case, we consider the transformer to have failed to pass the test.

1.10. The sweep frequency response analysis

The sweep frequency response analysis test is a nonintrusive way used to identify even minor mechanical or electrical changes inside a power transformer. it is extremely sensitive to any changes in the transformer even to the insulation temperature. changes in the internal configuration produce different frequency responses that indicate a range of failure modes [16]. The quintessence of this way is avoiding the process remove the winding from the core. Which keeps the insulator (paper and oil) from moisture. FRA is widely recognized as the best tool, which measures the transfer function response of a transformer winding electrically over a wide frequency range. The input of winding is injected with low voltage, which, symbolizes it by V_{input}. To be measured exit voltage at the other end, that designated by V_{ouput}. The process is repeated for various frequencies in a predetermined frequency range. This range is typically from 20 Hz to 2 MHz as suggested in the IEC standard [56]. It is easier to understand and give more information about any change that occurs within the active parts of the electrical power transformer, by synthesizing and analyzing the magnitude plot. However, throughout the measure of two frequency responses, the expert can judge the correctness of the transformer winding. The first response is obtained while the transformer is devoid of all defects, such as during the commissioning process or at the factory before shipping. The second measurement depends on some requirements, which could be one of the following demandingness for acceptance tests, during commissioning, relocation of the transformer, after a fault, routine inspection, and asset management tool [57,58]. This method allows us to detect and know the severity of the majority of mechanical or electrical damage to the power transformer.

Typical internal mechanical problems identify ed in transformers with FRA are: • Core movement • Winding deformation and displacement • Faulty core grounds • Partial winding

collapse • Hoop buckling • Broken or loosened clamping structures • Shorted turns and open windings.

1.10.1. The method for FRA Test Connections

To detect mechanical faults, Short-circuits between windings or between turns and Open circuits in parallel strands in winding. Or some faults, like the Floating core ground in the core, Open circuit, shorted turns, or high resistance connections in the OLTC preventative autotransformer. The FRA method has become one of the most reliable methods since was introduced by the IEC 60076-18 standard to identify mechanical or electrical faults in power transformers [59]. There are four different methods used to measure the FRA method, below we discuss these available test configurations.

a. The end-to-end open-circuit test: This type of connection is used in the case of FRA measuring one winding, in the primary winding or the second. This concept is performed in type delta-connections windings or signal winding. Where it is connected as follows:

- feeds the entrance of the winding with the signal, while the output signal is measured from the other end of the same winding.
- The secondary winding of the same phase must be left open or moved during the measurement.
- All unmetered windings, including windings from phases, must be left in an open circuit.

Figure 1.21 shows how this test can be connected, which is one of the accepted tests, or when needed. from the salient features of this type of connection six measurements are required to test all HV and LV windings of a two-winding three-phase transformer [60,61].

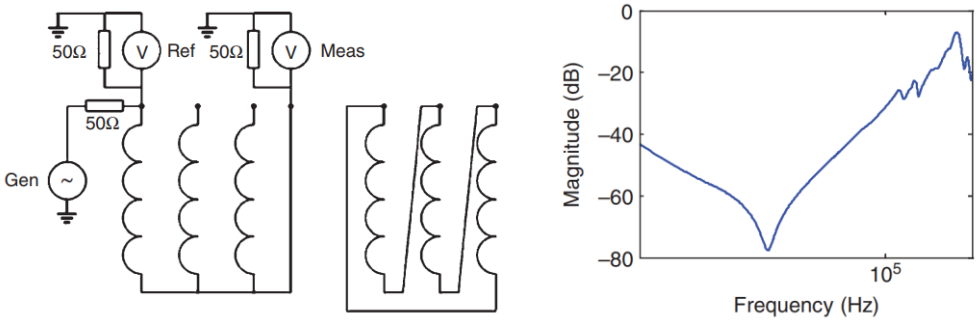


Figure 1.21: The end-to-end open-circuit test.

b. the open-circuit test: The fundamental difference between this type of connection and the previous connection is the two terminals of the secondary winding are connected together for the short-circuit test as presented in figure 1.22. The complementing strength of this connection is that it removes the effect of magnetizing induction from the response, unlike the first connection, where the effect of magnetizing is strongly anti-resonance. In general, it is sufficient to distinguish whether the damage is in the core or elsewhere [59].

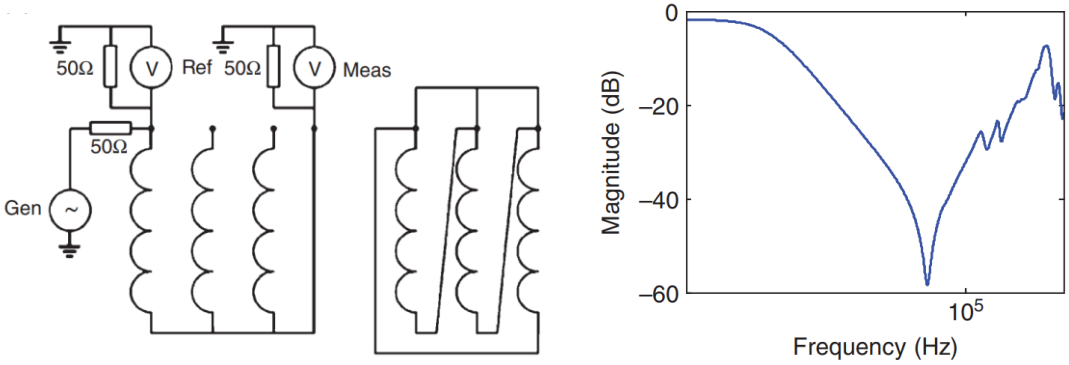


Figure 1.22: The open-circuit test.

c. The capacitive inter-winding test: The process of this connection is performed as follows: the first winding is fed, and recovery of the exit signal is from the second winding. For the rest of the phases, it is left floating. The characteristic of this type of connection is that in the low frequency, the effect of the capacitance between the two windings is directly observed on the measurement, as shown in figure 1. 23. Where in this case the impedance is very large, the plot of magnitude starts at low value. However, the capacitive inter-winding test has a high sensitivity to radial deformation of a winding [61].

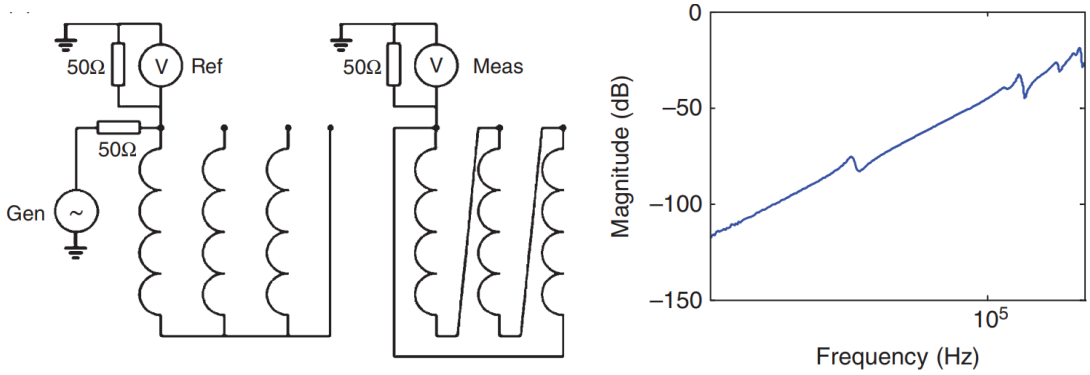


Figure 1. 23: Method of the capacitive inter-winding test.

d. the inductive inter-winding test: This type of connection is similar to the previous one, where the point of disagreement lies between them is the open terminals of the primary and secondary

measured windings are connected to ground. to avoid undesirable effects on the measurement, make the rest of the other phases floating. This configuration of the test is performed in the detection of some faults such as to determine the winding turns ratio from its low-frequency response. Also, as a complementary test for the main turns ratio test (TTR). Where the figure below shows the connection method and the measurement scheme in this type of configuration.

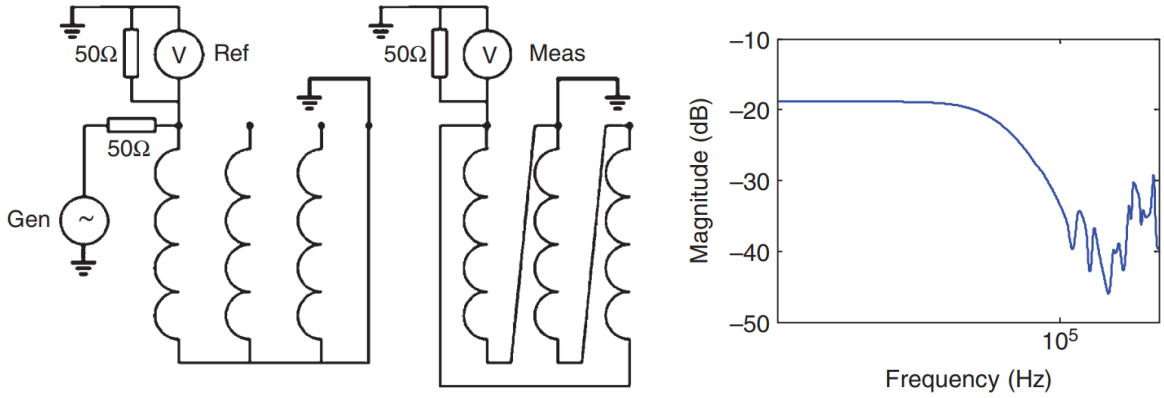


Figure 1.24: Method of the inductive inter-winding test.

1.11. Conclusion

Power transformers are considered the least vulnerable equipment to breakdowns or collapses due to the fact that they are designed to hold out against transient faults. Also, since it does not contain moving parts. However, Power transformer can fail from any combination of electrical, mechanical, or thermal factors. In the introduction to this chapter begins with a brief discussion of the main and active parts of the power transformers and their characteristics. Then, the chapter continues with the background of the most famous types of power transformer windings, where it is divided into interleave windings: where the conductors are a tape with a rectangular or square section. The windings are formed in the form of a pancake, this type of winding allows the transfer of heat from the conductors to the cooling medium, and thus we overcome the excess heat in the transformers. the second type is concentric winding: the most famous of them as mentioned in this chapter where, spiral, crossover, helical and continuous type. Afterward, in this chapter, it has been discussed the main cause of physical damage to power transformers. Mechanical pressures, mechanical failures, or mechanical damages are terms for abnormal states that affect electrical transformers windings during their life, in which occur disturbance or weakness in the active parts. Finally, this chapter presents several popular methods available for detecting defects of power transformer, as each component has a method used to detect its own faults. FRA is a fashionable way most well-known recently, and most widely currently used fulfil to achieve the required. In recent decades, the invention of the power-sensitive method FRA made possible to early detection of mechanical deformations windings of the power transformer. The success of this method of detecting minor mechanical defects has clear foundations. the early detection of these faults also leads to a significant reduction in the financial effects of it: not only are the maintenance costs in its early stages much lower than its other stages, but it also enables it to avoid falling into a breakdown.

Tests generally must be carried out according to specific specifications, as they must be standard, and if they are conducted in any country, they are done in the same way. To ensure that the FRA test is standardized, in the subsequent chapter, FRA test methods connections are standardized according to connection technique, based on IEC 60076-18.

Chapter 2: State-Space Equations of The Equivalent Lumped Model for Transformer Winding.

Chapter 2: *state-space equations of the equivalent lumped model for transformer winding.*

2.1. Introduction

The modelling of power transformers is a task nearly as old as transformer manufacturing. Establishing a reliable methodology to develop an electric equivalent circuit model that can yield to be used for diagnostic mechanical deformation is the issue in this chapter [63,64].

In this chapter our aim is to explore tow complementary power tools state-space equations and transfer-function matrices for analysis and synthesis deeply transformer behavior during transient faults. Frequency Response Analysis (FRA) is a suitable tool used for modelling power transformer is recommended. It is essential to determine the new FRA fingerprint to be as close as possible to the original fingerprint of the FRA trend of the real power transformer. This chapter proposes automation constructing the equivalent model of the transformer winding, which considers the winding structure, shunt and series capacitances and all mutual inductances. estimation details of the model's parameters are presented [65]. This model as mentioned before reflects the internal physical structure of the power transformer and allows studying the impacts of various winding deformations on the FRA response. The objectives of this chapter can be listed as follows:

- Determine the parameters of the model with high precision using analytical simplifications to reduce their search spaces. This approach has been accessed by the MATLAB program and is updated in the last chapter and made more practical using the LabVIEW program.
- One of the main advantages of using the state space model is to achieve accurate fault detection and access to its severity.

The novel self-synthesis method is proposed to construct the mutually coupled equivalent circuit of an insulated air-core transformer winding based on the signal morphology interpretation of the measured frequency response only [66,67]. This approach aims to determine the parameters of the model from the frequency sub-bands, each of which reflects its dominant parameters, where the parameter identification procedure is carried out from their corresponding sub-band separately. This approach is based on one of the modern optimization algorithms.

2.2. The simplified meaning of optimization

Optimization is a powerful skill that can use to find the best solution among a set of feasible solutions for complex and multidisciplinary problems in various domains. In mathematical terms definition, it deals with the problem of minimizing or maximizing a function with several variables subject to some constraints [68,69]. optimization plays a central role in operation research management science, and engineering. To clarify the meaning of optimization in a larger sense, we use the following example. Let there be two points A and B, if someone wants to move from A to B, for this person has several solutions that he can use to get from point A to point B, either by walking as a means, by using a bicycle, or by car, and he also has two means. Others are the train and the plane.

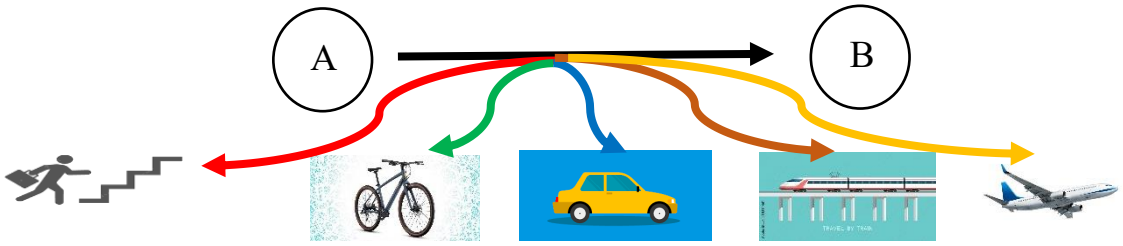


Figure 2.1: Example of the possible solutions to the optimization problems.

All of these solutions are considered possible for this person to move from point A to point B.

If it is taken into account the time required as the objective function in the process of moving from point A to B. Where the moving by walking costs 250 hours, moving by bicycle costs 105 hours, for example, while moving by car, by train, and by plane costs 17, 20, and 2 hours respectively. the constraint set in this process is the arrival time which selects as 25 hours. We find that the first two solutions walking and cycling are not possible (infeasible solution), while the rest of the solutions are considered possible solutions (feasible solution). If we set another objective function, which is to minimize cost, where the process of moving from A to B by car, by train, and by plane costs respectively, $150, $50, and $350, we find that the best solution is the train.

Classical optimization techniques: these methods assume that the function is differentiable twice with respect to the design variables and that derivatives are continuous [70].

heuristic algorithms are algorithms developed to solve a specific problem without the possibility of generalization or application to other similar problems. It is also called a problem-dependent technique. heuristics are rules that can be developed based on past experiences. heuristics aren't about making the perfect decision or judgment, just about making one quickly [71].

The heuristic is divided into three essential sections:

Greedy approach: is the simplest and most straightforward approach. It is not an algorithm, but it is a technique. The main function of this approach is that the decision is taken on the basis of the currently available information [72]. whatever the current information is present, the decision is made without worrying about the effect of the current decision in the future. In order to provide a clearer and more accurate explanation, we consider the following example in figure

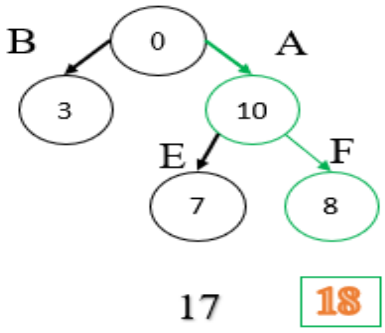


Figure 2.2: The method to get optimal solution in greedy approach.

The algorithm has two paths, you can choose one of them while the objective function is the maximization. the algorithm selects A, where the value is 10, after selecting A other options appear. the same things at the first step the algorithm selects F so the result is 18. On the other hand, if the problem was taken in the long term (run), the optimization algorithm took B and C, and the result would be 53, which is the best solution from the first path A or F. This is one of the drawbacks of the greedy algorithm, as it does not search for the global solution, but instead takes the solution found, meaning it may fall into the local solution, as illustrated in figure below.

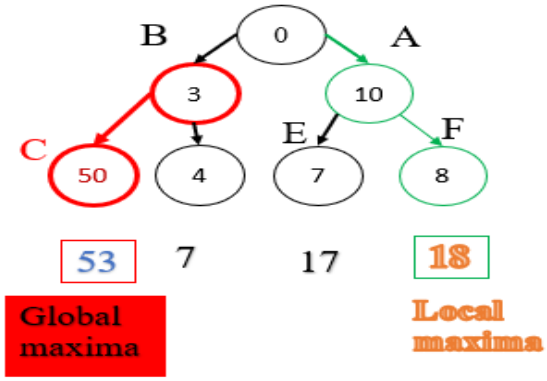


Figure 2.3: The method to get global solution in greedy approach.

Brute force approach: A brute force approach is an approach that finds all the possible solutions to find a satisfactory solution to a given problem. The brute force algorithm tries out all the possibilities till a satisfactory solution is not found [73].

In the case of a small problem like the previous example, the global situation is obtained easier, and this method is better and more effective, but in contrast, for example, to find a password consisting of four numbers, the algorithm tries each number ten times, which the algorithm must do 10,000 operations and is a method considered ineffective.

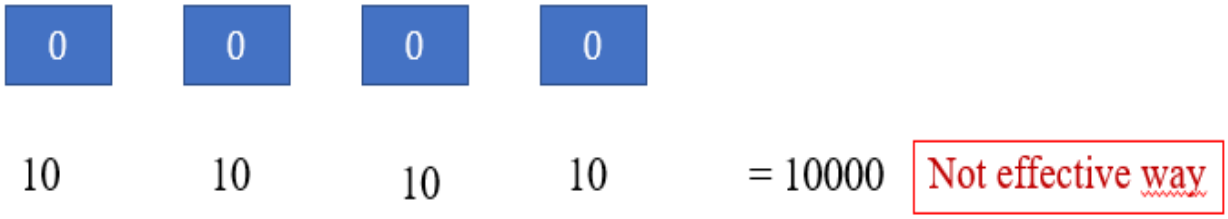
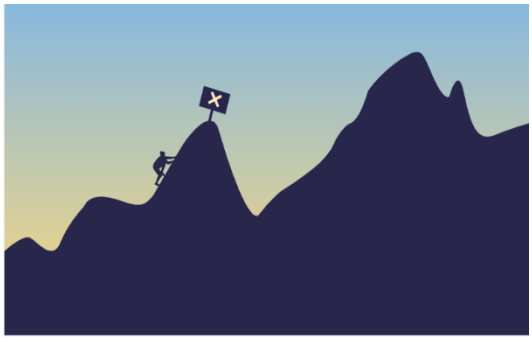


Figure 2.4: Example of brute force approach.

The hill climb algorithm: This algorithm mixes the two previous methods; The hill climb algorithm is a local search algorithm that moves continuously in the direction of increasing elevation/value to find the top of the mountain or the best solution to the problem. It ends when it reaches the peak value as there is no neighbor with a higher value. This algorithm is used to improve



mathematical problems. One widely discussed example of a hill-climbing algorithm is the traveling salesman problem in which we need to minimize the distance traveled by the salesman [73].

algorithm:

- generation possible solution
- if the new solution is better than **old solution**

yes ⟶ best solution = new solution

no ⟶ best solution = old solution

Figure 2.5: The hill climb algorithm.

- Go to 1

2.3. Particle swarm optimization used for determine equivalent model

Before delving into the definition of the swarm intelligence algorithm, a swift brief presentation of the main feature of the SI system. The self-organization on which this system is built is its main feature, in which the components of an initially perturbed system interact locally to produce a global coordination or order [86]. Particle swarm optimization (PSO) algorithm is a stochastic optimization technique based on swarm, which was proposed by Eberhart and Kennedy (1995) and Kennedy and Eberhart (1995) [74]. PSO is swarm intelligence inspired by the nature of social behavior and dynamic movement with communications of insects, birds and fish. A swarm has been moved to a specific search space to search for the best solution, where each element in this swarm flies according to its own flying experience, taking into account the flying experience of the swarm.

2.3.1. Standard PSO Structure

To explain the basic idea on which the swarm intelligence algorithm is based, let a swarm of birds spread in a specific area for the purpose of searching for food, and food spread in this area randomly, in addition, the birds do not know the food locations clearly, so what is the best way to search for food? [75].

The ideal method is to spread out all the birds in an area, with the birds communicating with each other every time where the food is. Each particles start their trip in searching for best solution from random search space, and with each replay the particles get closer to the most accurate and optimal solution. Each particle within the algorithm is called a particle, and each

element has an appropriate value, and this value indicates the suitability of solving this particle compared to the rest of the particles. The best fit value recorded by the particle and symbolized by pbest. it in addition to the best fit value recorded within the swarm gbest, and finally the value of the best local positioning of a particle compared to the locally neighboring particles lbest. The particle optimization algorithm can be described mathematically as follows, let the size of the swarm be N, any possible solution named i in the search space [a b]. where each particle is assumed that have two characteristics: a position vector xi in D dimensional, a velocity vector symbolized by Vi. each particle keeps track individual's optimal position named Pi, and global best gbest.

By specifying the values of each particle, the velocity and position of each particle are changed in each iteration using the following two equations [75,76]:

$$V_{i,t+1}^{d}=\theta * V_{i,t}^{d} + c_1 r_1 * rand * (p_{i,t}^{d} - x_{i,t}^{d}) + c_2 r_2 * rand * (p_{g,t}^{d} - x_{i,t}^{d}) \quad (1)$$

$$x_{i,t+1}^{d}= x_{i,t}^{d} + V_{i,t+1}^{d} \quad (2)$$

Where, inertia weight θ it's a proportional agent that is related with the speed of last improvement, the value of θ is assumed to vary linearly from 0.9 to 0.4. $c_1$and c_2 are the cognitive (individual) and social distributed random numbers in the range 0 and 1.

The algorithm can be summarized into three main steps:

- Calculating the optimal value for each particle and the overall optimal value.
- Determine the optimal values.
- Update the velocity and topic for each item.

In the figure below is the structural diagram of the algorithm:

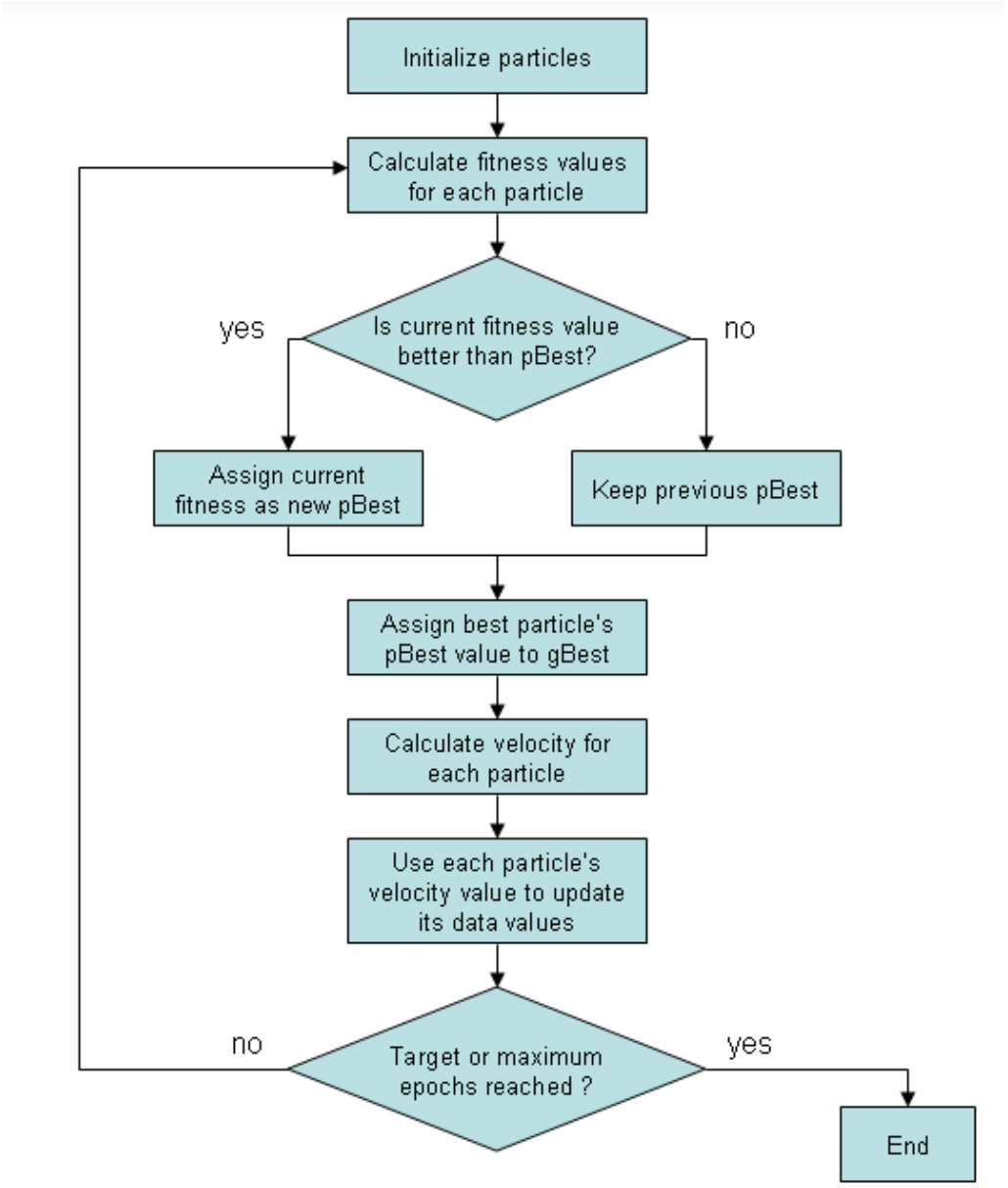


Figure 2.6: Framework of the IDE-PSO algorithm.

Optimization algorithms are a reliable tool and one of the basic elements in building a model of an electrical power transformer. Optimization algorithms help in performing various operations such as searching and sorting winding information values, for example, inductance matrices and capacitances matrices. Algorithms allow improved access to accurate parameter values and help save time and effort in arriving at the ideal winding model. In this chapter, the particle swarm optimization algorithm was used to optimize the winding parameters of the equivalent circuit: self-inductance, mutual inductance, series capacitance, and ground capacitance.

2.4. Equivalent model of an isolated electrical transformer winding

The testing idea of the frequency response analysis for a power transformer is based mainly on considering the transformer as a large group of RLC circuits. Therefore, determining all winding parameters is very crucial. Accordingly, if a signal is injected with a small voltage in the 1 volt, with a wide range of frequencies from 20 Hz to 2 MHz, each Waveform transformer will be different from other transformers, even if the transformers have the same voltage and capacity, and they also have the same directional group, it is radically different in terms of fingerprint or, in other words, in terms of winding parameters.

Providing a new iterative approach to ensure the synthesis of a mutually coupled equivalent power transformer winding model is the main objective of this chapter. This approach aims to determine the parameters of the model from the frequency sub-bands, each reflecting its dominant parameters, where the parameter identification procedure is performed from their corresponding sub-band separately [66,].

2.5. Identification of model parameters by the FRA-SMI method

The proposed of this method is mainly based on the subdivision of the FRA signal into three frequency sub-bands (low, medium and high frequency); each sub-band contains dominant parameters [78,144] which reflect on the behaviour of the winding response. First, in the Low-Frequency Response (LFR) range, the inductance effect is dominant, where resistance and inductances can be determined. Second, in the Medium Frequency Response MFR range, the effect is dual (inductive and capacitive), causing resonance and antiresonance frequencies, where the initial number of sections is inferred from the number of resonance frequencies detected in this sub-band. Finally, in the high-frequency response range (High-Frequency Response HFR), the capacitive effect is predominant; from the analytical relationships, the capabilities of the equivalent model are determined. In addition, to ensure an appropriate synthesis of the adopted model, analytical simplifications have been made to restrict the limits of the parameter search space [80]. The FRA-SMI method proposed by Abdel-Razzak Amara is a powerful approach based on the analysis of the morphology of the FRA signal, which is related to the physical components of the transformer (conductor sections, number of turns, insulator, etc.). However, it contains all the technical specifications of the transformer winding, which can be represented by electrical parameters (resistance, inductance, and capacitance). Depending on the approach all model parameters can be accessed with high accuracy only from the FRA input data in the sub-frequency ranges: low, medium and high

frequencies. Careful analysis and interpretation of the FRA signal in these regions can effectively improve the determination accuracy of equivalent model parameters [81,82].

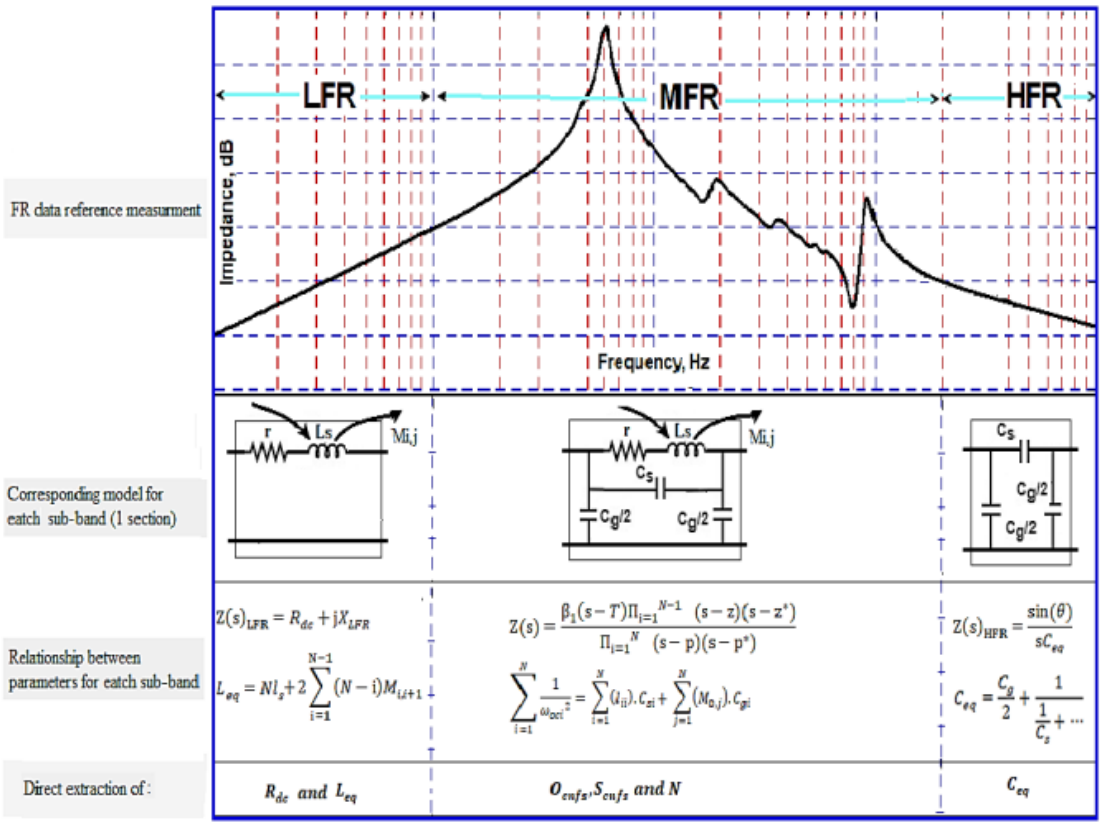


Figure 2.7: Decomposition of the frequency response FRA.

The intrinsic goal of this approach is to automate the determination of equivlant model parameters found in each frequency zone in previous figure.

- In the LFR region, at lower frequencies, the capacitive lattice behaves as a purely open lattice. Hence, current flows only through the series path which contains resistance and inductance. The effect is purely inductive, and the eigenvector and mutual inductances are the dominant parameters.
- In the MFR frequency region, the effect is dual inductive and capacitive, affected by series (Cs) capacitors, (Cg) and inductors.
- In the HFR frequency region, at higher frequencies, the inductive network behaves as a purely open network and current flows through the capacitive elements in the circuit. The effect is purely capacitive, affected by the global capacitance (Ceq) generated by the two dominant parameters of capacitance Cs and Cg.

Raghavan et al. [77] showed that an equivalent circuit of sections can be represented by a transfer function given by equation (6). The mathematical expressions for each subdomain are defined in the next section.

2.5.1. Low frequency response (LFR sub-band)

As mentioned, the equivalent circuit of isolated winding can be modelled by resistances, self-inductances and mutual inductances, for the current tends to flow only through the series path containing resistance and inductance [77].

At low frequencies, the impedance can be written as follow:

$$\lim_{s\to 0} Z(s) = R_{dc} + sL_{eq} \quad (1)$$

The impedance $Z(f)_{LFR} = R_{dc} + jX(f)_{LFR}$ (2)

As the Reactance ban be as $X(f)_{LFR} = 2\pi f L_{eq}$ (3)

The equivalent inductance can also be expressed as,

$$L_{eq} = Nl_s + 2\sum_{i=1}^{N-1}(N-i)M_{i,i+1} \cong l_s\left[N + 2\sum_{i=1}^{N-1}(N-i)\lambda^i\right] \quad (4)$$

With $M_{1,i+1} \cong l_s\lambda^i$ according to reference [87]

where, R_{dc} is the Resistance, L_{eq} is the equivalent inductance, l_s is the self- inductance, $M_{1,i+1}$is the mutual inductance, N number sections and λ Coefficient of mutual inductances, between 0 and 1.

For self-induction and mutual induction, the magnetic coupling between individual sections decreases when the separation distance between them increases [93]. It is therefore logical to consider that both self and co-inductance satisfy the following constraints:

$$l_s > M_{12} > M_{13} > M_{14} > M_{15} > M_{16} \quad (5)$$

$$\lambda_{min}^i\, l_s < M_{i,i+1} < \lambda_{max}^i\, l_s$$

With $0 < \lambda_{min} < \lambda < \lambda_{max} < 1$, and $M_{12} = \lambda\, l_s$, $M_{13} = \lambda^2 l_s$, $M_{14} = \lambda^3 l_s$, $M_{15} = \lambda^4 l_s$, $M_{16} = \lambda^5 l_s$.

2.5.2. Mid-frequency response (sub-band MFR)

In the mid-frequency band, the current tends to flow through the parallel path containing serie capacitance and inductance in series with resistance. The interaction between the inductive and capacitive effect induces the resonant and ant resonant frequencies. The development relationship between resonant frequencies and the model parameters (capacitances and inductances), it's can be rewritten as [66]:

$$\sum_1^N \frac{1}{\omega_{oci}^2} = \sum_{i=1}^N l_{ii} C_{si} + \sum_{j=1}^N M_{0j} C_{gj} \quad (6)$$

ω_{oci}^2 is the resonant frequency

l_{ii} is Self-inductance of the i_{th} disk

C_{si} is serie capacity of the i_{th} disk

C_{gj} is shunt capacity of the i_{th} disk

$M_{0j}$is mutual inductance of the i_{th} disk

2.5.3. High frequency response (HFR sub-band)

It has also been confirmed previously, e. At high frequencies, the inductive network behaves as a purely open network and the current flows through the capacitive elements in the circuit. Hence the equivalent circuit of transformer winding consists of only capacitive elements such as C_s and C_g[83]. The driving-point impedance function of an n-section equivalent circuit with its neutral grounded can be expressed as:

$$Z(f)_{HFR} = \frac{\sin\theta}{sC_{eq}} \quad (7)$$

The equivalent capacitance value (C_{eq}) of the ladder network with N sections can be estimated as:

$$C_{eq} = \frac{C_g}{2} + \frac{1}{\frac{1}{C_s} + \frac{1}{c_g + \frac{1}{C_s} + \cdots}} \quad (8)$$

2.6. Estimation of the parameters of the isolated winding using the method by the "FRA-SMI".

The FRA-SMI method was applied on a real winding illustrated in figure 2.7. The synthesis of the mutually coupled circuit begins with the measurement of the frequency response FRA. the FRA-SMI method should identify all tested winding parameters. In order to support and strengthened the approach and prove its validity, have been monitoring a set of experiments on it. to reach the desired signal isolated winding for 06 disks of high voltage primary winding simulated as shown figure 2. 8. Where each disk contains 66 turns. the winding was wound using a copper flat wire with a width of 3mm and a thickness of 0.8 mm. Has been used the LCR meter to measure the winding parameters and the impedance with the following characteristics:

- Frequency range 20Hz -5 MHz
- Measured using 50ohm coaxial cable
- Basic accuracy of 0.1%, with 6-digit resolution.



Figure 2. 8: Conceptual model for the basic elements in the experiment.

2.6.1. Parameters can be measure

model parameters	Recommendations should be made when measuring winding parameters
C_{geff}(pf)	It is assumed that there are three important steps in measuring the ground capacity. First, the neutral must be isolated from the ground, so connect it to the end of the line, then choose a low frequency as the current becomes weak.
C_{eq} (pf)	After the last peak and trough of the impedance, its value is constant throughout the rest of the frequency range and the phase shift approximately 90°. In this range preferred measured the total winding capacity of the winding.
L_{eq} (mH)	The operation of feeding winding by tens of kHz, producing an increase in the eddy current inside the core. The radial flux increases and the axial flux decreases due to the reduction in the mutual couplings between the turns/discs. Therefore, causes a significant decrease in the total inductance. As a result of an increase in the frequency, the core becomes resilient to flux, and the total inductance in this field becomes constant. In this range of frequency that the total inductance is measured.

Table 2.1: Recommendations before measure parameters.

Parameters measurement is one of the effective methods of diagnosing power transformer malfunctions. The inductance is the most affected component in failures such as disk deformation, core deformation, and short circuit winding. and most influencing in the magnitude and frequencies resonances of impedance (FRA).

The second element, which is no less important in determining faults is the ground capacitances, for example, radial displacement and moisture ingress. Table 2. 2 highlights the fields, the frequencies in which the health parameters were measured.

Model Parameters	The frequency range in which the parameters measured

	0khz	1Khz	50khz	2Mhz
C_{geff}(pf)	-	18 .85 -	-	-
C_{eq}(pf)	-	-		33 .11
L_{eq}(mH)	-	-	9 .7204	-
R(ohm)	2 .4	- -	-	

Table 2.2: Parameters measured using LCR meter, each according to its range of frequency in which to measure it.

The strengths of the third element use for health inspection of an electrical transformer is the series capacitance. In cases of radial displacements or axial displacement, the series capacitance has an important role in determining the shape FRA with the induction and the ground capacitance in the field of 20 kHz to 2 Mhz. in general, has been estimated by one of the algorithms or analytical methods. To obtain accurate data and reliable results from which to build the first footprint of the electrical transformer. The bat algorithm was used to estimate the serial capacitance which its value C_s = 6.242 pf.

One of the fundamental and huge data that we rely on in this paper M_{0i}in determining the location of axial and radial displacement. it's tabulated in 3.

M_{00} = 0.701	M_{01} = 2.329	M_{02} = 3.755	M_{03} = 5.534	M_{04} = 7.468	M_{05} = 9.720

Table 2.3: Various M_{0i} that have been estimate.

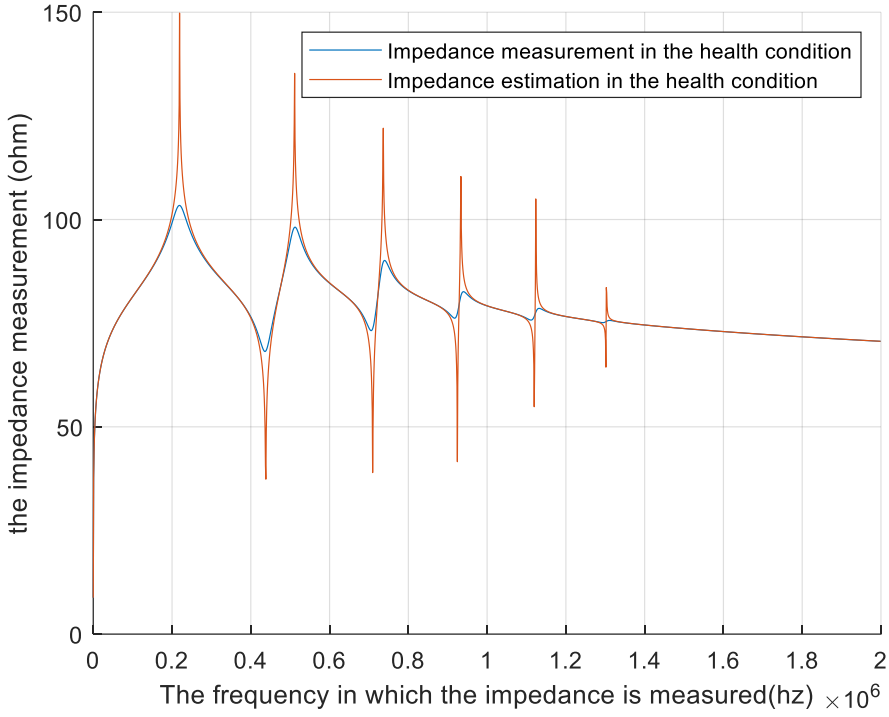


Figure 2.9: The FRA fingerprint corresponding to the healthy winding and the impedance estimation in the health condition.

2.6.2. Inductance matrix estimation

The inductance matrix is n by n matrix, where n = 6 to the number of sections of the ladder network. Calculation of the mutual inductances $M_{i,j}$ (mH) by substituting the value of L_s (mH) and λ into equation (4). The estimated values of the self-inductance and mutual inductances are given in as follows:

L = [0.7014 0.3538 0.1617 0.0913 0.0464 0.0236;
0.3538 0.7014 0.3538 0.1617 0.0913 0.0464;
0.1617 0.3538 0.7014 0.3538 0.1617 0.0913;
0.0913 0.1617 0.3538 0.7014 0.3538 0.1617;
0.0464 0.0913 0.1617 0.3538 0.7014 0.3538;
0.0236 0.0464 0.0913 0.1617 0.3538 0.7014] * 1e-3 mH

R is a diagonal matrix, where r = 0.4 Ω

R = [0.4 0 0 0 0 0;
0 0.4 0 0 0 0;
0 0 0.4 0 0 0;
0 0 0 0.4 0 0;
0 0 0 0 0.4 0;
0 0 0 0 0 0.4];

In the HFR sub-band, equation (8) was used as the objective function, the approximate values of capacitance Cg and Cs are Cg = 1.885e-11 and Cs = 6.2420e-11. Therefore, the capacity

search space can be determined by multiplying and dividing the approximate capacity values by the coefficient n.

2.7. State-space equations of the equivalent lumped model for winding defects simulation

The state variable is the most obvious method that emphasizes to description deeply of the internal structure of the system. In addition, it can provide an explanation of the control variables (input) and the response variables (output) [17], [84]. The distinguishing characteristic of state variables is that the non-zero initial conditions can be combined. In the following, the important steps carried out to construct the model winding dedicated to short-circuit faults in turns are outlined. In this section, we tackle the problem of finding state-space equations associated with of the equivalent lumped model for transformer winding. The solution to this problem, coupled with an ability to solve the state-space equations, means that we can analyze and synthesise transformer winding faults using state-space equations [85].

2.7.1. State-space equation for the coupled ladder network

The lumped mutually coupled model shown in Fig.2 is currently considered to be one of the best reliable tools for diagnosing power transformer winding failures [101], as it has the ability to simulate all physical properties of windings such as; the magnetic couplings between the windings and the disks of a winding, and the electrical coupling between the windings and between the turns, and between the winding and the ground by self and mutual inductances, series capacitances between turns, and shunt capacitances between the winding and the ground respectively. Furthermore, the necessary steps to define state-space equations of the coupled ladder network are described as follow:

- In the first part, Kirchhoff's voltage law or current law is used to analyze the coupled ladder network depicted in Figure 2.10.
- Expression of each current that passes through inductors depending on Kirchhoff's first law. Identify any voltage on both ends of capacitors and inductors approval on Kirchhoff's second law in the coupled ladder network.
- Write the state-space equations describing the system by the derivation of the homogeneous equation, and the output equation with identification of the four systems matrices (A, B, C and D).

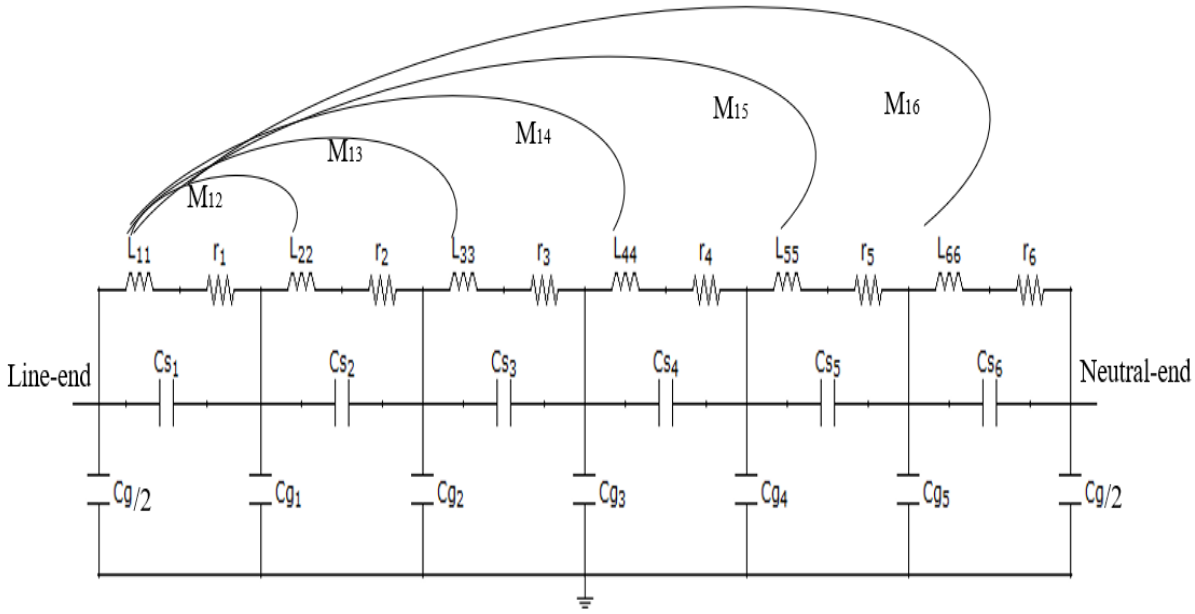


Figure 2.10: The lumped model scheme of transformer winding.

The most format representation of the state-space equations are assigned below.

Sate equation: $\dot{x} = [A]x + [B]u$ (1)

Output equation: $y = [C]x + [D]u$ (2)

Where x- column vector of the state variables;

$\dot{x}$- time derivatives of the state variables;

u- excitation or input vector;

y- response or output vector;

2.7.2. Determination of the percentage of the short-circuited turn's number in each winding disk

The short-circuited turns number in each disk is designated by n_{sc1} for the disc 1, n_{sc2} for the disc 2 and n_{sci} for the disk i. Let n_T be the total number of turns per disk in the case of a healthy isolated transformer winding. The coefficients n_1, n_2 and n_i are the percentage of the short-circuited turns at disks 1, 2 and i respectively of the winding, which are defined as follows:

$n_1 = \frac{n_{sc1}}{n_T}$

$$n_2 = \frac{n_{sc2}}{n_T} \tag{3}$$

$$\vdots \quad \vdots$$

$$n_i = \frac{n_{sci}}{n_T}$$

The coefficients f_i represent the percentage of turns not short-circuited by each disk of the winding. These coefficients defined by:

$$f_1 = 1 - n_1$$
$$f_2 = 1 - n_2 \tag{4}$$
$$\vdots \quad \vdots$$
$$f_i = 1 - n_i$$

The resistances and the self and, mutual inductances of the winding are expressed as a function of their nominal values and of the coefficients f_i , which are given by the following matrices:

$$R = r * \begin{bmatrix} f_1 & 0 & \cdots & 0 \\ 0 & f_2 & \cdots & 0 \\ \vdots & \vdots & \ddots & \vdots \\ 0 & 0 & \cdots & f_i \end{bmatrix} \tag{5}$$

$$L = \begin{bmatrix} f_1^2 l_{11} & f_1 f_2 M_{12} & \cdots & f_1 f_j M_{1j} \\ f_2 f_1 M_{21} & f_2^2 l_{22} & \cdots & f_2 f_j M_{2j} \\ \vdots & \vdots & \ddots & \vdots \\ f_1 f_i M_{i1} & f_i f_2 M_{i2} & \cdots & f_{ij}^2 l_{ij} \end{bmatrix} \tag{6}$$

The K matrix represents the series and shunt capacitances as a function of their nominal values and of the coefficients f_i.

$$K = \begin{bmatrix} \frac{c_s}{f_1} + \frac{c_{g1}}{2} & \frac{-c_s}{f_1} & \cdots & 0 \\ \frac{-c_s}{f_2} & \frac{2c_s}{f_2} + c_{g2} & \cdots & 0 \\ \vdots & \vdots & \ddots & \vdots \\ 0 & 0 & \cdots & \frac{2c_s}{f_i} + c_{gn} \end{bmatrix} \tag{7}$$

Note: The effective shunt capacitance can be defined by the capacitance between winding and ground. However, this capacitance is the equivalent of the capacitances between each turn and the ground. In the event of a short-circuit fault, the shunt capacitance of the short-circuited turns is eliminated and therefore the value of the total effective shunt capacitance changes. However, if a small short circuit fault (e.g., 10%, 20%) is produced on one disk of the winding, this affects the disk capacitance slightly and therefore its influence on the total shunt capacitances is very slight, finally, its effect on the frequency response will be very negligible.

$$\begin{bmatrix} \frac{di_1}{dt} \\ \frac{di_2}{dt} \\ \vdots \\ \frac{di_n}{dt} \end{bmatrix} = [L]^{-1} \begin{bmatrix} v_1 \\ v_2 \\ \vdots \\ v_n \end{bmatrix} \tag{8}$$

were, $[L]^{-1}$ inverse matrix of $[L]$. Since, the voltage across the inductances can be expressed in terms of the nodal voltages, the above gets modified to,

$$\begin{bmatrix} \frac{di_1}{dt} \\ \frac{di_2}{dt} \\ \frac{di_n}{dt} \end{bmatrix} = [L]^{-1} \begin{bmatrix} e_1 - e_2 - i_1 r \\ e_2 - e_3 - i_2 r \\ e_n - i_n r \end{bmatrix} \tag{9}$$

Let $[R]$be a diagonal matrix with its element equal to the sectional value of the resistance 'r'. Expressing the inductor voltages in terms of node voltages and the resistive voltage drops, the above equation gets modified to the following form,

$$\begin{bmatrix} \frac{di_1}{dt} \\ \frac{di_2}{dt} \\ \vdots \\ \frac{di_n}{dt} \end{bmatrix} = [L]^{-1} \begin{bmatrix} e_1 - e_2 \\ e_2 - e_3 \\ \vdots \\ e_n \end{bmatrix} + [L]^{-1} \begin{bmatrix} -i_1 r \\ -i_2 r \\ \vdots \\ -i_n r \end{bmatrix} = [L]^{-1}[T]^t \begin{bmatrix} e_1 \\ e_2 \\ \vdots \\ e_n \end{bmatrix} - [L]^{-1}[R] \begin{bmatrix} i_1 \\ i_2 \\ \vdots \\ i_n \end{bmatrix} \tag{10}$$

$[T]$ matrix has the following form:

$$[T] = \begin{bmatrix} 1 & 0 & \cdots & 0 & 0 \\ -1 & 1 & \cdots & 0 & 0 \\ \vdots & \vdots & \vdots & \vdots & \vdots \\ 0 & 0 & \cdots & -1 & 1 \end{bmatrix} \tag{11}$$

Assigning $[I_e] = - [L]^{-1}[T]^t$ and $[I_i] = - [L]^{-1}[T]$, equation becomes,

$$\begin{bmatrix} \frac{di_1}{dt} \\ \frac{di_2}{dt} \\ \vdots \\ \frac{di_n}{dt} \end{bmatrix} = [I_e] \begin{bmatrix} e_1 \\ e_2 \\ \vdots \\ e_n \end{bmatrix} - [I_i] \begin{bmatrix} i_1 \\ i_2 \\ \vdots \\ i_n \end{bmatrix} \tag{12}$$

Time Derivatives of the Nodal Voltages. Applying KCL (Kirchhoff's current law) to the circuit of Figure 3.1, that is, the sum of the currents diverging from the nodes through the inductances and the capacitances equals the currents fed to the nodes, results in,

$$\begin{bmatrix} i_1 \\ i_2 - i_1 \\ \vdots \\ i_n - i_{n-1} \end{bmatrix} + [K] \begin{bmatrix} \frac{de_1}{dt} \\ \frac{de_2}{dt} \\ \vdots \\ \frac{de_n}{dt} \end{bmatrix} = 0 \tag{13}$$

Where, [K] represents the node capacitance matrix of the circuit as represent before.

$$[T]\begin{bmatrix} i_1 \\ i_2 \\ \vdots \\ i_n \end{bmatrix} + [K]\begin{bmatrix} \frac{de_1}{dt} \\ \frac{de_2}{dt} \\ \vdots \\ \frac{de_n}{dt} \end{bmatrix} = 0 \qquad (14)$$

Assigning $[E_i]$ = - $[K]^{-1}[T]$, time-derivatives of node voltages can be expressed as,

$$\begin{bmatrix} \frac{de_1}{dt} \\ \frac{de_2}{dt} \\ \vdots \\ \frac{de_n}{dt} \end{bmatrix} = [E_i]\begin{bmatrix} i_1 \\ i_2 \\ \vdots \\ i_n \end{bmatrix} \qquad (15)$$

d) State equation. By merging equations (12) and (15), state equation corresponding to the circuit in figure 2.9, is obtained as,

$$\begin{bmatrix} \frac{de_1}{dt} \\ \frac{de_2}{dt} \\ \vdots \\ \frac{de_n}{dt} \end{bmatrix} = \begin{bmatrix} 0 & E_i \\ I_e & I_i \end{bmatrix}\begin{bmatrix} e_1 \\ e_2 \\ \vdots \\ e_n \end{bmatrix} \qquad (16)$$

The above equation can also be expressed as,

$$\dot{x} = [A]x \qquad (17)$$

e) Output Equation. Neutral current of the primary winding is chosen as the output variable 'y' of the state model, so it is to be expressed in terms of the state variables (x) and the input (u). From Figure 3.1, it is obvious that, neutral current is the sum of the currents through the inductance and the series capacitance of *n*th section of the primary winding, that is,

$$i = i_n + C_s \frac{de_n}{dt} \qquad (18)$$

Using the definition of state variables and making use of (17), the above equation can be rewritten as,

$$y = x_n + C_s([A_y]x + [B_y]u) \qquad (19)$$

where, $[A_y]$ and $[B_y]$ represent *n*th row of [A] and [B] respectively. The first two terms of the above equation can be merged together by assigning

$Cx = x_n C_s([A_y]x$ and let $D = C_s[B_y]$. Now, (8) modifies to,

$$y = Cx + Du \qquad (20)$$

Thus, the output variable of the state model is expressed in terms of the state variables and the input vector. Equations (17) and (20) together constitute the state model of the network.

The complete model of the state-space model represents the coupled ladder network, taking a considerably short circuit of turns in the faulty disk; can take the form of an equation of state

and output:

$$\dot{x} = A(0, E_i, I_e, I_i, f)x + B(I_u, 0,0,0) \quad (21)$$

$$y = C\big(C_s, A_y, f\big)x + D(C_s, B_y, f) \quad (22)$$

The vector of the defects f is given by:

$$f = \begin{vmatrix} f_1 \\ f_2 \\ \vdots \\ f_i \end{vmatrix} \quad (23)$$

2.8. Conclusion

This chapter presents a robust methodology FRA-SMI applied to synthesize the mutually coupled equivalent model of the transformer winding based on interpreting the FRA signal morphology. Optimization algorithms have an effective tool in scientific research, as they are used to find a close solution to a specific problem by exploring and improving the solutions available in the vicinity of the current solution. As previously mentioned, the reliance on the particle swarm optimization algorithm was used to model the equivalent winding of an insulated electrical transformer. The investigation of the frequency response of a transformer winding to determine the matrices of inductances and capacitances has been multi-advantaged, which can be easy to implement, with only FRA measurement signal input required, and a significant reduction in parameter search space. However, the parameters of the power transformer coils vary during operation, due to short circuit faults and mechanical displacement. It is then necessary to assess the impact of these variations on the developed state space model to interpret short-circuit faults in the winding. Especially since the synthesis of the frequency response used for fault detection is carried out on the basis of one of these models. So, the greatest advantage of this approach is to perform a short-circuit fault synthesis task, through this advanced model, can be simulated in various proportions the short circuit faults. Furthermore, the extreme of this approach the results of the simulation were close to the experimenta

Chapter 3: The extent to which the impedance of the power transformer is affected by short circuit faults.

Chapter 3: ***The extent to which the impedance of the power transformer is affected by short circuit faults.***

3.1 Introduction

Power transformers can operate under certain circumstances during their service life. There are five types of currents that are subject to power transformers [88]:

- Transient in-rush current in primary winding when it is switched in.
- Steady no-load current in primary winding when it has no load on the secondary side.
- Steady load currents in all windings when a load is connected to the secondary winding.
- Transient short-circuit currents in all windings during external short-circuit event.
- Geomagnetically induced currents, which are possible when the winding has a grounding point.

Undoubtedly, only the transient short-circuits currents have direr consequentially for the power transformer winding. A short circuit faults are significant a huge problem in power transformers and can eventually develop into catastrophic failures. Massive electromagnetic forces are produced practically by short circuit currents in a short period. Electromagnetic forces may deform the windings in two states, the first one is if the mechanical structure of the power transformer is not robust to withstand the strength of electromagnetic forces when it is poorly designed or manufactured. In the second one with service years accumulating, the winding mechanical structure is not as tight as the original one [89,90].

The phenomenon of short circuits in the transformer windings leads to instability in the active parts of the transformer. Short-circuits of the transformer windings are due to the loss of insulation between adjacent conductors due to the destruction of the protective enamel (varnish) or the insulation papers may have become aged and brittle. Every short-circuits forms a hot spot and creates a black point placed in the transformer winding, and little by little becomes perishable. In this part, we devote all our attention to the careful study of the effect of a short circuit on the electrical transformer winding in the event of a short-circuit failure in one disk and short-circuit failure in multiple disks of the transformer winding [90].

3.2.Percentage Impedance written in nameplates

The percentage impedance of a transformer is defined as the voltage drop at full load due to the winding resistance and leakage reactance expressed as a percentage of the rated voltage.

It is also defined as the percentage of normal terminal voltage required to drive full load current under short circuit conditions [91]. In other words, the percentage impedance of a transformer is the percentage of the rated voltage applied at one side (primary winding) to circulate rated current on transformer keeping its other side (secondary winding) under short circuit conditions.

This value expresses the amount of drop in voltage when the transformer is loaded with full capacity. To make this point clear, we have to explain the following example. We have the Impedance% value equal to 4 and the voltage on the transformer is 415/11000 volts. Therefore, the amount of drop in voltage on the side will be 11 kV = 110000 * .04 = 440 Volts when the transformer is loaded to full capacity, and certainly this is reflected in the value of the transformer voltage under load, but does this mean that the lower this value, the better for the transformer? Here we have to clarify the second point, which is that the greater the value of the Impedance%, the lower the value of the Short Circuit Capacity. In order for this important point to become clear, we now want to calculate the short circuit current on the transformer in the 415-volt direction = the rated current of the transformer / Impedance% equals 3475 A. Through this we find The Impedance% value is of utmost importance when talking about short circuit current calculations. Sometimes the Impedance% is written on the Name Plate with the value of X% only because the value of R is neglected in relation to the value of. When conducting the Short Circuit Test, there is also a need to know the Impedance% value because it represents the voltage required to be applied to one of the two coils of the transformer in order to pass a rated current through both coils when a short circuit is placed on the other coil. To clarify further, this percentage is the same as for (percentage impedance voltage). If its value is equal to, for example, 4%, this means that you only need 4% of the rated voltage value in the short-circuit test to pass the rated current value. There is also the importance of the Impedance% value when connecting transformers in parallel, but this point requires some detail.

Chapter 3: ***The extent to which the impedance of the power transformer is affected by short circuit faults.***

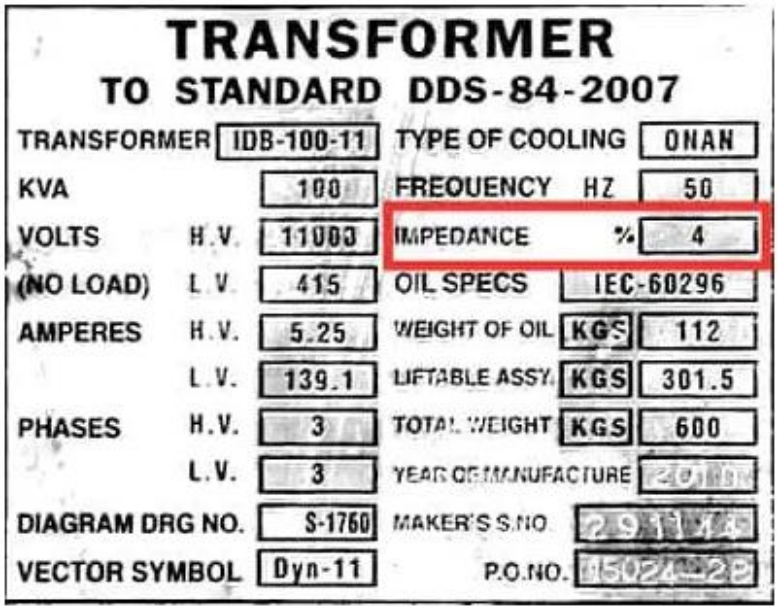


Figure 3.1: Percentage Impedance written in nameplates.

3.3.Transformer impedance in case of short circuit fault

Transformer impedance is an invincible heart, which plays an important role in the case of magnitudes of short-circuit current faults and the consequent short-circuit forces. The higher the impedance is, the lower the short-circuit current and the forces are. There is a so-called "natural" short-circuit impedance value for each transformer. By selecting it, the overall design can be well balanced with the best compromise among different requirements [102]. Determine model parameters corresponding to the impedance is the fingerprint of transformer, so changes in the frequency response trace would almost certainly be caused by changes or displacements in the winding structure [103]. The state space equation of the lumped model may be a useful tool for simulating the short-circuit of transformer winding in autonomously manner by changing the faulty coefficients (f_1, f_2, ... f_i.). The coefficients f_i represent the percentage of turns not short-circuited by each disk of the winding. However, these coefficients have been introduced added on the matrices of resistance, inductance and capacitance instead of realizing real faults in the winding as previously mentioned. However, the coefficient f_i represents the percentage of non-short-circuited turns per winding disk that affects the parameters of the faulty disk. This coefficient increases and decreases according to the number of short-circuited turns of the winding as presented in previous chapter. In a healthy state, it is equal to one. This approach made it possible to obtain a state model for the detection of short-circuit faults in the winding of the transformer, by determining approximately the ratio of faults. The main advantage of the

approach is that it not only can estimate the ratio faults but also can be used to compare it with mechanical deformation accompanied by short circuit faults.

These coefficients represent the percentage of turns not short-circuited by each disk defined by:

$$f_1 = 1 - n_1$$
$$f_2 = 1 - n_2 \qquad (1)$$
$$\vdots \qquad \vdots$$
$$f_i = 1 - n_i$$

3.4.short-circuit failure in one disk in isolated winding

Representing the transformer winding in a circuit model aims to capture the physical length of the winding. In itself, it is a powerful tool because it visualizes the spin physically from the line to the neutral end. In turn, it shows the same properties for winding. The synthesized circuit should reach a small difference or a limited tolerance between the measured and estimated resonant frequencies, in other words, to all corresponding short circuit natural frequencies (S_{cnf}) and open circuit natural frequencies (O_{cnf}) equally [92].

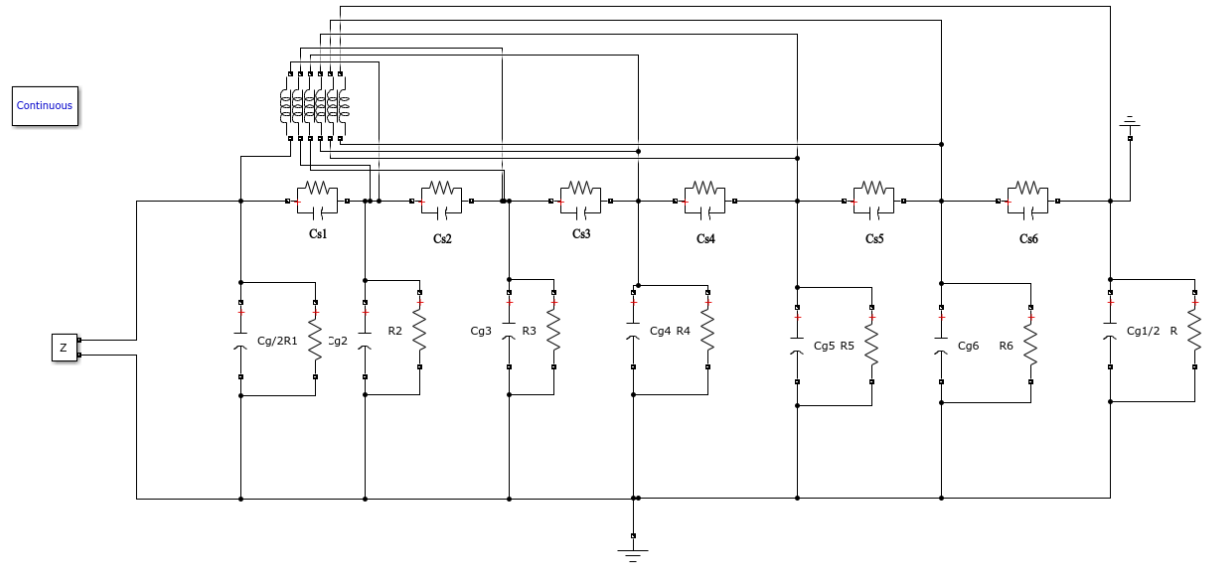


Figure 3.2: Equivalent circuit of a transformer winding in MATLAB Simulink.

3.5.Simulation of isolated model winding

In this part, the simulation of the short-circuit faults in an isolated power transformer winding is presented. The defects are introduced in the form of different proportions which are, in fact, in proportions very close to the simulated ratios. The state space model is a reliable and efficient method for simulating short-circuit faults in the winding of an electrical transformer. A defect

between 5% and 40% is considered in this case. These reports are simulated on all disks individually and simulated in the event that more than one fault occurs on more than one disk. Short-circuit faults were created on an isolated winding power transformer consisting of 6 disks, where the faults were created at the top of the winding on the first disk and in different proportions, after which a short-circuit fault was created in the same proportions at the level of the middle of the winding, to conclude in the end with the same fault type and the same proportions on the bottom disk. A short-circuit malfunction is created by 5 % incrementally in each case to see the extent of the short-circuit's impact on the transformer's behavior. The impedance spectrum is divided into three parts, which are low frequency, medium frequency, and high frequency, and then study the effect of a short circuit on the impedance spectrum in each case. Simulation results are discussed in Table 3.1. to study the influence of different short circuit portions on winding frequency characteristics. The results recorded in the following table show the effect of short-circuit failure on the behavior of the transformer. If changes portion of the short circuit there change in the series capacitive, self-inductance, and mutual inductances components of winding, therefore, a shift in the frequency characteristic of winding indicates winding deformation. The results also show that in the low frequency, there is no significant effect on the resonance frequencies, and this is because the elements responsible determine this resonance are the inductances and ground capacitance. The ground capacitance, where has no exciting mathematical relationship with the number of turns. While in the middle frequencies, it is evident the displacement appears clearly in the resonance frequencies, they determine due to the new element ground capacitance, series capacitance, self-inductance and mutual inductances. At higher tensions, a significant displacement of the resonant torsions is also observed, and in this case, the equivalent circuit of transformer winding consists of only capacitive elements such as Cs and Cg.

Chapter 3: *The extent to which the impedance of the power transformer is affected by short circuit faults.*

Case of short circuit fault in isolated electrical power transformer winding disks		Estimated natural frequencies for isolated power transformer winding using the simulation model	
		O_{cnfs}(Khz)	S_{cnfs} (Khz)
		1st 2nd 3rd 4th 5th	1st 2nd 3rd 4th 5th
A1	5% of SC in Disk 1	220 516 747 948 1138	0 442 712 923 1115
	5% of SC in Disk 3	222 515 744 947 1135	0 438 711 923 1113
A2	10% of SC in Disk 3	223 518 748 952 1137	0 439 716 928 1115
	10% of SC in Disk 6	225 521 752 953 1142	0 447 718 929 1120
A3	15% of SC in Disk 1	221 522 760 963 1150	0 451 725 937 1126
	15% of SC in Disk 3	225 520 751 958 1139	0 439 721 934 1118
A4	20% of SC in Disk 1	221 525 766 971 1157	0 456 731 945 1134
A5	30% of SC in Disk 1	221 530 778 989 1178	0 464 744 963 1154
	30% of SC in Disk 3	229 528 762 976 1145	0 441 735 951 1125
	30% of SC in Disk 6	234 537 776 984 1173	0 464 743 961 1152
A7	35% of SC in Disk 1	221 533 783 998 1191	0 469 750 972 1166
	35% of SC in Disk 6	236 541 782 992 1185	0 469 749 970 1164
A8	40 % of SC in Disk 1	221 535 789 1007 1206	0 473 756 981 1180
	40 % of SC in Disk 3	232 532 768 989 1149	0 441 743 964 1130
	40 % of SC in Disk 6	238 545 788 1002 1198	0 473 756 979 1178

Table 3.1: Short-circuit on disks of isolated winding.

Chapter 3: *The extent to which the impedance of the power transformer is affected by short circuit faults.*

3.6.Influence of short circuit for winding frequency characteristics

The figure below represents the influence of short circuit faults for winding frequency characteristic in disk 4. An analytical investigation of frequency-domain responses using circuit simulation software (MATLAB), shows the extent of the influence of different ratios SC on the behavior of the frequency response analysis. the process of changes in the number of turns of the winding means that there is a change in the square of the self-inductance component of the winding, therefore the mutual inductance and series characteristic capacitances of the coil indicate that the winding is deformed. Figure 3.3. shows the decrease in the numbers turn (ratios of SC), In addition, the resonant frequency of winding shifts right side. The phase response was also changed, changing the winding parameters causes a noticeable change in the phase, as the greater the failure percentage, the greater the change in the phase as presented in figure 3.3.

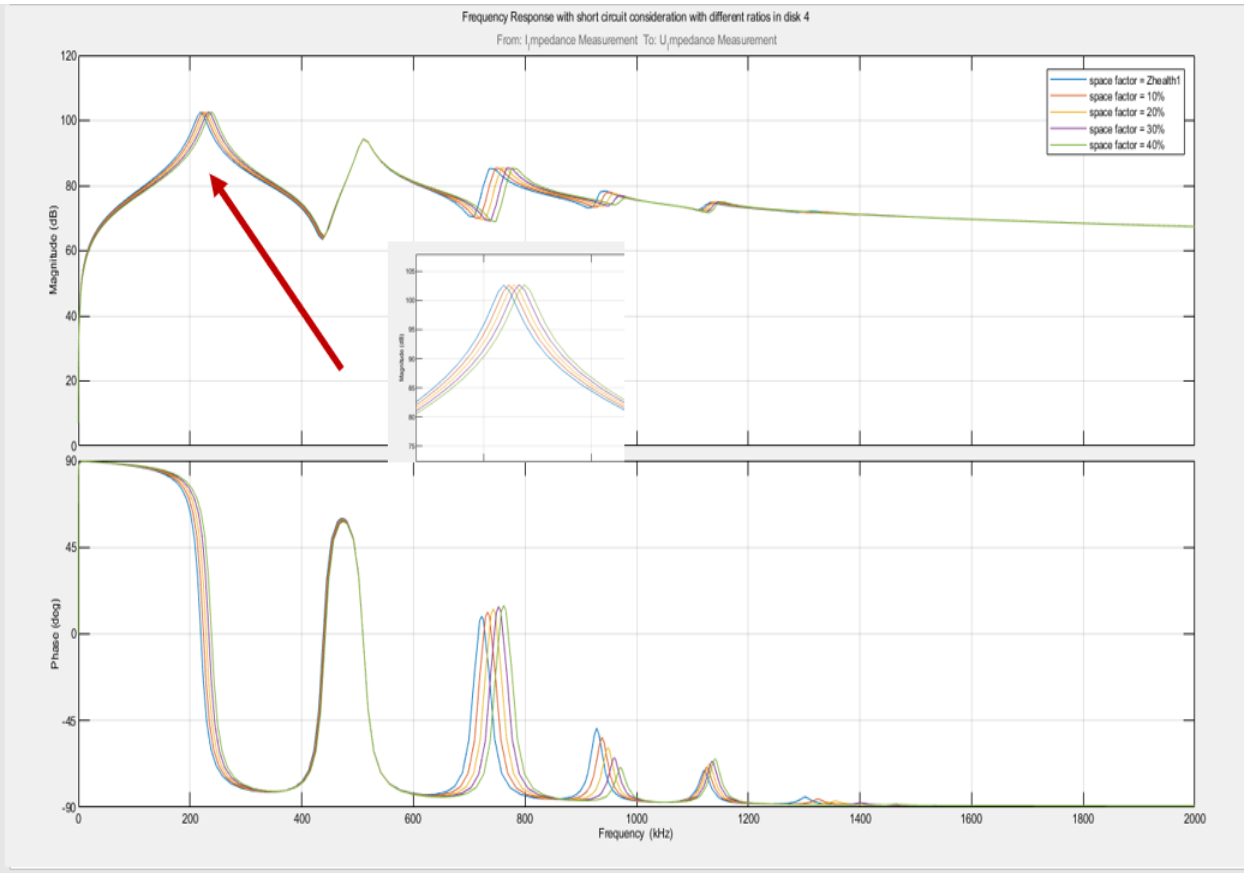


Figure 3.3: Frequency response analysis in disk 4 with SC excite.

3.6.1. Short circuit fault simulation results in disk 6

In this part, perform the simulation of the state space model given in the previous chapter. The Figure.3.4 appears the impedance of the winding isolate before the appearance of the fault in red with the impedance estimate of two different short-circuit faults in disk 6 with 5% and 40% respectively. Almost, this sees its amplitude increase significantly., with an offset important in the resonance frequencies. As the fault of SC percentage in one disk increases, it increases with the change in the winding parameters, and accordingly, the displacement in the resonance frequencies appears clearly.

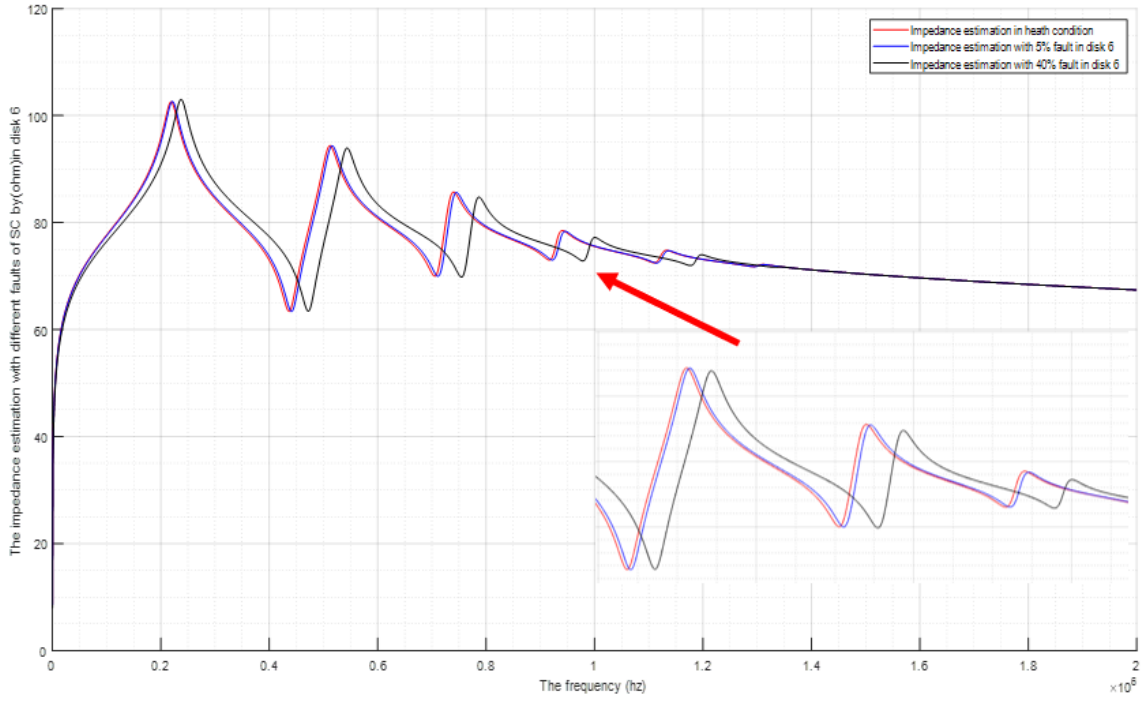


Figure 3.4: The impedance estimation with different faults of SC by (ohm)in disk 6.

3.6.2. Case of multiple faults of short circuit in isolated winding

In order to maintain the integrity and continuity of the electrical system, the power transformer must be protected from short circuits. Detecting electrical shorts in power transformers and treating them is extremely important. This requires us to search for a reliable way to determine the location of the fault and the extent of the damage. In this part has been devoted to the analysis performances of the state space model developed for the purpose of analysis the behavior of the power transformer in the event of a short circuit in more than one disk. In what follows, a consideration of the case of short circuit faults in isolated power transformer winding that may occur in two disks or three disks simultaneously.

3.6.3. Short circuit faults on disks 5 and 6 by 5% ($f_5 = f_6$ 0.95 and $n_5 = n_6 = 95$)

In this part, a consideration to the detection of multiple short circuit faults in the in isolated winding using state space model. The figure 3.5. gives the impedance measurement, in case of multiple short circuit in power transformer winding in disk 5 and 6 simultaneously with 5% of SC, comparing with healthy impedance. The salient feature, in this case, is that low values of the percentage of turns in short-circuit indicated the fault appearance of SC. The difference between the healthy and faulty frequencies resonances measurements increases when this percentage increases.

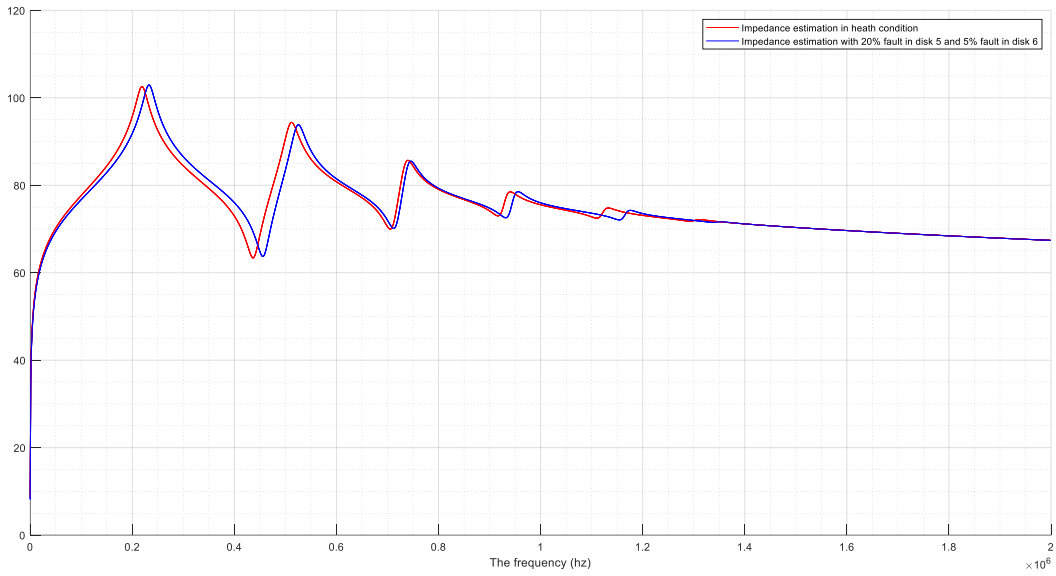


Figure 3.5: Impedance estimation with 20% fault in disks 5, 5% fault in disk 6.

In this case, after introducing change the number of spires in two disks simultaneously, was measured the frequencies of transformer winding and are noted as in table 3.2. The defects are introduced in the form of different percentages. consideration the appearance of a 5% defect on disk 5 (reduction of the number of turns of disk 5 by 5%), a defect on disk 6 by 5%. It is noted that there is a huge displacement in all pecks of the resonance frequencies as shown in table 3.2.

Case of multiple faults of short circuit in isolated electrical power transformer winding disks		Estimated natural frequencies for isolated power transformer winding using the simulation model	
		O_{cnfs}(Khz)	S_{cnfs} (Khz)
		1st 2nd 3rd 4th 5th	1st 2nd 3rd 4th 5th
A1	5 % of SC in disk 5 5% of SC in disk 6	234 526 747 957 1177	0 457 713 933 1155

Table 3.2: short-circuit 5% in disk 5 and 6.

3.6.4. Short circuit in disk 2 with 20%, 25% in disk 3 and 40 in disk 4

In this section, we consider the case of a multiple SC fault in disk 2 with 20% shorted turns, in disk 3 with 25% SC and 40% in disk 4. The figures 3.6. following shows the results of simulation. They are identical to those obtained in the case of multiple faults. The variations in the amplitudes of the impedances and the variation in the offset of the resonance frequencies result in the appearance of short-circuit faults in the winding. A short circuit causes a change in the winding parameters, which is reflected by the observed displacement at the resonance frequencies.

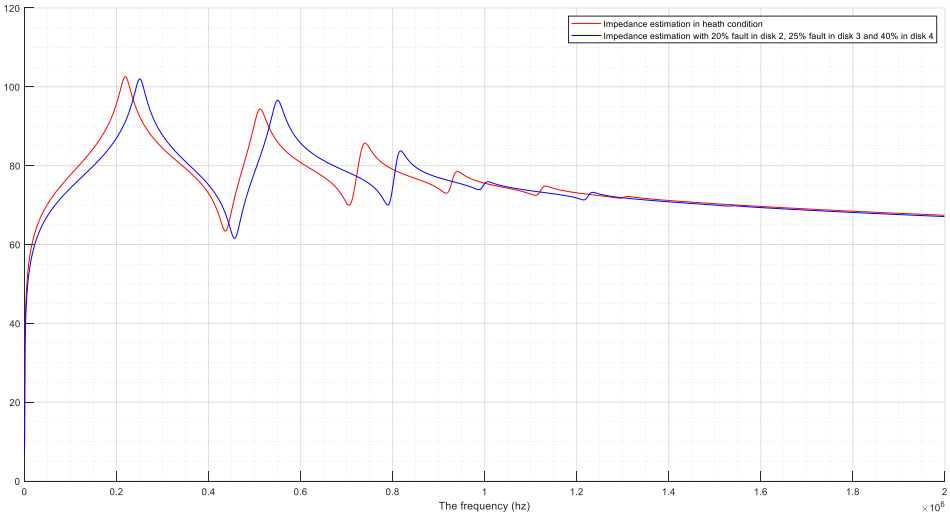


Figure 3.6: Impedance estimation with 20% fault in disk 2, 25% fault in disk 3 and 40% in disk 4.

In this part, we analyze the influence of the variation of the parameters on the behavior of the power transformer. These simulation results show that the influence of the parametric variation is reflected by the change on the resonance frequency peaks. the amplitude of the impedance

indicates the appearance of the fault, on the other hand, the resonance frequencies are a strong indication. This is what can be seen in the following table.

Case of multiple faults of short circuit in isolated electrical power transformer winding disks		Estimated natural frequencies for isolated power transformer winding using the simulation model	
		O_{cnfs}(Khz)	S_{cnfs} (Khz)
		1st 2nd 3rd 4th 5th	1st 2nd 3rd 4th 5th
A1	20 % of SC in disk 2 25 % of SC in disk 3 40 % of SC in disk 4	251 551 818 1008 1236	0 458 790 988 1216

Table 3.3: Case of multiple faults of short circuit in different disks.

3.6.5. Short circuit in disk 1 with 10%, disk 2 with 20% and disk3 with 25%

We consider the case of a fault of 10% of short-circuited turns which occurs on disk 1, 20% in disk 2 and 25% in disk 3. Figure 3.4 shows the results of this simulation. There is a significant shift in the resonance frequencies, as shown in the image and the following table, which proves the presence of the defect. The difference between the impedance curve in red in the healthy state of the transformer and in blue in the event of a malfunction shows the magnitude of the change in the winding parameters, which is reflected by the resonance frequencies.

Case of multiple faults of short circuit in isolated electrical power transformer winding disks		Estimated natural frequencies for isolated power transformer winding using the simulation model	
		O_{cnfs}(Khz)	S_{cnfs} (Khz)
		1st 2nd 3rd 4th 5th	1st 2nd 3rd 4th 5th
A1	10 % of SC in disk 1 20 % of SC in disk 2 25 % of SC in disk 3	231 559 773 1001 1180	0 467 741 979 1159

Table 3.4: Case of multiple faults of short circuit in different disks.

As seen in Figure 3.7, in case of multiple faults of short circuits in different disks. It is indicated that the fault causes a clear shift in the resonance frequencies, and this is because the short circuit changes the winding parameters.

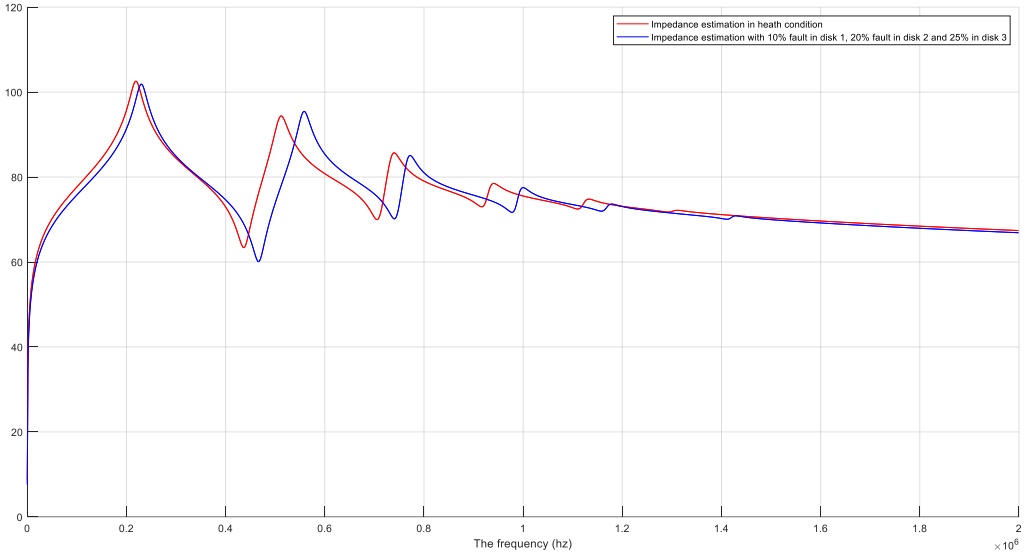


Figure 3.7: Impedance estimation with 10% fault in disk 1, 20% fault in disk 2 and 25% in disk 4.

3.7. Short circuit faults in isolated transformer winding in case experimental

A short circuit in the power transformer coil is a serious problem. This occurs when an unintended electrical connection is created between two or more points in the coil. This can lead to several consequences, such as overheating, voltage Imbalance, mechanical stress, and other unwanted consequences. After the study of the forms of short-circuit failure of an isolated transformer winding was simulated in the first section, the second part of this chapter is dedicated to the study of short-circuit failure on an experimentally isolated winding in the laboratory. In this case, the short circuit fault can occur on one disk i. We consider the case of a fault of 5%, 10%,20%,30%, and 40% of short-circuited turns which occurs on disk 5. Figures 3.8 a and b show the results of this simulation. The figures show that the results obtained are very close to the experimental. This is confirmed by figure b. This effective method for early detection of power transformer faults is capable of detecting short circuit faults of up to 1%. The investigate the sensitivity of transformer frequency response experimental. Form figure 3.8, various short-circuit ratios are simulated on disk 5. To see the extent of damage to an isolated winding. Figure.3.8, illustrates the effect of increased short-circuit ratios on the faulty disk. As the resonance peaks are shifted to the right with increasing ratios of SC, this is due to the effect of series capacitance and inductance significantly. the Impact of change in amplitude is also due to the effect of induction. The extent of influence of the parameters directly affects the resonance frequencies of the impedance spectrum.

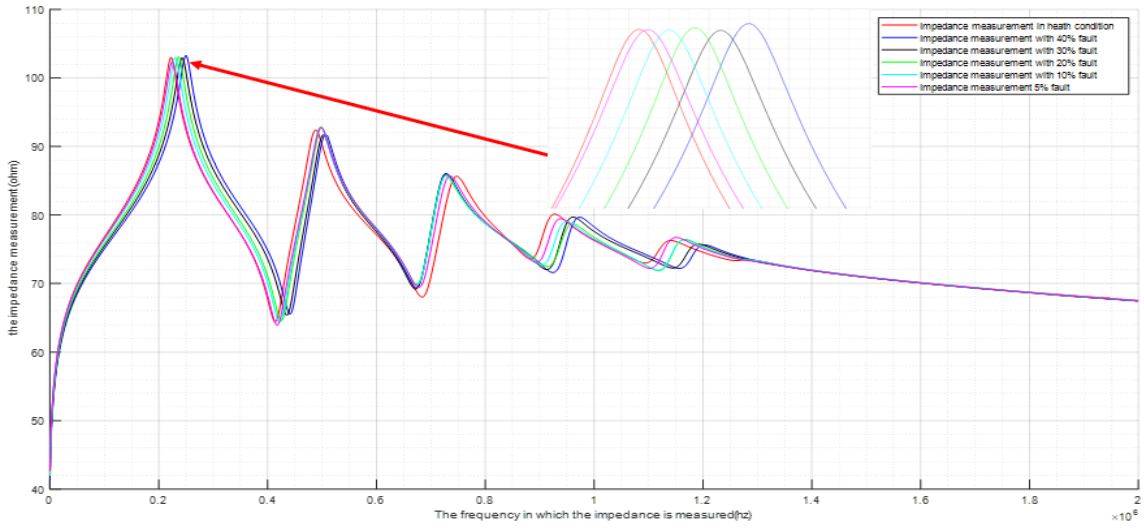


Figure 3.8: Short-circuit faults in disk 5 with different levels, (a) reel faults.

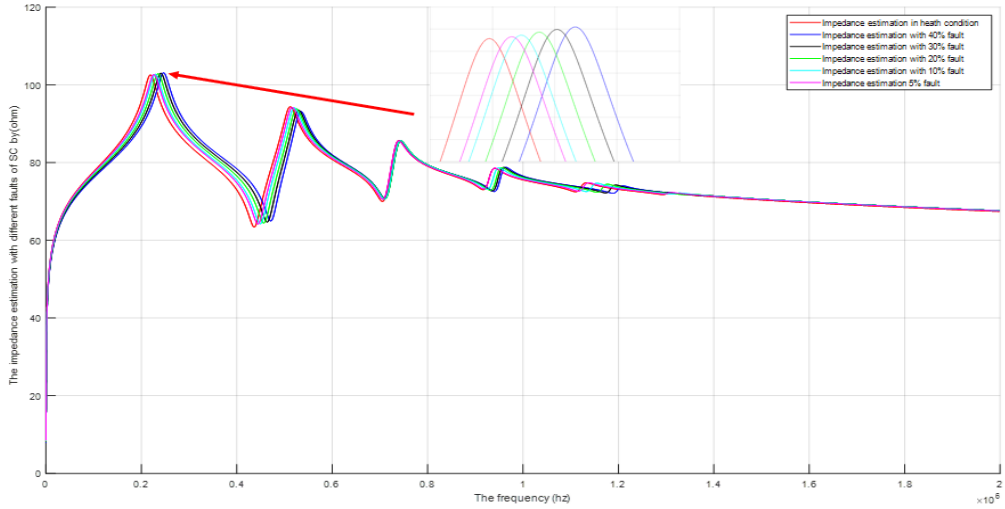


Figure 3.9: Short-circuit faults in disk 5 with different levels, (b) simulation faults.

	N° Discs	SCNFs (kHz) measured to take into consideration of SC in various disks					$\Delta Leq\ (mH)$
		1st	2nd	3rd	4th	5th	
5%	3	225	494	742	945	1145	-0.367
	5	224	498	734	938	1150	-0.282
20%	1	220	494	760	960	1144	-0.487
	3	226	511	750	943	1147	-0.837
	5	236	499	727	959	1166	-0.882

Table 3.5: In the case of failure of CC in one disk of insulated winding.

3.7.1. short-circuit failure in multiple disks in isolated winding

In the following, the case of faults that may arise produce on both disk i and j simultaneously. When two disks are shorted together in equal proportions, and two disks are shortened together in different proportions. The contrast is evident in both resonant frequencies and parameters as shown in table 3.6.

	N° Discs	SCNFs (kHz) measured to take into consideration of SC in various disks					ΔLeq (mH)
		1st	2nd	3rd	4th	5th	
5%	4 and 5	230	502	725	946	1146	-0.594
20 %	4 and 5	248	506	753	976	1180	-1.508
40% (3) 30 % (4)	3 and 4	250	533	818	981	1154	-2.532

Table 3.6: Occurrence of a short circuit fault in several disks of insulated winding.

3.8.Estimation of the severity of short-circuit faults in disks

In this part, we consider detecting faults using the variation of the equivalent winding inductance. The defects of SC are introduced in the form of percentages. If a short circuit failure occurs in one of the winding disks, the higher the percentage of short circuits, the greater the change in the equivalent inductance.

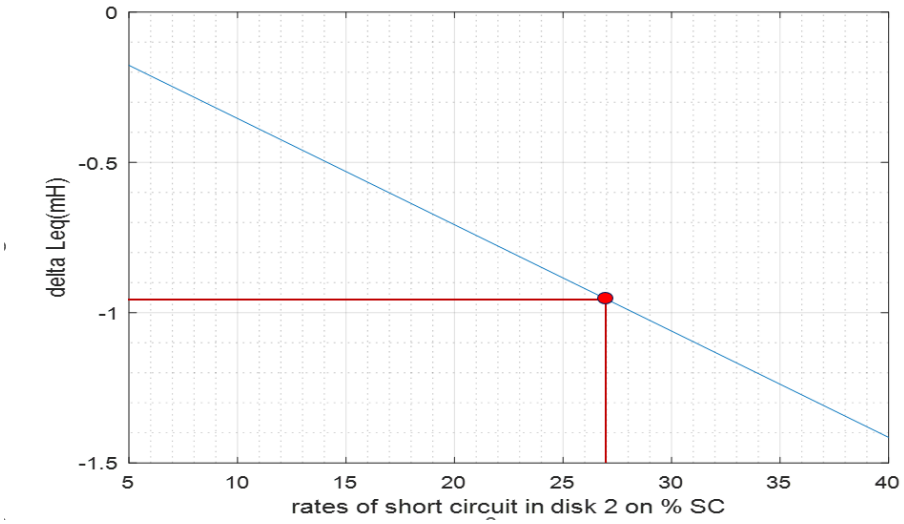


Figure 3.10: Rates of short-circuits in disk 2.

Chapter 3: ***The extent to which the impedance of the power transformer is affected by short circuit faults.***

3.9.The salient features extract

In the following, we deal with the phenomenon of short circuit in the transformer windings which leads to instability in the active parts in the transformer. The short circuit of the transformer windings is due to the loss of insulation between adjacent conductors, due to the destruction of the protective enamel (varnish). This phenomenon occurs locally and forms a hot spot, which affects a very small number of turns. Then it propagates, involving an increasing number of turns because the short-circuit current is being very important.

Short-circuit turns of winding twist slowly, slowly, to destroy the active part of the electrical transformer. With every short-circuit turn a black point is placed in the transformer winding, and little by little it becomes perishable.

- Knowing the levels of short-circuit winding helps to predict the risk.
- where it makes a remarkable change in the self-inductance (L_i), series capacitance (C_s) and the mutual inductance (M_{ij}) between disks.
- The process of increasing the percentage of short-circuit winding at the normal level by 5 % or 10 % clearly shows a decrease in the amplitudes of impedance and increases in the displacement of frequencies resonance. This ratio indicates the existence of a slight or moderate risk if it is not rectified due to the increase in the short circuit in the disk, but it has not reached at this stage the level of great danger.
- as for 20% to 40% in a disk, indicating a significant increase in the short circuit level, which indicates a high risk.

In this part, we devote all our attention to care to study the effect of a short circuit on the electrical transformer winding in the event of a short-circuit failure in one disk and short-circuit failure in multiple disks of the transformer winding.

3.10. Conclusion

The possibility of a short circuit occurring between the windings in the power transformer windings has several reasons. When the transformer is exposed to vibrations during loading, or is subjected to repeated electromagnetic shocks, as a result of connecting to an external short, these sharp edges cut the insulation, and allow the metal of the adjacent windings to touch, causing a short circuit castle. In addition, the humidity factor may be a major cause of short circuits. As the insulation becomes saturated with moisture, the possibility of a short circuit between the windings becomes possible as a result of insulation corrosion. In transformers used for large electrical systems, the manufacturer takes care to connect and install the coil cushions to prevent any problems from occurring if the coil insulation shrinks. If the connection is not made and fixed at a certain pressure during manufacturing, some conductors are susceptible to displacement under operating conditions, resulting in insulation collapse and a short circuit between the windings. These and other reasons could cause an emergency short circuit and can lead to the ending of the life of the transformer completely. The first healthiest ways and most famous methods ever to find out the correctness of the electrical transformer winding after the occurrence of short circuit or mechanical damage is the analysis of the frequency response (FRA). This chapter exposure a new method of modelling the transformer winding with respect to a short circuit fault in turns in the winding. This approximation is valid as long as n_i is small in front of 1, is used to analyse and synthesise how the model behaves when n_i varies. Where required redefining the resistance, inductance and capacitance matrices by introducing the coefficients quantifying the faults of short-circuiting in this model. The simulations that have been presented in the first section assist in the evaluation and interpretation of FRA measurement when a short-circuit occurs by introducing series faults of 5%, 10%, 20%, 30% and 40%.

In this chapter, as previously mentioned an approximation study to develop a model of the frequency response of the transformer winding concerning turn short-circuit faults. This approximation is valid as long as n_i is small compared to 1. Determine a model examining the characteristics of the frequency response analysis due to short circuit deformations when n_i varies. A practical approach proposing for interpretation of the deformation regarding the response.

Chapter 4: Deformations Instigated by AD, AD with SC and Radial

Chapter 5: *Test Platform Dedicated to Power Transformer Winding Diagnostics*

4.1. Introduction

The power transformer parameters vary during its operational lifetime. The change occurring has appeared more with increasing age, and more clearly in the event of a malfunction. These parameters variations and alterations in symmetry in the power transformer windings are some of the reasons caused by the axial displacement which affects the dynamic behavior of the power transformer. In a transformer áxial displacement can occur in more than one way, and each of them as mentioned before has varying effects on winding parameters viz, L and C [93]. However, several case investigations on signal-isolated winding are presented in this chapter, based on its measured spectral impedance. Frequency response analysis, which is referred to as FRA or SFRA, is a powerful and sensitive method for testing the axial displacement integrity of a power transformer. The principle of frequency response analysis can be explained in a simple way as each electrical transformer has a unique frequency response - what is called the transformer fingerprint. Network faults or vibrations can cause changes in this frequency response and thus distort the original fingerprint. Comparing the measurements to the original fingerprint of the same transformer provides indications of any mechanical or electrical changes. In this case, the difference between the two fingerprints is clear. In the event that it is proved that the winding has been subjected to a large extent of damage, it is necessary to initiate other procedures, such as stopping the transformer from service permanently. When an axial displacement occurs or an axial displacement associated with a short circuit occurs, in this case each point on the frequency response curve deviates from the original coordinates, and this leads to the prominence of a new frequency response curve that differs radically from the original curve of the same transformer. The proposed of this case study can provide an analysis of how the extent of failure has affected the response and how it's reflected in the physical behavior of whole system. Finally, the influence of axial displacement with short-circuit consideration on the frequency response has been an aspect of this section. The axial displacement with SC components of the forces can cause various forms of structural damage on a transformer winding if its mechanical structure is not robust when poorly designed or manufactured [59]. Among the available methods for assessing and severity transformer axial displacement with SC condition, propose a new coefficient to locate and assess the severity of mechanical deformations of the transformer winding by using the relationship relaying the model parameters to the sum of the inverse squares of natural frequencies of the impedance transfer function curve [94].

4.2. Deformations Instigated by Axial displacement

Axial displacement caused by electromagnetic forces can cause catastrophic results in the active part of the power transformer (the windings). Where the types of failure come in several patterns through the events of collapse in the winding, and this is the result of breaking the supporting rings installed. Bends can also occur in joints. or by compressing the insulation to the point where loosening occurs which can lead to displacement of spacers and subsequent failure. Naturally, there are axial compressive forces in the winding, and the direction of these forces is towards the center of the winding. The magnetic energy stored in this winding system is expressed as follows [95]:

$$W = \frac{\pi.\mu_0(NI)^2}{H_{wdg}}\left(\frac{1}{3}r_1a_1 + r_{12}a_{12} + \frac{1}{3}r_2a_2\right) \quad (1)$$

where the dimensions used in the equation are shown in Figure.4.1. The axial force exerting on winding pair per leg, F_{ax} is

$$F_{ax} = \frac{\partial W}{\partial H_{wdg}} = \frac{\pi.\mu_0(NI)^2}{2.H_{wdg}^2}\left(\frac{D_1a_1}{3} + D_{12}a_{12} + \frac{D_2a_2}{3}\right) \quad (2)$$

where $D_1 = 2r_1$, $D_2 = 2r_2$, $D_{12} = 2r_{12}$, the mean diameters of winding 1, winding 2 and the gap in between respectively. This is axial force under rated current, I. Under the short-circuit situation, this force becomes

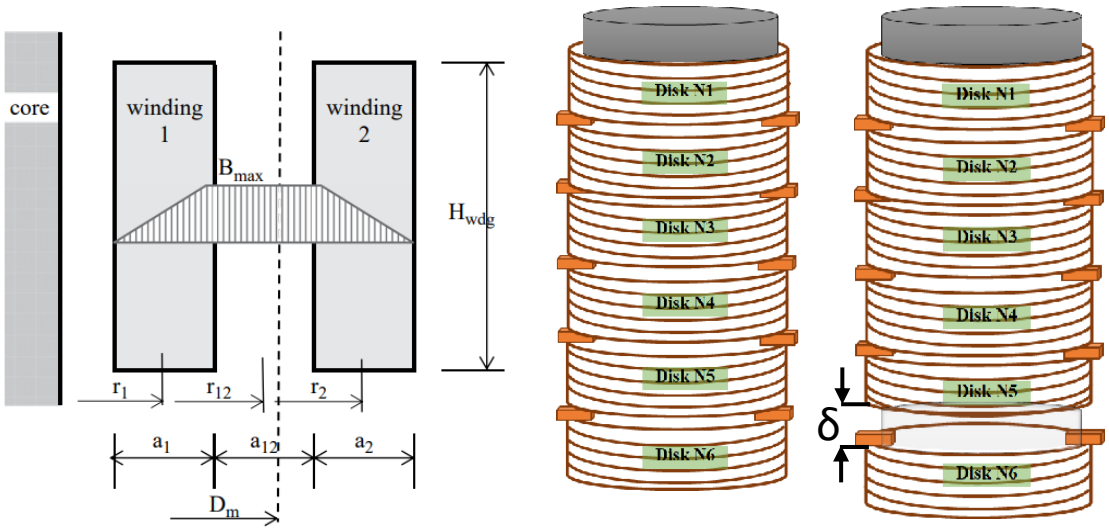
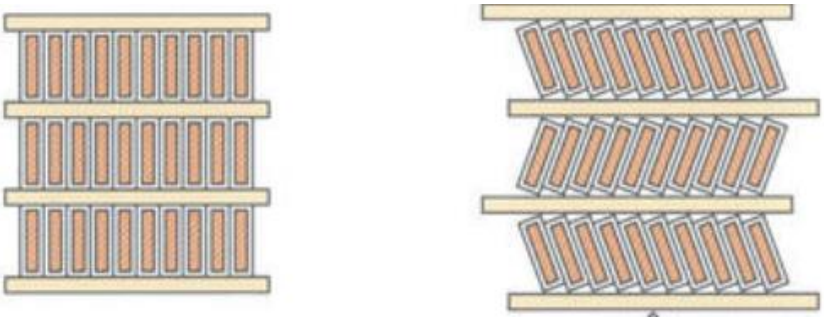


Figure 4.1: Illustration schematic for axial displacement before and after.

4.2.1. Failure mode caused by axial forces

Tilting: Axial forces may trigger different failure modes, according to the mechanisms described here below: - loss of winding axial stability, consisting of a significant turning of conductor cross-sections around the respective perpendicular axis of symmetry. this mode of collapse is called "tilting", and makes the whole set of adjacent conductors inside the radial width of the winding turn in the same direction whereas the next axially adjacent set of conductors turns in the opposite direction. the result is a zig-zag pattern assumed by the winding conductors (the figure below shows some explanation).

tilting may result in broken conductor displacements as well as internal short circuits between conductors [18].



(a) Normal position (b)Tilting conductors

Figure 4.2: Conductors tilting in power transformer winding.

Axial bending: This phenomenon of axial bending failure of conductors is relatively less serious of damage compared to winding displacement. In this failure mode, the distances between the disks are varied and uneven, and this is unlike the first type. And this situation of failure will be more in fact. In this case, axial forces are not large enough to displace the entire winding. However, this type of failure can cause bending of the conductors between the supporting spacers as shown in figure 4.3. This changes the oil-filled gap between the conductors.

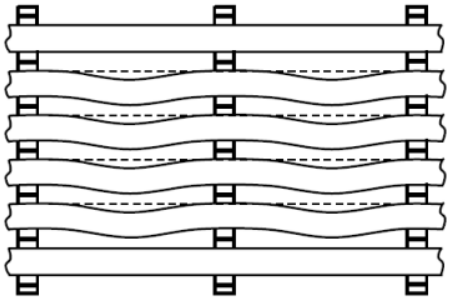


Figure 4.3: Schematic of axial bending failure of conductors.

Telescoping: The axial collapse of the winding is due to the conductor's'' telescoping'' which is typical of layer-type windings. Telescoping consists of some turns driven axially past adjacent turns because of radial looseness caused by stretched conductors (figure 4.4).

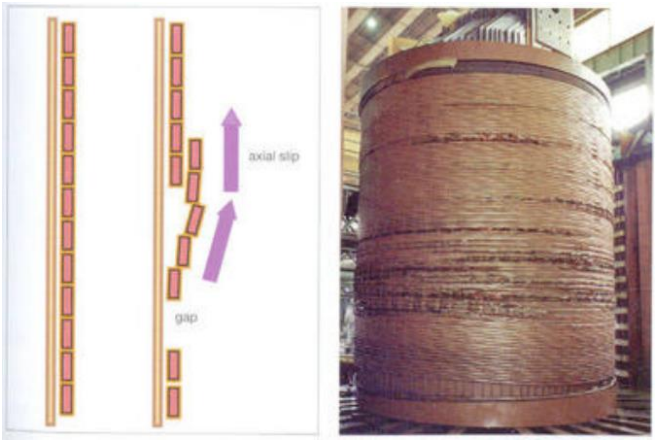


Figure 4.4 Axial collapse due to conductor 'telescoping.

Collapse of winding end supports: due either to overstressed materials or instability within the support structure, which can result in momentary axial deformation of the winding (see figure 4.5), increased forces, and sometimes a burst major insulation or turn insulation [10].



Figure 4.5: Collapse of winding in power transformer.

As previously mentioned, axial displacement may come in many forms and patterns. In the section, in order to facilitate the application of the theory for the detection of axial displacement and its severity. Figure 2.7 in chapter 2 is depicted a signal-isolated transformer winding consisting of six disks. The figure 4.1 is an illustration of the axial displacement process. The axial displacement is in this case by creating a gap between the disks and increasing the gap each time. With the occurrence of an axial displacement in the winding, it causes a clear displacement in the resonance frequencies as shown in the figure 4.6. As the displacement ratio increases, the resonance frequencies are shifted to the right. In the following example (figure 4.6.), the graph compares the axial displacement in the case of 5 mm and the axial displacement in the case of 20 mm. It also caused a decrease in the corresponding mutual inductance. As a result, L_{eq} decreases, so ΔL_{eq} becomes negative.

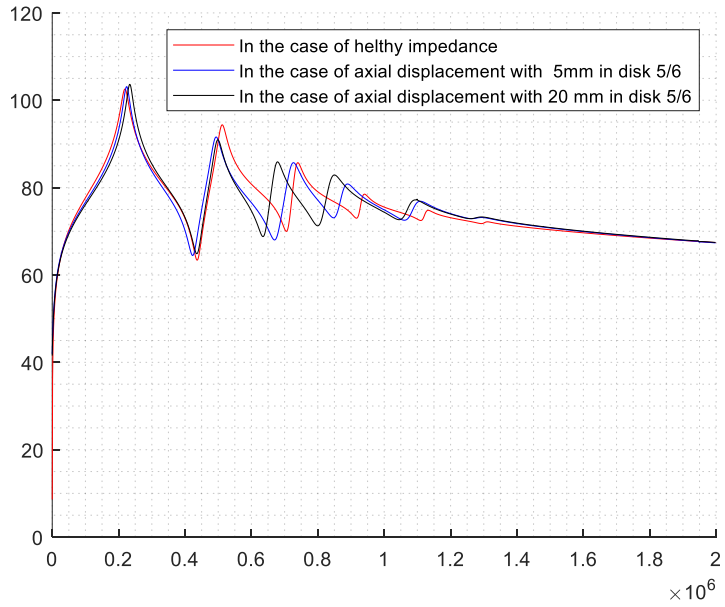


Figure 4.6: A graphical representation of the impedance in the event of an axial displacement between disk 5 and 6.

4.3.Deformations Instigated by Axial displacement with SC

The occurrence of an axial displacement with SC causes a radical change in all winding parameters, which is reflected by the deviation of the events of the frequency response. The axial displacement accompanied by a short circuit greatly affects the behavior of the transformer, increasing as the displacement ratio increases or the number of shorted turns increases. Pictured above is an illustrative schematic diagram, due to the occurrence of an axial displacement associated with the short circuit at the bottom of the winding, and this is the most

common axial displacement occurrence. Where a small portion was created between the two disks D5 and D6, and then a measurement of the resonance frequencies was taken. Conventionally, the axial displacement changes the induction more than the capacitance, where this change is witnessed in mutual induction. The colored elements in the matrix are the elements that have changed after an AD shift.

$$L = \begin{bmatrix} l_{11} & m_{12} & m_{13} & m_{14} & m_{15} & m_{16} \\ m_{21} & l_{22} & m_{23} & m_{24} & m_{25} & m_{26} \\ m_{31} & m_{32} & l_{33} & m_{34} & m_{35} & m_{36} \\ m_{41} & m_{42} & m_{43} & l_{44} & m_{45} & m_{46} \\ m_{51} & m_{52} & m_{53} & m_{54} & l_{55} & m_{56} \\ m_{61} & m_{62} & m_{63} & m_{64} & m_{65} & l_{66} \end{bmatrix} \quad (3)$$

On the other hand, the occurrence of axial displacement with SC has a greater effect on all winding parameters as previously mentioned. Where a short circuit causing loss of insulation. So, the number of turns of the winding concerned undergoes a reduction. A short-circuit begins with a very small number of turns, causing the circulation of a very high current compared to the rated current. For AD is also more deadly to the winding. It can be causing failure by producing collapse of the winding, fracture of the end rings or clamping system, and bending of the conductors between spacers. The occurrence of AD with SC simultaneously have varying effects on winding parameters viz: R, L, and C.

Evidently, after occurrence AD with SC simultaneously have to be estimated the change parameters, starting from the resistance, which is directly related to the coefficient f_i, as it represents the percentage of turns not short-circuited by each disk of the winding. then self-inductance which has to do with a square f_i, the mutual inductance, and the series capacitance which each of them is affected by the SC. In addition to the great impact of mutual inductance in case of AD. As shown in the following matrices in color.

$$R = \begin{bmatrix} r_1 & 0 & 0 & 0 & 0 & 0 \\ 0 & r_2 & 0 & 0 & 0 & 0 \\ 0 & 0 & r_3 & 0 & 0 & 0 \\ 0 & 0 & 0 & r_4 & 0 & 0 \\ 0 & 0 & 0 & 0 & r_5 & 0 \\ 0 & 0 & 0 & 0 & 0 & r_6 \end{bmatrix} \quad (4)$$

The self-inductances of the winding, as well as the mutual inductances, are expressed according to their nominal values and the coefficients fi. which does axial displacement associated with short circuits affect these parameters.

$$L = \begin{bmatrix} l_{11} & m_{12} & m_{13} & m_{14} & m_{15} & m_{16} \\ m_{21} & l_{22} & m_{23} & m_{24} & m_{25} & m_{26} \\ m_{31} & m_{32} & l_{33} & m_{34} & m_{35} & m_{36} \\ m_{41} & m_{42} & m_{43} & l_{44} & m_{45} & m_{46} \\ m_{51} & m_{52} & m_{53} & m_{54} & l_{55} & m_{56} \\ m_{61} & m_{62} & m_{63} & m_{64} & m_{65} & l_{66} \end{bmatrix} \quad (5)$$

The change of series capacitive by AD with SC in the model winding affects frequency response by changing the frequency range, by changing the transfer function poles and zeros (S_{scnfs} and O_{scnfs} of equivalent circuit).

$$K = \begin{bmatrix} \frac{c_s}{f_1} + \frac{c_{g1}}{2} & \frac{-c_s}{f_1} & \cdots & 0 \\ \frac{-c_s}{f_2} & \frac{2c_s}{f_2} + c_{g2} & \cdots & 0 \\ \vdots & \vdots & \ddots & \vdots \\ 0 & 0 & \cdots & \frac{2c_{s6}}{f_6} + c_{gn} \end{bmatrix} \quad (6)$$

4.4.Axial displacement accompanied by the phenomenon of short-circuit faults in turns

The imbalance and asymmetry in the winding of the transformer by axial displacement accompanied by the phenomenon of short-circuit faults in turns can be seriously damaged all parameters of winding. Figure 4.1 depicts a formal single isolated winding for a probability of axial displacement (AD). For example, between discs 5 and 6 which are often more abundant at the bottom of the winding. The series capacitance and the self-inductance in an AD state without being SC are constant and without any change. In the case of both occurrences, the faulty disk parameters must be taken into account.

For instance, when AD occurs in disks 02 for example with N = 3 the coefficients f_1 and f_3 equal 1 and they have no effect. Taking into account the short-circuit in the winding, can be written succinctly as follows:

$$\sum_{1}^{3} \frac{1}{\omega_{SCi}^2} = L_{11}C_{S1} + L_{22}f_2^2 C_{S2}\, 1/f_2 + L_{33}C_{S3}$$

$$+ L_{11}C_{g1}$$
$$+ (L_{11} + L_{22}f_2^2 + 2L_{12}f_2)C_{g2}$$
$$+ (L_{11} + L_{22}f_2^2 + L_{33} + 2L_{12}f_2$$
$$+ 2L_{23}f_2 + 2L_{13})\, C_{g3} \quad (7)$$

In this allusion, considering the short circuit in the second disk be what follows:

$$\sum_{1}^{3}\frac{1}{\omega_{SCi}^{2}} - L_{22}f_2^2C_{S2}\,1/f_2 = \quad L_{11}C_{S1} + L_{33}C_{S3}$$

$$+ L_{11}C_{g1}$$
$$+ (L_{11} + \ L_{22}f_2^2 + 2L_{12}f_2)C_{g2}$$
$$+ (L_{11} + \ L_{22}f_2^2 + \ L_{33} + 2L_{12}f_2$$
$$+ \quad 2L_{23}f_2 + \ \ 2L_{13})\ C_{g3} \qquad (8)$$

- The series capacity and self-inductance of disk one and three constants.
- Various methods have been proposed to evaluateM_{0i}, the analytical method which is based on the analytical calculation of inductances equivalent to $M_{0i}$and can be estimated by optimization. These methods produce close results. Whether it is a convention M_{0i} estimated as M_{0m}.
- Let it be a convention on the left part as follows

  $\hat{\psi}_{ocnf} = \sum_{1}^{3}\frac{1}{\omega_{SCi}^{2}} - L_{22}f_2^2C_{S2}\,1/f_2$ (9)
- As previously mentioned before that the series capacity and self-inductance in non-defective disks, it's considered constants and it will be the following:
- Calculate the amount of ψ_{Ocnf}

  $\psi_{ocnf} = \sum_{1}^{3}\frac{1}{\omega_{SCi}^{2}} - L_{22}C_{S2}$ (10)
- Let the difference between before and the occurrence of the displacement be calculated as follows:

$\Delta\psi_{\mathrm{ocnf}} = \hat{\psi}_{\mathrm{ocnf}} - \psi_{\mathrm{ocnf}}$ (11)

The imbalance of the turns of the coil of the transformer in per disc with a high number of turns or low (short circuit) causes many damages to the body of the transformer and changes its lifestyle. can be seriously damaged all parameters of winding.

4.4.1. Axial displacement (5mm) with SC (40%) in disk 5

In fact, axial displacement and short circuits often lead to catastrophic damage to the active parts of the transformer. Thus, it is interesting to simulate such a situation as closely as possible. such as this malfunctions affect the frequency response clearly. A comparison of the frequency response of the reference model and that of a shift of 5 mm and a short-circuit of 40 % is presented and the difference in the frequency bands can be clearly seen in the figure 4.7.



Figure 4.7: A graphical representation of the impedance in the event of an axial displacement between disk 5 and 6 with SC.

4.4.2. Axial displacement (20mm) with SC (40%) in disk 5

In this case, the displacement ratio is large, as well as the short-circuit ratio. A big difference appears between the displacement of the resonance frequencies. This type of fault also causes a significant change in winding symmetry. The following figure 4.8 shows how different the resonant frequency shifts are from the frequency response of the reference model.

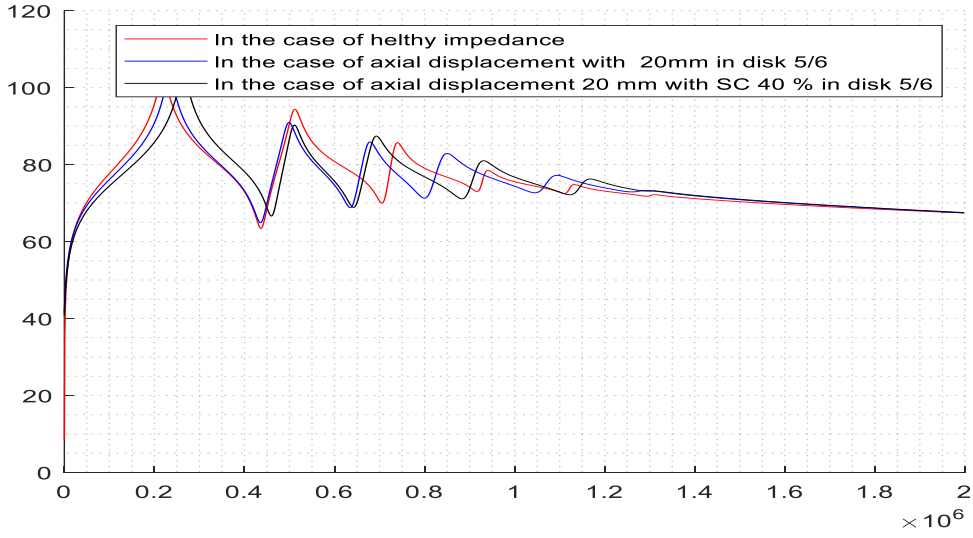


Figure 4.8: Axial displacement (20mm) with SC (40%) in disk 5.

The process of estimating the severity and the location of axial displacement has to be studied extensively. it is needless to emphasize that early detection of such a winding condition is crucial. wherein avoided falling into exorbitant costs of maintenance. Figure 4.9 depicted the accuracy of AD in winding direct effect on winding parameters, resonance frequencies, and transformer behavior in general.

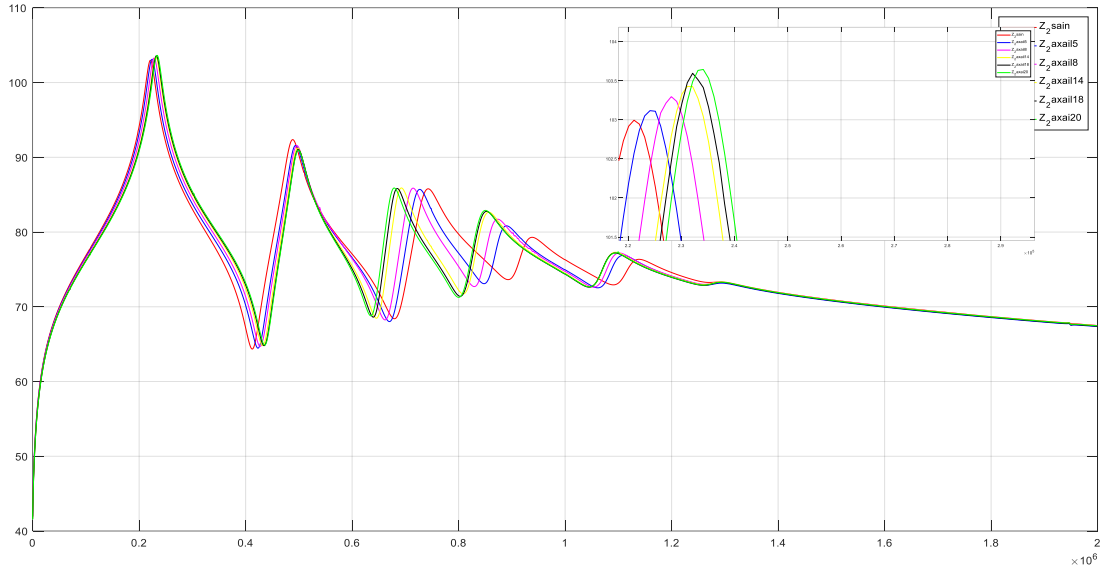


Figure 4.9: Measured of FRA for isolated winding with AD between D5 and D6.

As mentioned previously, this study aims to study the axial displacement by taking into account the short circuit in turns in isolated winding disks. This phenomenon has been studied with displacement ratios 5 mm, 8 mm, 14 mm, 17 mm and 20 in the case of short circuit ratios in each disk by 5% 10%, 20%, 30%, and 40%, which was summarized in Table 4.1, to measure the parameters of the winding before the occurrence of the malfunction and after its occurrence, then calculate the difference each time, in order to know the extent of displacement and the location of displacement on one side and on the other hand, to show the extent of the ratios of the short circuit.

Case AD with degree of SC	O_{cnfs} (KHZ)					Δcg (pf)	ΔLeq (mH)	δ (mm)	ψ_{ocnf} D (e-13)	$\Delta\psi_{ocnf}$	degree of SC
	1ST	2nd	3rd	4th	5th						
D5- D6	241	503	715	924	1135	1.75	-0.0010	5mm	7.3626	1.2844	20%
	244	504	706	907	1125	2.4	-0.0011	8mm	7.4634	1.7949	20%
	236	506	682	868	1108	5.6	-0.8644	17mm	7.7077	4.2381	5%
	227	492	766	881	1132	4.5	-0.0015	17mm	7.4536	1.6964	20%

D3-D4	227 475 762 888 1129	3.8	-0.89830	14mm	7.4294	1.4549	5%
D2-D3	227 495 765 886 1135	3.7	-0.0014	14mm	7.4124	1.2844	20%

Table 4.1: Results of axial displacement with short-circuit consideration for different disks winding.

4.5. An illustrative example of AD with SC consideration in disk 5

After an axial displacement with 05 mm, accompanied by a 20 % short circuit in winding the new and old equivalent inductance respectively are $\mathcal{L}_{eq} = 8.6863\ \mathrm{m}H$ and $L_{eq} = 9.7204\ mH$. The equivalent inductance decreases with reason of the axial displacement and the short circuit in the turns. The change also affects both the resonant frequencies and the total capacitance.

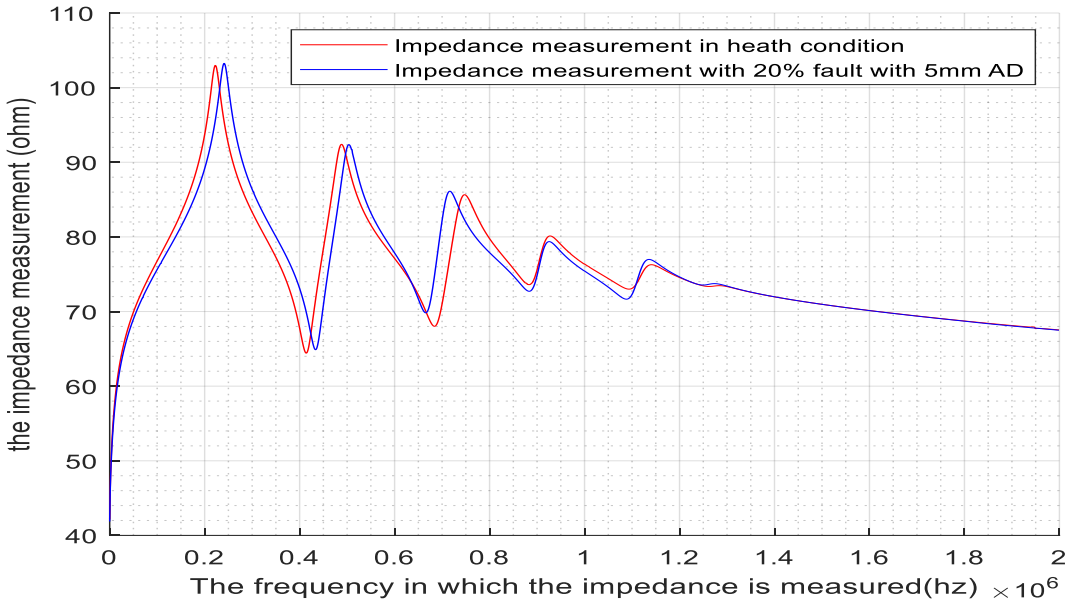


Figure 4.10: Example of AD with cc consideration in disk 5.

4.6.Deformation instigated by radial

The flow of an electric current within a magnetic field creates an electromagnetic force. The exposure of the winding to this force is proportional to the current passing through it and the strength of the flux. As shown in Figure 4.11 the gap between the windings has the highest radial forces because the leakage fluxes are highest in these locations; the conductors on the other side of the windings have zero radial forces because of zero leakage flux. When the winding is wound tightly, higher radial forces on conductors are transferred next to conductors which have lower forces. As a result, the total radial force exerted on the winding is shared by each conductor evenly, so the average radial force on one electrical turn (can be several conductors) per unit circumference length based on Equation (18) is

$$F_{unit\ length} = (B_{max} I_{peak})/2 \tag{12}$$

where I_{peak} is the peak amplitude of the winding rated current I. The total radial force on a complete winding, if ignoring the reduction of the axial flux at winding ends, is

$$F_{rad} = F_{unit\ length} * \pi * D_{mwdg} * N = \frac{\mu_0}{2} * \frac{\sqrt{2}(NI)}{H_{wdg}} * I_{peak} * \pi * D_{mwdg} * N \tag{13}$$

$$F_{rad} = \frac{\mu_0}{2} * \frac{(NI_{peak})^2}{H_{wdg}} * \pi * D_{mwdg} \tag{14}$$

where $D_{mwdg}$is the mean diameter of the winding, m. $F_{rad}$is the maximum radial force generated by current I_{peak},

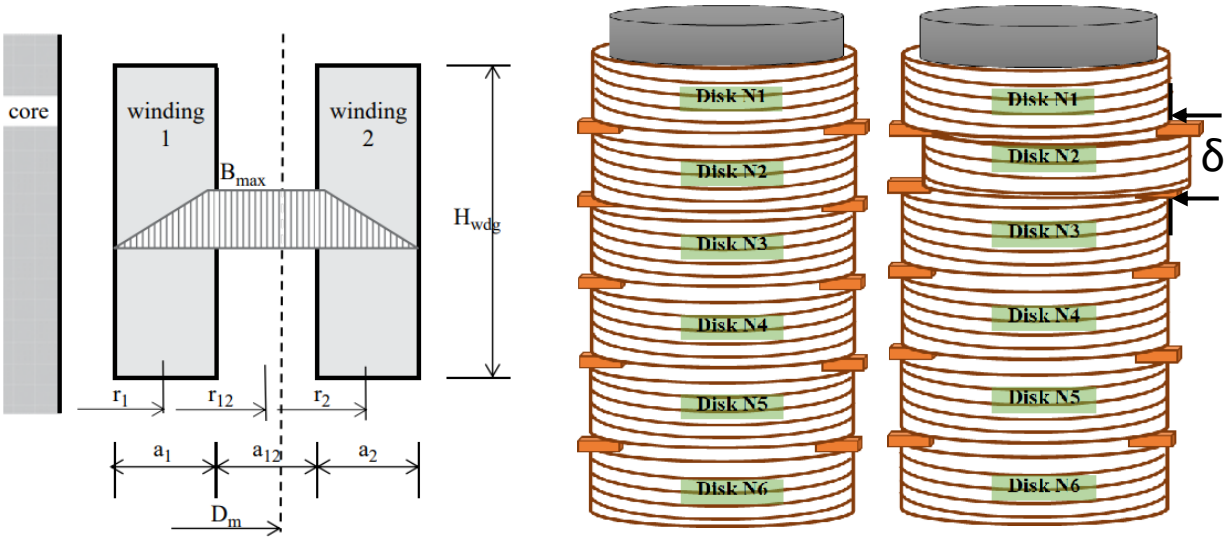


Figure 4.11: Leakage flux in two windings.

4.7.Failure mode caused by radial forces

There are three forces that arise from the radial force, which was dealt with carefully in the first chapter of this thesis.

The tensile stress: The tensile stress to which the outer windings are subjected, which change their circular shape in case the displacement is greater than the materials resisting this tensile, this leads to isolation of the broken conductor and a breakdown in the axial stability of the winding due to local swelling outside the circumference of the spacer [96].

Buckling: The winding is twisted or deformed in the form of buckling as a result of the excessive pressure caused by the electromagnetic force. The windings are exposed to two types of buckling as sketched in figure 4.12: forced buckling, in which the conductors bend inwards, and free bending, this type of deformation is more frequent. A number of factors that contribute to the occurrence of free buckling, including the initial deflection and the diameter of the winding, and the geometry of the conductor are decisive factors in the free deformation of the critical stress [97]. This type of torsion reduces the capacitance between the windings and the mutual inductance between the two windings in the deformation position. Moreover, the shunting capacity of the LV winding will increase due to the reduction of the distance between the LV winding and the core [18]. It also increases the average distance between HV and LV files. This will result in a decrease in the amplitude of capacitance winding between HV to LV. This type of deformation is known as forced buckling (figure 4.12 a) [19].

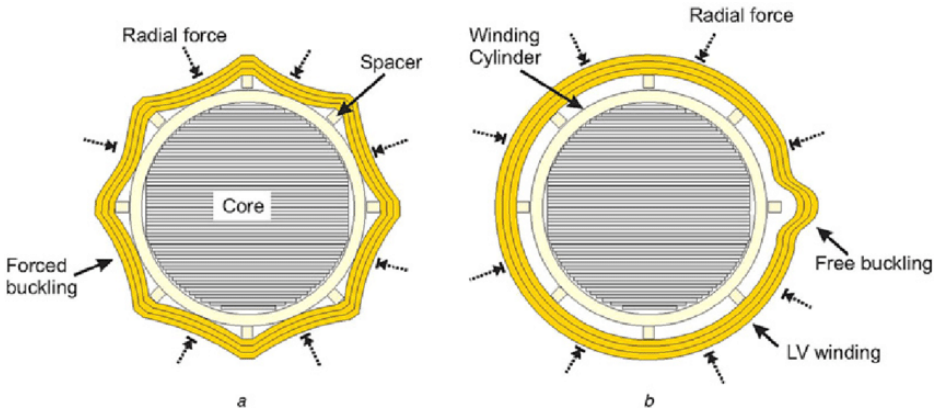


Figure 4.12: Deformation by buckling (a. Shape after free buckling. b. Shape after forced buckling).

Spiraling: The following image depicts a pattern of radial deformation that occurs frequently in the helical winding. The spiraling conductors in a transformer helical winding may result in catastrophic failure under the action of torsional short-circuit electromagnetic forces [98].

Torsional electromagnetic forces are responsible for the deformation of the winding in the circumferential direction. When helical winding has high pitch, such as one electrical turn consisting of several cables axially stacked, the risk of spiraling is high [99].

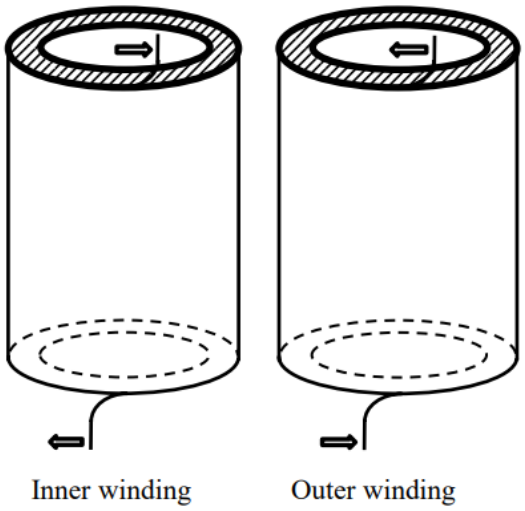


Figure 4.13: Spiraling Failure.

4.7.1. Radial displacement in disk 2 by change Cg2 with 20%

The study of the effect of the ground capacitance is a lofty goal because of the importance of knowing the behavior of the transformer during transient faults. whrere, Yıldırım Özüpak observed that changing the value of the ground capacitance decreases and increases the value of voltage. The most important element in the coupled ladder network that clearly reflects the radial displacement is the ground capacitance. In this case, Here the shunt capacitance at the line end is increased from the reference value of 18.85 pF to 22.62 pF in disk 2. It is observed that there is a displacement in the resonance frequencies.

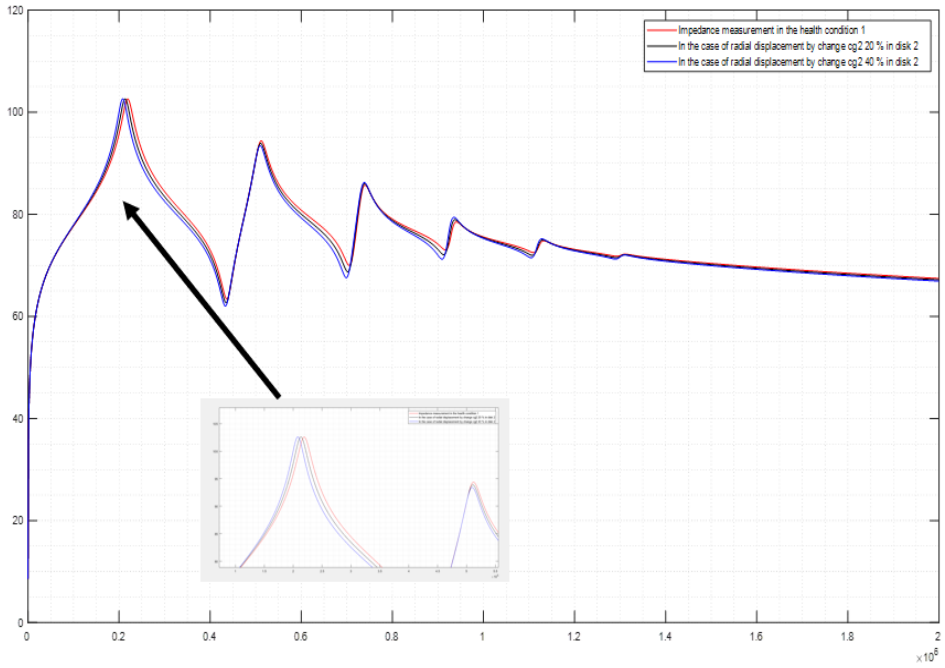


Figure 4.14: Radial displacement in disk 2 by change Cg2 with 20%.

The FRA measurement traces in figure 4.15 the end short circuit test of isolated power transformer winding has showed the effect of radial displacement. The figure depicts the FRA signature in case of radial displacement for simultaneous fault in disks 3 and 4 by changing C_{g3} to and Cg to compared with the corresponding base FRA fingerprint. the frequencies of resonances of the DPF have been changed, this change is evident in the initial frequencies as shown in figure 4.15 the low frequencies have changed much.

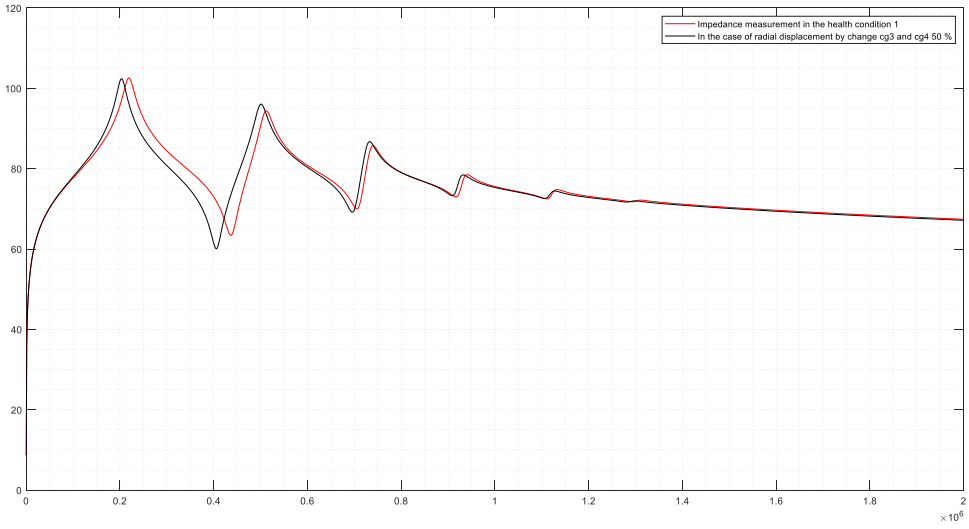


Figure 4.15: Radial displacement by change Cg3 and Cg 4 with 50%.

Case RD Fault	O_{cnfs} (KHZ)					C'_g (pf)	ΔC_g (pf)	$\Delta\psi_{ocnf}$	degree of C_g Change
	1^{ST}	2^{nd}	3^{rd}	4^{th}	5^{th}				
D3 and D4	204	502	734	933	1129	2.827e-11	-0.0010	1.2844	50%
D3-D4	214	506	739	937	1132	4.5	-0.0015	1.69	10% and 30%

Table 4.2: Radial displacement in disk D3 and D4.

4.8. Conclusion

Frequency response analysis (FRA) is among the tests that do not leave the power transformer during its lifetime for the early detection of distortion of windings. Accurate diagnosis can detect the internal fault of the transformer winding based on measuring FRA and the internal transformer's characteristic parameters. The frequency response analysis measurement process of the transformer winding is to determine the degree of changes in the inner windings of the transformer based on the change amount, the size, the area affecting the change and the direction of the frequency response change which is quoted from the response changes in different frequency domains of the inner winding parameters of the transformer, then it can help you to determine if the transformer is severely damaged or needs an overhaul based on the measurement results. The proposed of this chapter is to examine the condition of transformer windings, in the event of one of the three transient mechanical failures. The failure modes in the power transformer due to axial forces are divided into three modes, which are axial displacement, axial bending, and tilting of the conductor, which were discussed in the previous sections. Each of them causes a radical change in the behavior of the power transformer, and therefore it was necessary to study one of these types of failure by simulating how it occurs on the winding of an insulated electrical transformer. The first section in this chapter the effect of the axial displacement has been treated. The study showed that a small displacement between the winding discs leads to an asymmetry in the distribution of forces, causing a change in the winding parameters, which is reflected in the displacement in the resonance frequencies. The second section in this chapter serves to alert the risk of axial displacement with a short circuit and the need to take into account its side effects. The analysis of the FRA spectral is an appreciable help to distinguish between an alarm generated by an axial displacement is a global solution to diagnostic the problem of axial displacement with SC consideration. moreover, the implementation of a platform combining to calculate the differences $\Delta\psi_{ocnf}$ and ΔL_{eq} which

allows better access to detailed information on the characteristics of the axial displacement with SC consideration by determining the location and percentage of the damage.

The conclusion that can be deduced by analysis of the FRA traces is that at the law and medium frequencies, the FRA trace is mostly affected by AD fault damage, in this zone, the effect of the equivalent induction is significant on the resonance frequencies, which in turn is greatly affected in the case of axial displacement. Whereas at high frequencies RD mainly influences FRA trace.

Chapter 5: Test Platform Dedicated to Power Transformer Winding Diagnostics

5.1. Introduction

This chapter has broached the development of a platform to control the LCR meters via computer. This approach has been developed with two software MATLAB and LabVIEW in order to facilitate the control of the device and to make engineering user's work comfortable. This platform can also transfer large datasets from LCR meter devices to computer memory at a high speed, and save data. Use this approach in the testing routine of electrical power transformers which is usually recommended before it leaves the factory and after installation, during the equipment that exists in service to assess its condition. The ultimate goal of which is to chart the deterioration of the equipment during its life course. Setting up and developing a reliable platform for diagnostic power transformer has always been a primary destination and challenging task in this thesis. Using this test platform, it is possible to detect mechanical malfunctions of the electrical power transformer windings that can cause it to go out of service and cause an electrical service outage. Also, early detection of mechanical and electrical malfunctions of its winding will reduce the risks to the life of the power transformer. Property maintenance and detection reduce downtime by minimizing catastrophic failures. To carry out the successful operation of the power transformer it is necessary to prepare an effective test platform. a test bench can be performed basic tests of the power transformer can be carried out. The realization and preparation of a test bench will allow to be carried out:

a. Carry out communication and data loading between the LCR and the PC.
b. Control of LCR with MATLAB and LabVIEW.
c. Carry out the various tests on the coils to determine the shape of the coil and to determine the change in frequency responses in the event of the fault.

Development of a test platform dedicated to analyzing and assessing mechanical deformation of power transformer windings is has a prominent importance in the early detection of mechanical failures, by reducing failure, reducing downtime and enhancing operational efficiency. Also, facilitating the testing process by developing new test platforms helps provide the information needed to design the maintenance plan.

5.2. Software design and instrumentation

5.2.1 Data acquisition

For most engineers and scientists, data acquisitions are the key to analyzing most of the problems. It is often frequently necessary to monitor the equipment from the inside not possible due to the difficulty of the cost, or the process itself being harmful to the rest of the parts. Dealing with signal change over time is the appropriate solution [2]. The process of reading electrical signals into a computer from sensor equipment may represent the state of the physical condition of the equipment. The occurrence of a change in the power transformer winding parameters with an increase in the capacitance or a decrease in the equivalent inductance from the normal levels indicates the onset of a radial or axial displacement. The process of detecting such these faults in its early stage by the frequency response measurement is very important and necessary for any transformer to correct their faults. Using a computer to control LCR meters automates measuring the parameters of the power transformer and the data acquisition process, enabling more data collection in less time with fewer errors. This methodology facilitates early detection and analysis of possible faults as mentioned previous [100]. The basic steps in the development of this diagnostic platform used for detection faults are covered in this chapter step by step from the measurement networks of various parameters, such as the equivalent inductance, capacitance and resistor. Using algorithms to form an equivalent reference circuit of isolated transformer winding. Obtaining data and transferring it to the platform for processing and analysis. All important steps are explained in this chapter. In this chapter, we consider the detection of mechanical winding faults using the test platform. The defects were introduced by inserting a reflection wedge in the case of AD. the development platform assesses the location of the defect and its severity. The same recent method developed to determine AD can be also used to estimate RD.

5.3 Design of the platform

Developing a test platform to detect the electrical and mechanical faults of the power transformer is essential, especially in recent times with the increasing demand for electricity dramatically. Firstly, the test platform consists of hardware device LCR meter and PC. The figure below illustrates the frame structure that enable to connect LCR meter by PC via RS-232 to save the data or measure parameters winding. while the second section includes a successful FRA-SMI methodology that has been developed for the contraction of a mutually equivalent model of a transformer winding based on the interpretation of the FRA signal morphology by using metaheuristics optimization algorithms. In the last section of platform development that

can be detected and located faults and failures in power transformer windings, such as axial and radial deformation of windings; short circuits or cuts. Through this platform, it is possible to detect earlier the electrical and mechanical faults of the power transformer windings as previously mentioned. In addition, the efficient operation of the transformer is maintained. To ensure the continuity of the service, a maintenance plan is necessary, the basis of this plan is to collect the data and through this platform, the necessary data can be obtained.

The main characteristics of the platform are summarized as follows:

- The development of a new approach that is able to form the equivalent model construction structure of a winding.
- Provide a concise and intuitive visual interface for calculating and assessing the severity of damage. By drawing the curves on the interface, the displacement of the resonance frequencies in the event of a fault can be determined.
- Based on the data obtained by measuring the impedance of the power transformer and simulating faults on the equivalent model construction can be assessed and detected the severity of the damage through this platform.
- Collecting data through routine tests, and this is especially for detecting faults of the type of short circuit, and this is very important for detecting faults in its early stage.

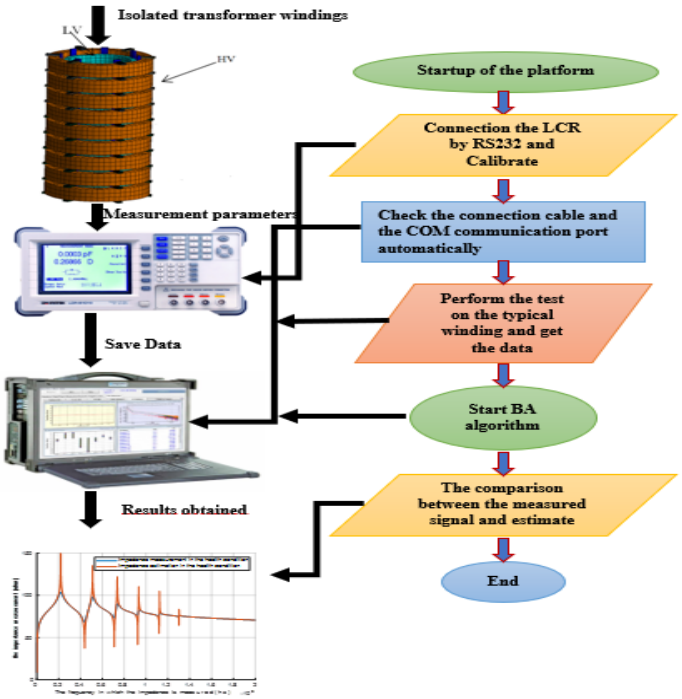


Figure 5.1: Block diagram explain the main steps of the platform.

5.4. LCR meter via PC connection

The test platform consists of hardware device LCR meter and PC. The two Figures 2 and 3. below illustrates a program interface that was developed to enable the connection of an LCR meter by PC via RS-232 to save the data or measure parameters winding. The program provided for the purpose of obtaining data about the start-up tests, maintenance tests, or even routine tests for some types of malfunctions. The data acquisition section of the test platform is designed to provide the measured data and historical simulation data for power transformer winding, to detect the changes that occurred during its life stages. The following most important steps used to achieve the objective:

step 1: install the USB driver

step 2: get the device information

step 3: add an event structure and awhile loop to the program

step 4: define the measurement mode using the command ‘’ conf’’

step 5: get the measurement value

step 6: set the frequency of the instrument by using the command ‘’freq’’

step 7: set the length unit by using the command ‘’range’’

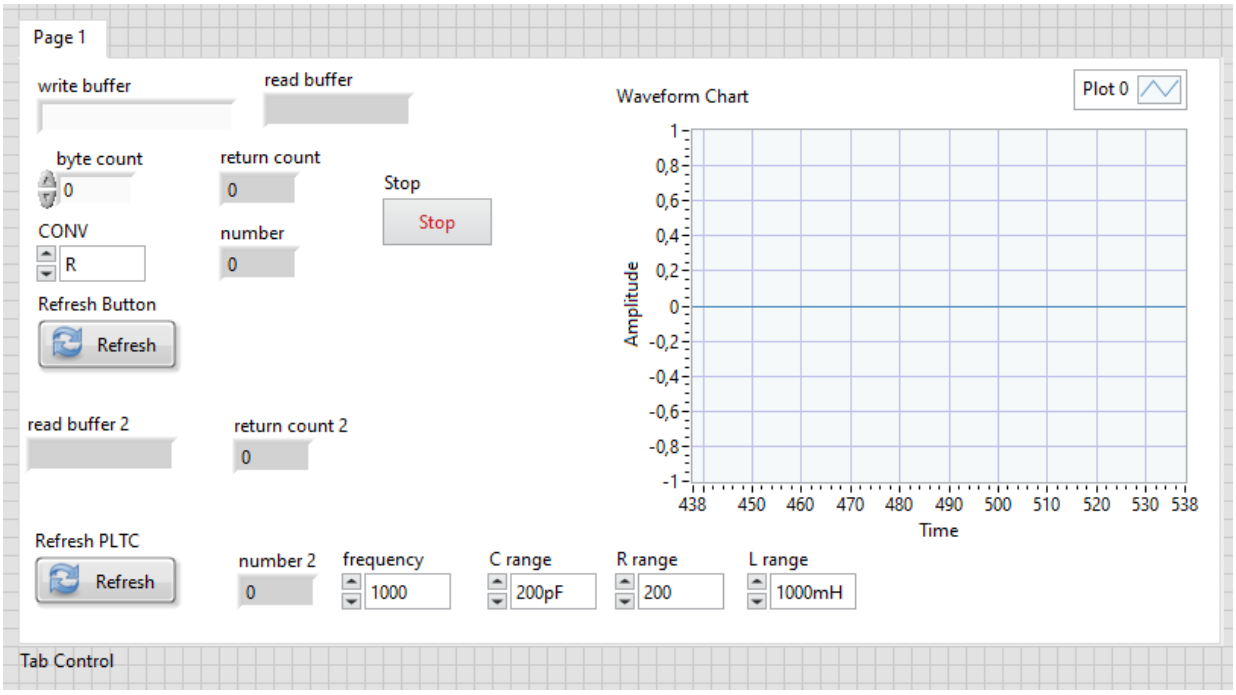


Figure 5. 2: Table for control LCR meter through LabVIEW.

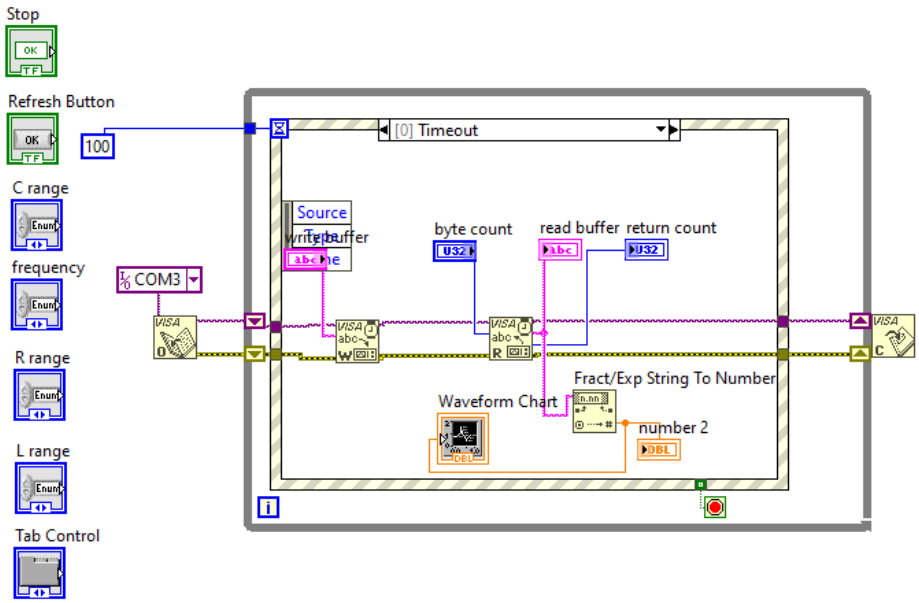


Figure 5.3: program for control LCR meter through LabVIEW.

5.5. Particle optimization algorithm (PSO)

In this section, a new efficient method is proposed to construct an equivalent mutually coupled transformer circuit for an insulated air-core transformer. This approach aims to determine the model parameters of self-inductance, mutual inductance, series capacitance, and ground capacitance. Two programs have been developed in this chapter, in the first program both self-inductance and mutual inductance are determined, while in the second program, the series and ground capacities are determined.

5.5.1. The process of estimates of self and mutual inductances l_s and M_{ij}

To find the optimal solution that fits the measurement data, the expression for the equivalent inductance has been simplified to obtain the equation that contains two unknowns l_s and λ, which is taken as the objective function of the search algorithm for estimate l_s and λ then the mutual inductances M_{ij}. In this case, the coefficient λ must be substantially constant for the different mutual inductances in case of an isolated and uniform transformer winding ($M_{i,ij} \cong M_{ij,i}$).

The equivalent inductance can also be expressed as the objective function,

$$L_{eq} = Nl_s + 2\sum_{i=1}^{N-1}(N-i)M_{i,i+1} \cong l_s\left[N + 2\sum_{i=1}^{N-1}(N-i)\lambda^i\right] \quad (1)$$

as mentioned in chapter 2, we have the following mathematical inventory:

$$l_s > M_{12} > M_{13} > M_{14} > M_{15} > M_{16} \quad (2)$$

$\lambda_{min}^{i}\, l_s < M_{i,i+1} < \lambda_{max}^{i}\, l_s$

With $0 < \lambda_{min} < \lambda < \lambda_{max} < 1$

With $M_{12} = \lambda\, l_s, M_{13} = \lambda^2 l_s, M_{14} = \lambda^3 l_s, M_{15} = \lambda^4 l_s, M_{16} = \lambda^5 l_s.$

The main steps of the swarm algorithm used in constructing an equivalent model of the isolated winding of a power transformer are summarized in the following steps:

The first step: enter the data that is divided into the objective function:

$L_{eq} \cong l_s\left[N + 2\sum_{i=1}^{N-1}(N-i)\lambda^i\right]$ with two variables l_s and λ

The second step: Determine the input matrices for each of the two variables and enter the values for each W represents the weight of inertia. C1 and C1 are positive constants called learning factors. r1 and r2 are two random values within the range [0,1].



Figure 5.4: Initialize parameters.

The third step: start implementing the swarm optimization algorithm based on the input data.

The fourth step: Calculate the fitness function for the values for each individual (so that P_{best} represents the best personal position) initially, which depends on the objective function, as the function represents the equation number (1).

Step five: Calculate the value of g_{best} (best overall location), comparing the value of the fitness function with the best location in the swarm as a whole. If the current value is better than g_{best}, then the value of g_{best} is set equal to the current location.

The process is repeated according to the programming of the algorithm, as there are two ways to stop the algorithm, either by the number of iterations or when the algorithm reaches a known error rate.

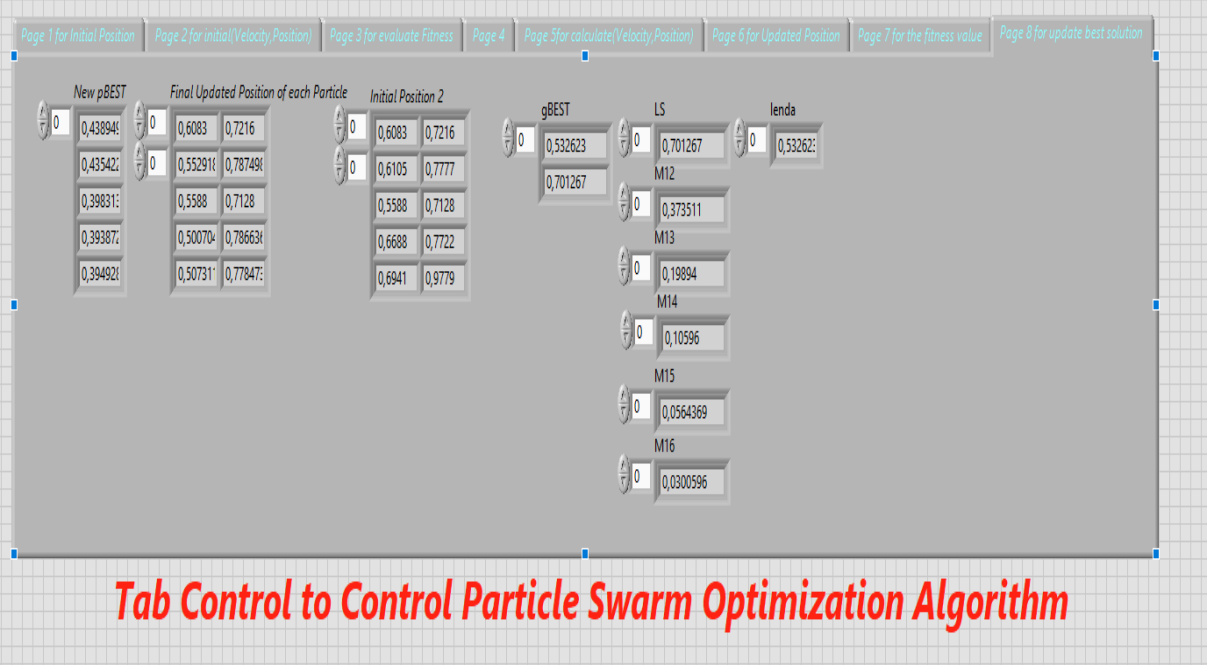


Figure 5.5: Update best solution**,** with calculate self-inductance and mutual inductances.

The parameter identification of the isolated power transformer winding is carried out according to the flowchart in the presiding figure, where all the input parameters of the algorithm are entered directly as follows:

- Initial position: the two-vector of λ and l_s.
- The number of sections N of the equivalent circuit, which is initially equal to the number of frequencies O_{cnfs} extracted $N = 6$.
- To find the optimal solution of self-inductance and mutual inductances, the objective function and search space must be specified for the optimization algorithm. Additionally, to restrict the bounds of the search space for the proper and mutual inductances, the upper and lower values of λ and $l_s$are randomly chosen as present in the initial position.
- The algorithm was used to optimize the self-inductance ls and the coefficient λ to achieve an equivalent model of an insulating transformer coil, in which the estimated results for a small number of iterations are $\lambda = 0.5326$ and $l_s = 0.7012$mH.

Calculation of mutual inductances $M_{1,1+i}$ by substituting the value of l_s and λ into equation $M_{1,1+i} \approx \lambda^i l_s$. The estimated values of the self-inductance and mutual inductances are given in the output vector as shown in the previous figure.

5.5.2. The process of estimates of the series capacitance $C_s$and the ground capacitance C_g

In this section, we choose the following function $C_{eq} = \sqrt{C_s C_g}$ as an objective function to determine the optimal values of C_s and C_g of this equivalent model.

The approximate estimated values of the capacities C_g and C_s are C_g = 19.02 pf, and C_s = 62.29 pf, and which are close to the values obtained using the bat algorithm in MATLAB.

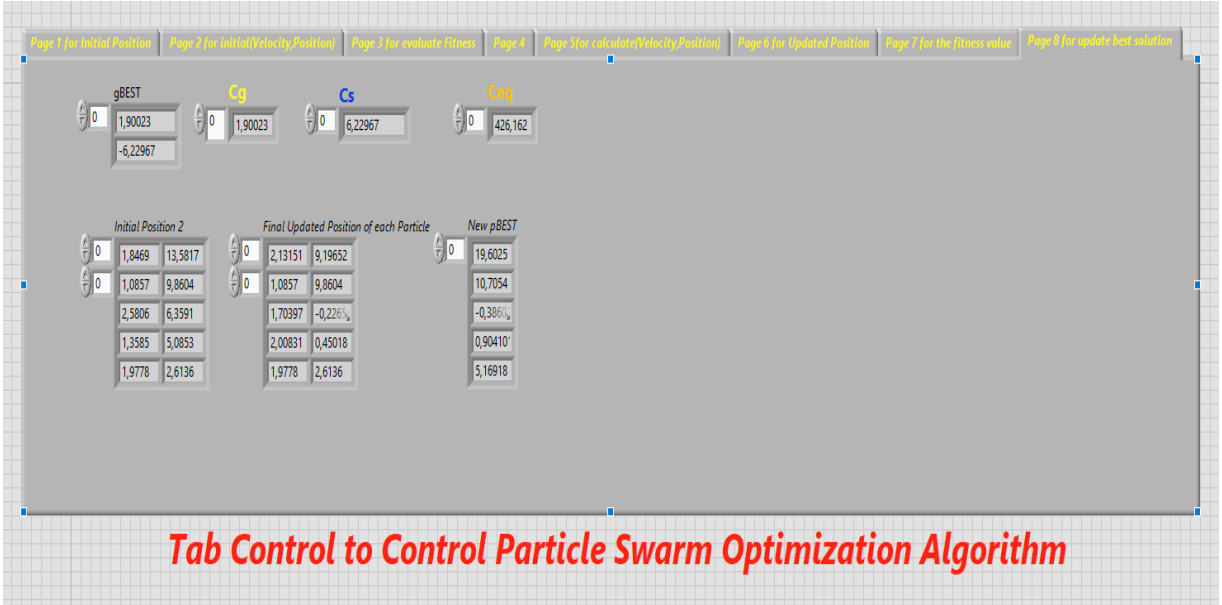


Figure 5.6: Update best solution**,** with calculate series and shunt capacitance.

5.6.Qualitative evaluation of short-circuit condition in power transformer windings

In this case, the ability of ψ_{ocnf} to capture the short-circuit extent in a number of turns is investigated. Careful analysis reveals that after a short circuit, ψ_{ocnf} is directly proportional to the quantities of the winding parameters. The factor ψ_{ocnf} decreases with increasing short-circuit rates in one disk. Therefore, through the platform, it is possible to determine the extent of the short circuit ratios in a single disk. This is the first time that the extent of short-circuiting (distortion in general) has been analytically linked to the deviation in FRA by introducing short-circuiting coefficients into the state space model as introduced in Chapter Two.

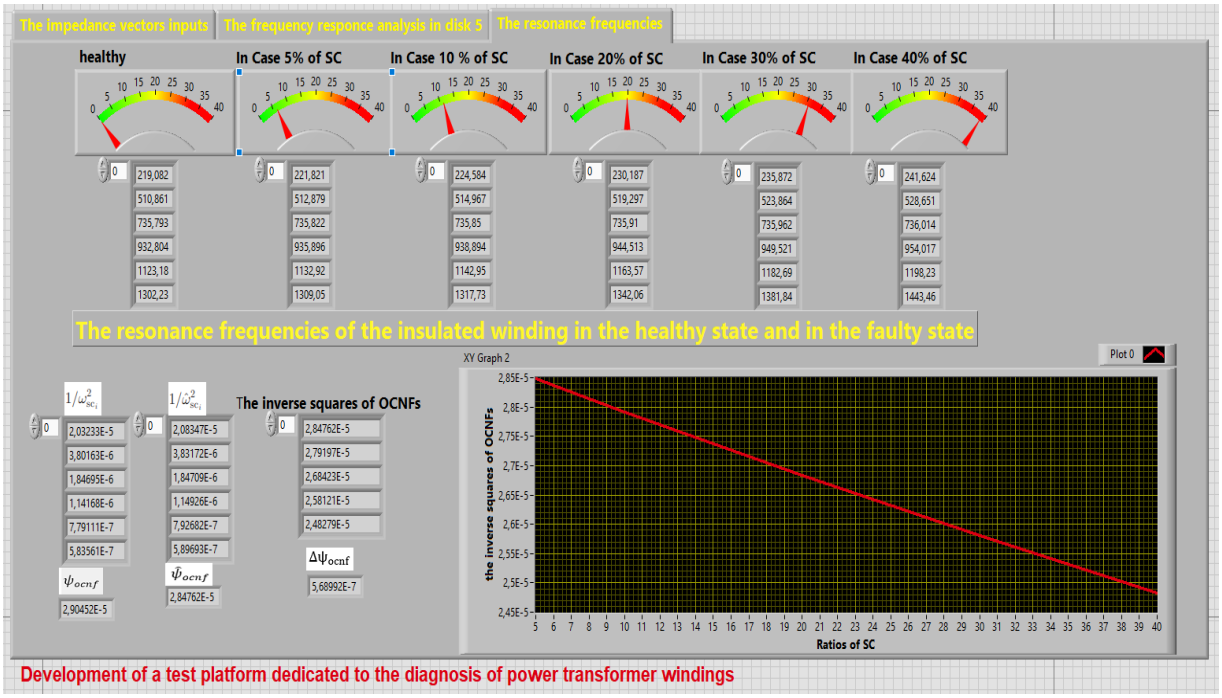


Figure 5.7: Test platform to diagnosis short circuit fault.

The simulation of the models obtained in the preceding chapter two is carried out. The objective is to validate these models, and to show that the results obtained are consistent. The simulation is carried out in two stages. The first concerns the absence of defects. The second step highlights the appearance of defects of 05%, 10%, 20%, 30% and 40% on disk 5. Figure 5.8 represents the simulation results for the model developed in chapter two.

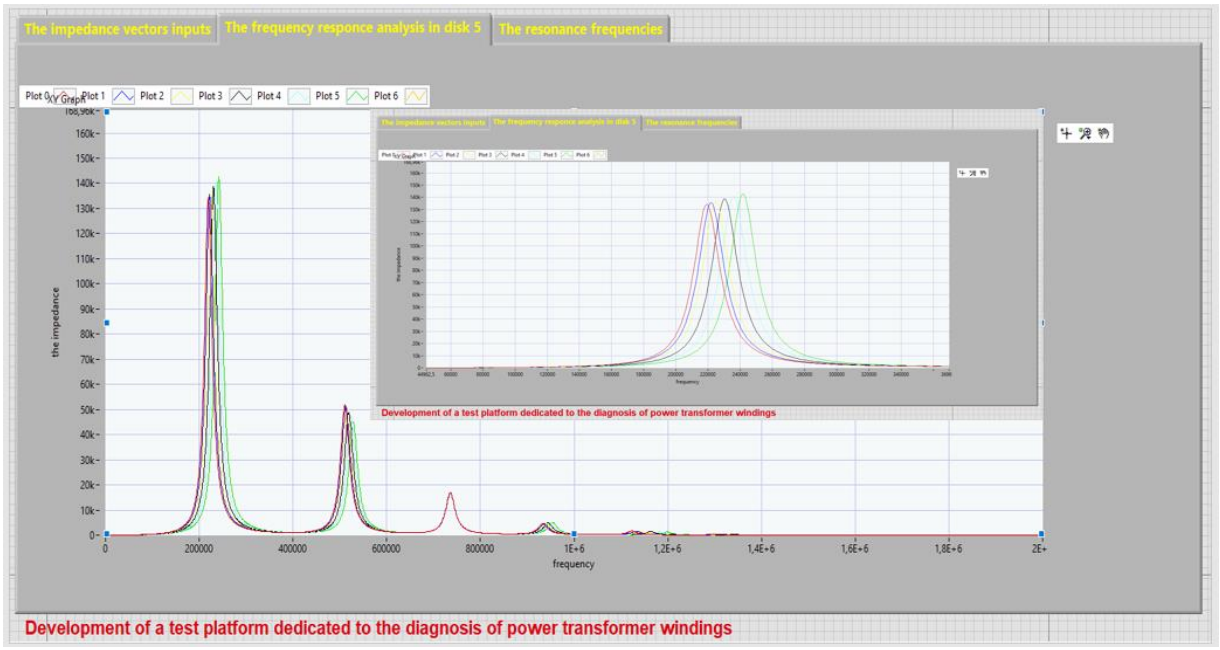


Figure 5.7: Frequency response analysis in the event of short circuit.

5.7. Qualitative evaluation of radial displacement condition in power transformer windings

Radial displacement and axial displacement are among the widespread electrical faults that affect the power transformer core and its windings. This section aims to develop a test platform capable of early detection of radial displacement and determining its location along with its severity. An example is presented in the figure below: the displacement occurring in the resonance frequencies after the occurrence of radial displacement. By measuring the impedance of the insulated winding in a healthy state before the fault occurs and after the fault occurs by inserting a wooden wedge between the disk and the rail. The investigation the resonance frequencies of the peaks that appear in the figure 5.8 and measure the equivalent ground capacitance before and after sufficient data for this platform to determine Location of damage.

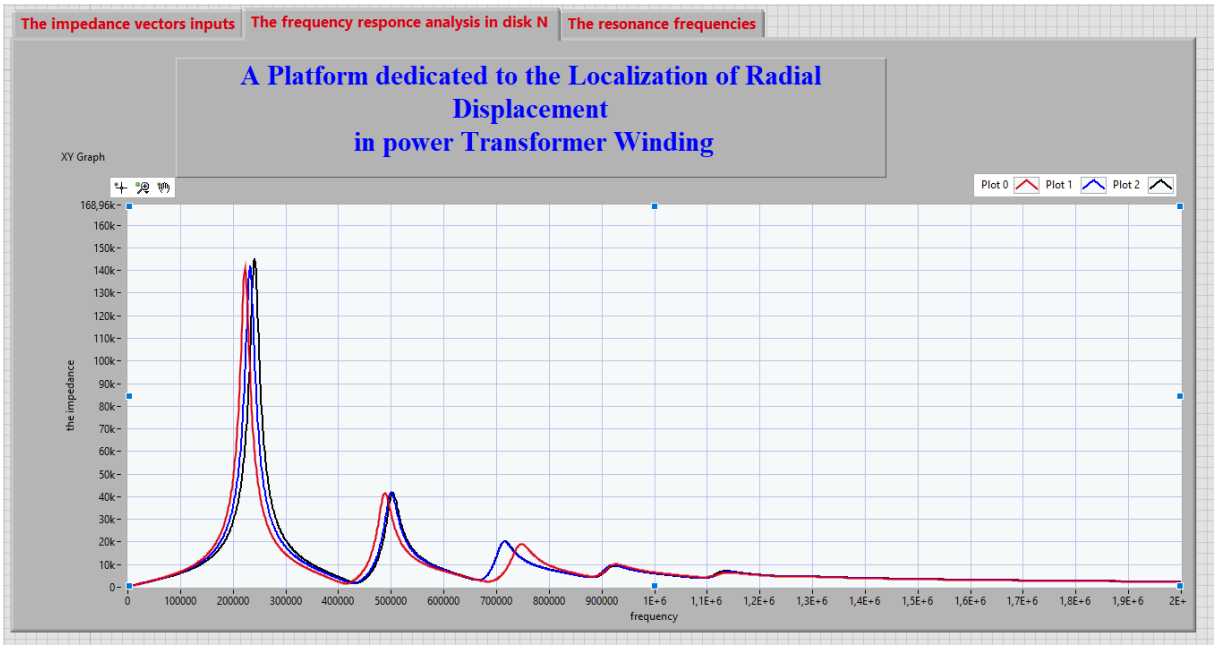


Figure 5.8: Measured FRA of the winding before and after RD.

The work presented by the Pritam Mukherjee and L Satish team in [95], by developing and generalizing a relationship between SCNFs or OCNFs and ladder network parameters is a powerful tool in determining the location and severity of damage as mentioned above, by calculating the difference between ψ_{ocnf}, which is the inverse sum of squares for SCNFs, and calculating the difference between the ground capacitance (ΔC_g) is sufficient to determine the location fault.

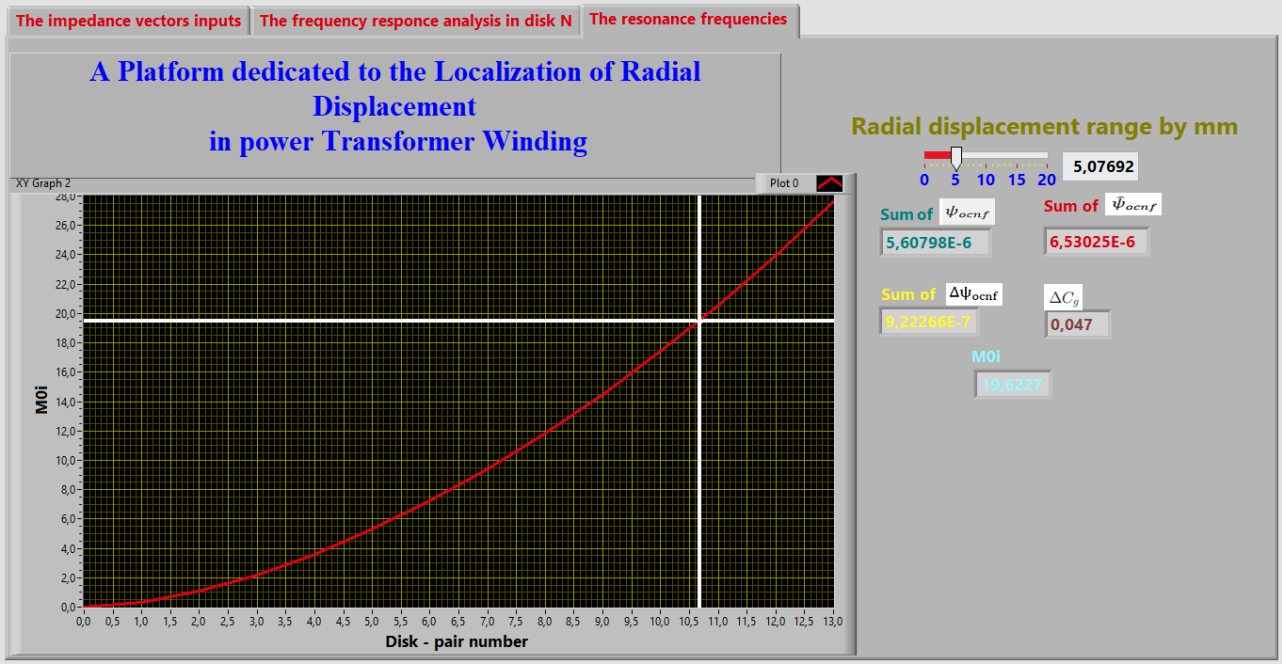


Figure 5.9: platform for Localization process of radial displacement.

5.8. localization of AD escorted by SC

Monitoring and assessing the AD, and supporting and prove the hypothesis that was submitted. The experiment of the AD with SC was repeated on all the winding disks with different displacement rates. After these experiments, it is evident that the monotonicity of $\Delta\psi_{ocnf}$ versus the disks.

To determine the axial displacement graphically, we use the $\Delta\psi$ curve in terms of X, and we follow the following steps:

- The calculation of the variation of $\Delta\psi_{ocnf} = 1.6964$
- Then the projection on the curve of $\Delta\psi_{ocnf}$ versus X
- Reading in the axis of displacement ratio with the disks of winding Which was identified between the two disks 5 and 6.
- Accordingly, we conclude that the axial displacement in the disk 5.

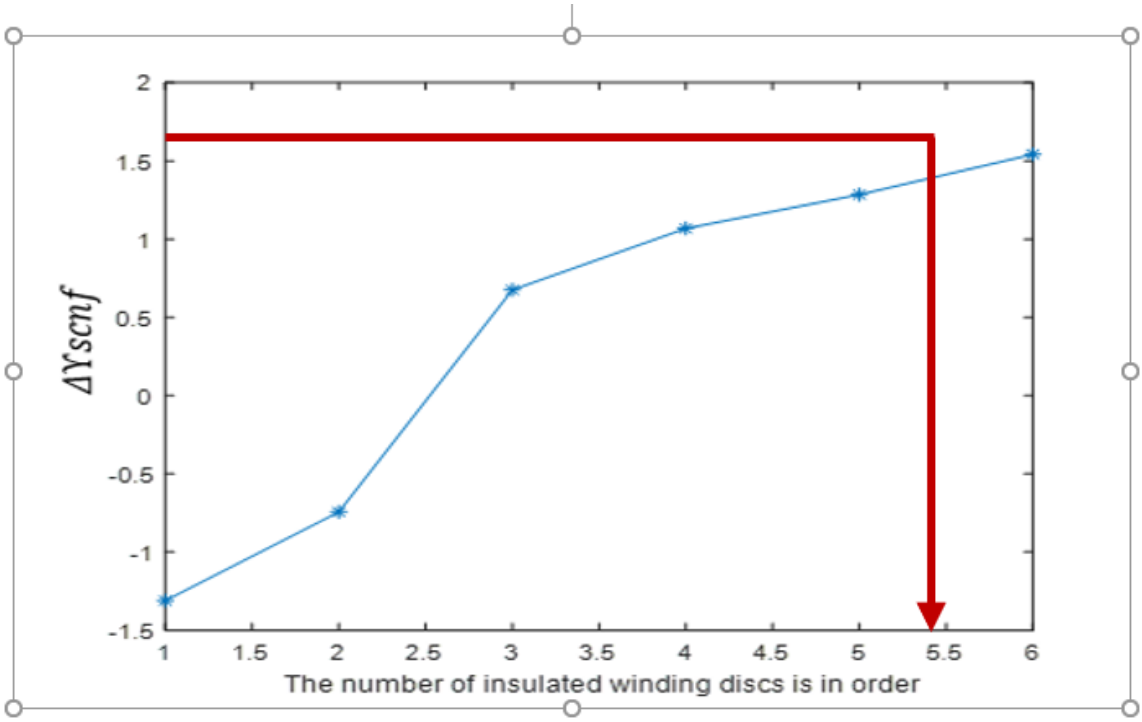


Figure 5.10: Plotted the change of $\Delta\psi_{scnf}$ in terms of x (number of disks).

5.9. Study of the change of the equivalent inductance as a function of the percentage of SC

In this part, have been analyzed the variation of ΔLeq in the case of the influence of AD with a short-circuit consideration on the model. The short-circuit effect is clearly evident in the transfer function merely of 5 % of SC in one of the rewinding disks. Figure 5.11. below shows the graphical representation of equivalent inductance as a function of short-circuit ratios proportion of 5 %, 10%, 20%, 30% and 40% in disk 5, although the displacement ratio δ was taken (5mm, 8mm, 14mm, 17mm and 20mm). This section presents several examples of the induction equivalent in terms of short-circuit ratios, and also explain the main steps to reach the degree after occurs of short-circuit in the winding accompanied by the axial displacement. An example can be provided to illustrate this point, let it be the inductance equivalent before and after an AC with SC respectively $L_{eq} = 9.7204mH$ and $\mathcal{L}_{eq} = 8.6863mH$, With an AD ratio of 5mm where ΔL_{eq} calculated is $\Delta L_{eq} = -1.0341mH$. By projecting the obtained value on the short-circuit ratio curves in the figure below, the value is between 10% and 20% and approximately 20% where the two lines intersect at the redpoint. In the second example, we have a value of $\Delta L_{eq} = -0.8644\text{m}H$ where the two lines intersect at the orange point so that the error ratio is 5 in milliseconds with an axial displacement of 17 mm.

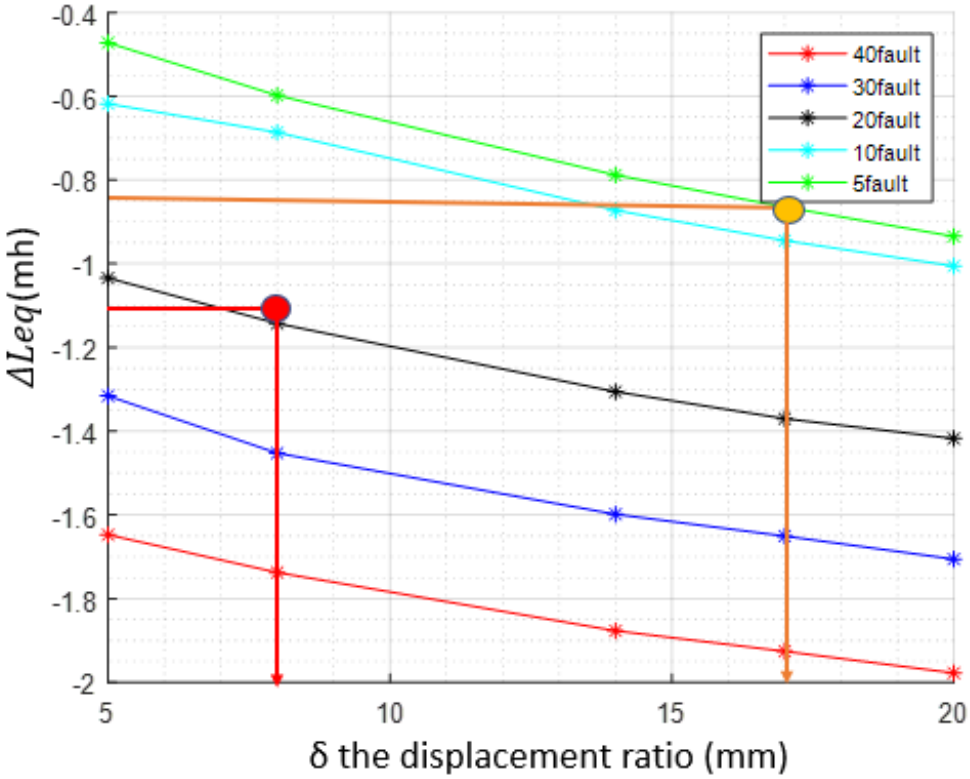


Figure 5.11: The change of the equivalent induction in terms of the displacement range in the case of different ratios of SC

5.10. Conclusion

This chapter was devoted to a platform to build an equivalent model for an isolated power transformer winding and also dedicated to analysing and detecting electrical and mechanical deformations. The biggest advantage of this approach is to perform a standalone synthesis task in a non-destructive way. This platform provides the technician with the necessary reports and evaluations about the health of the transformer after each test he performs. This makes the test more valuable and useful, as the technician can identify the level of damage, its severity, and weak points in the active parts of power transformers. In contrast to the traditional testing system, which only provides the technician with a malfunction.

- This system works to reduce the effort spent on establishing maintenance tests or factory tests.
- It gives the engineer the possibility of making an equivalent model of the transformer winding and performing some tests on it, such as short-circuiting the disks, observing the differences, and drawing conclusions.
- It provides many questionnaires about the health of the power transformer, to identify the problems it faces and work to fix them.
- The error rate in this type of test is almost non-existent.

The solution proposed throughout this work presents interesting performances and constitutes a realistic and achievable response at lower costs, to the problem of detecting short-circuit faults of turns in the disks in power transformers.

Conclusions

Conclusions

The search presented in this thesis deals with the diagnosis of electrical and mechanical faults in power transformer windings. The power transformer is subjected to frequent electromagnetic forces due the external short circuit, or when lightning strikes occur. These are the most prominent reasons. The voltage is concentrated on the ends of the pillows, and the voltage rise occurs when the impedance changes to the current waves and the overwhelming voltage at the change points between the transformer and the line. In addition to reflecting and transmitting transient waves of voltage and current (Traveling Wave). This voltage affects the ends of the cushions, causing a breakdown in the transformer windings, causing an axial or radial displacement. Also, the exposure of the transformer to vibrations when transporting it from the factory to the generation station is a reason for the occurrence of such types of malfunctions. The Sweep Frequency Response Analysis (SFRA) method is provided comprehensive information about the mechanical and electrical integrity of the active part of power transformers. In contrast to the traditional diagnostic method which is limited only to the detection of some defects. The SFRA is sensitive to external electrical interferences which may limit the comparability and can consequently lead to misinterpretation of the measurement results. In this thesis, the most important forms of failure affecting the transformer windings were discussed, and the sensitivity of the frequency response analysis for this type of failure showed a convincing explanation. The symmetry of the power transformer is altered when a fault occurs such as short-circuit. In transformers used for large electrical systems, the factory takes care of attaching and fixing the coil cushions to prevent the occurrence of any problems, if the insulation of the coils contract or dwindle. If it is not bonded and fixed at a certain pressure during manufacturing, some conductors are subject to displacement under operating conditions and the result is insulation breakdown and a short circuit between the windings. In addition, the insulation saturation with moisture the possibility of a short circuit between the windings becomes possible as a result of insulation corrosion. During the normal operation of a transformer in a state of load, subjecting it to severe and frequent electromagnetic shocks, which may lead to short circuit winding. These and other factors cause a short circuit in the transformer winding. Initially, the development of a state space model dedicated to the diagnosis of short circuit faults was established, taking into account the faults of short circuits of turns in the winding disks. Moreover, this model is appropriate for the use of diagnostic methods based on analytical models. As indicated previously, the behavior of the transformer was altered at the

time of the occurrence of a fault of short-circuits in the discs, the development of this new model required the redefinition of the matrices resistances, inductors, and capacitance and the introduction coefficients quantifying the defects. This led to a model describing the behavior of the power transformer in short-circuit fault mode. Using this suitable model, the short-circuit faults were detected until they occurred in small proportions. It was found that even a slight change of 5% in one of the winding disks can be detected, as it creates a prominent discrepancy in the response frequencies. This difference was also observed for the winding parameters.

Afterwards, in this thesis, the axial displacement and the axial displacement accompanied by the short circuit were investigated experimentally. The sensitivity of winding response due to the connection end-to end short-circuit test Showed satisfactory results in both cases it malfunctions. The experiments show that in case of axial displacement type failure, the mutual inductance decreases obviously, on the other hand, the frequencies response shift left side. Otherwise, in the case of axial displacement accompanied by a short circuit, where does the short circuit fault affect the rest of the parameters. It is true that the axial displacement has a significant effect on the behavior of the power transformer, but if it is accompanied by a short circuit, its effect appears clearly in the winding parameters and in increasing the resonance frequencies shift to the left. Redefinition of an analytical formal was established to locate and assess the axial displacement accompanied by SC, by rewriting the relationship in terms of short-circuit coefficients. The influence of radial displacement content on the frequency response spectrum has recently been a topic discussion in this thesis. While the radial displacement was treated analytical, the radial deformation will change the shunt capacitance of the winding significantly. A detailed study of radial displacement for different tests by changes of ground capacitive 10 % to 50% in one disk or more than one disk, change in Cg will move the local FRA resonance and antiresonance peaks shift to the left. The effect of the ground capacitance on the impedance spectrum appears clearly with every change in the Cg, as for the series capacitances, the self-inductance and the mutual inductance, there is no significant change in them.

Additionally, developing a program to obtain the transformer impedance measurement (data acquisition) is one of the highlight objectives of this thesis. Whereas the data acquisition systems, as their name indicates is the process used to gather information in order to analyze the behavior of system. Developing programs that allow communication between the device and the computer for the process of obtaining data acquisition in a shorter time and with fewer errors is very important in arranging the maintenance time and detect the changes that occurred

on the device. In this thesis and in its last chapter a program in LabVIEW was presented to exchange data between an LCR meter and a PC by using RS 232 serial communications.

Finally in this thesis, investigation in particle swarm optimization to determine parameters of isolated power transformer winding. the synthesis of the equivalent model of the transformer winding has been proposed to determine the inductance matrix. Mathematical simplifications are used to sufficiently reduce the search space for the optimization algorithm to obtain an accurate solution with an effective time in the low frequency range. On the other hand, A procedure for building the capacity matrix has been proposed. to determine the shunt and series capacitances of the equivalent model of the winding. A stand-alone diagnostic approach has been proposed to simultaneously locate and assess the severity of axial geometric deformations in the transformer winding. Since winding failures lead to changes in frequency behavior as well as changes in model parameters, this method is based on model parameters, where the characteristics of the inverse sum of the square of the frequencies of resonances with respect to variation in equivalent inductance change were used to locate and capture the severity of damage due to axial displacements. The direct extraction of the parameters used from the frequency response makes this method automatic. Developing a LabView program based on analytical method for identifying and evaluating the severity of mechanical faults, which can be a powerful and reliable tool in diagnosing mechanical faults of power transformers.

List of References

1. Jaspreet Singh. Transformer Failure Analysis: Reasons and Methods. International Journal of Engineering Research & Technology (IJERT) ISSN: 2278-0181 Published by, www.ijert.org ACMEE - 2016 Conference Proceedings.
2. William H. Bartly P.E failure analysis of transformer the Hartford steam Boiler inspection and insrance Co. Hartford CT.
3. Ashok Chavda. Sweep Frequency Response Analysis (SFRA) an Important Digestions tool for Power Transformer. DOI:10.13140/RG.2.2.19429.60645.
4. Martin J. Heathcote. The J & P Transformer Book Twelfth Edition a practical technology of the power transformer. CEng, FIEE.
5. James H. Harlow. Electric power transformer engineering, Publisher: CRC Press, Year: 2004, ISBN: 0849317045; 9780849317040
6. Angelo Baggini; Christoph Ploetner; Jean-Christophe Riboud. Functional Definition and Classification of the Power Transformer. Published in: IEEE Transactions on Power Delivery (Volume: 38, Issue: 1, February 2023). DOI: 10.1109/TPWRD.2022.3180625
7. https://megger.com/applications/transformers/bushings.
8. Dr. Dieter Dohnal on-load tap- changers for power transformers.
9. Transformer bushings Oil condenser type UP To 420kv.
10. Xiangning Lin; Jing Ma; Qing Tian; Hanli Weng. Malfunction Mechanism Analysis due to Nonlinearity of Transformer Core. Publisher: Wiley-IEEE Press. DOI: 10.1002/9781118653838.ch2
11. Scott D. Sudhoff. Transformer Design. Publisher: Wiley-IEEE Press. DOI: 10.1002/9781119674658.ch7.
12. Ahmed Abu-Saida. Power transformer Condition Monitoring and Diagnosis. IET the institution engineering and Technology.
13. https://studyelectrical.com/2022/11/transformer-windings-types-and-design.html.
14. Manuel Bolotinha. Power transformers windings. Electrical Engineer (Power Systems) [IST-Instituto Superior Técnico/1974]; Master in Electrical Engineer and Computers [FCT/UNL - 2017].
15. Bai Baodong; Xie Dexin; Cui Jiefan; O.A. Mohammed. Optimal transposition design of transformer windings by Genetic Algorithms. Published in: IEEE Transactions on Magnetics (Volume: 31, Issue: 6, November 1995). DOI: 10.1109/20.489573.

List of References

16. Yi Zhao, Weijiang Chen, Mingkai Jin, Tao Wen. Effect of winding transposition structure on the distribution of transverse leakage magnetic field Wiley. DOI:10.1049/iet-epa.2020.0414.
17. Reference in electrical power transformers - Prof. Dr. Mahmoud Jilani.
18. G. Bertagnolli, The ABB Approach to Short-circuit Duty of Power Transformers, 3rd ed. Zurich, Switzerland: ABB Ltd., 1996.
19. Mitushi Nigam ; Charles R. Sullivan. Multi-Layer Barrel-Wound Foil Winding Design. Published in: 2008 IEEE Industry Applications Society Annual Meeting. DOI: 10.1109/08IAS.2008.357.
20. Types of Transformer Windings: Cylindrical, Helical, Crossover & Disc Winding. October 26, 2020 by Electrical4U.
21. Zarko Janic, Zvonimir Valkovic, Zeljko Stih. Helical winding's magnetic field in power transformers. DOI :10.1007/s00202-009-0130-1.
22. K. Usha; S. Usa. Inter disc fault location in transformer windings using SFRA. Published in: IEEE Transactions on Dielectrics and Electrical Insulation (Volume: 22, Issue: 6, December 2015). DOI: 10.1109/TDEI.2015.005060.
23. Ibrahim A. Metwally Failures, monitoring, and new trends of power transformers. Digital Object Identifier 10.1109/MPOT.2011.940233. Date of publication: 4 May 2011.IEEE POTENTIALS.
24. Christina AJ, M.A. Salam, Q.M. Rahman, Fushuan Wen, S.P. Ang, William Voon. Causes of transformer failures and diagnostic methods – A review. https://doi.org/10.1016/j.rser.2017.05.165.
25. Diagnostic testing and monitoring of power transformers OMICRON.
26. Power Transformer Bushings – Inspection, Testing and Refurbishment. KAREN CALLERY, M.Sc. E, P.Eng. Hydro One Canada. 2020 CIGRE Canada Conference Toronto, Ontario, October 19-22, 2020.
27. https://www.electricalvolt.com/2022/11/what-is-transformer-bushing-construction-operation-failures.
28. Chenguang Yan, Zhiguo Hao, Member, IEEE, Baohui Zhang, Senior Member, IEEE, Tao Zheng, Shifeng Zhang, Guang Chao, Xian Yang, Dan Zhou. Simulation and Analysis of Power Transformer Internal Arcing Faults Overpressure characteristics. 2014 International Conference on Power System Technology (POWER 2014) Chengdu, 20-22 Oct. 2014.

List of References

29. Jaspreet Singh, Sanjeev Singh. Transformer Failure Analysis: Reasons and Methods. International Journal of Engineering Research & Technology (IJERT) ISSN: 2278-0181 Published by, www.ijert.org ACMEE - 2016 Conference Proceedings.
30. https://vietnamtransformer.com/our-news/the-disadvantage-of-large-exciting-current-in transformer.
31. https://benzoil.com.au/inhibitors-and-oxidation-in-transformer-oil.
32. https://savree.com/en/encyclopedia/pressure-relief-device-prd.
33. https://www.linkedin.com/pulse/transformer-oil-degradation-analysis-oksana-bichurina.
34. https://www.safetyfrenzy.com/is-a-leaking-transformer-dangerous.
35. https://www.linkedin.com/pulse/what-effect-moisture-transformer-engr-omar-alghamdi.
36. Electrical Power Equipment Maintenance and Testing. Book by Paul Gill. 2nd ed. p. cm. ISBN 978-1-57444-656-2 (alk. paper).
37. Priti Gite; A. S. Sindekar. Investigating mechanical integrity in power transformer using sweep frequency response analysis (SFRA). Published in: 2017 IEEE International Conference on Electrical, Instrumentation and Communication Engineering (ICEICE). DOI: 10.1109/ICEICE.2017.8191911.
38. M. Arivamudhan; S. Santhi. Analysis of Mechanical integrity in power transformer using statistical techniques. Published in: 2019 IEEE International Conference on Electrical, Computer and Communication Technologies (ICECCT). DOI: 10.1109/ICECCT.2019.8869152.
39. T. Sano and K. Miyagi, "Influence of Measurement Parameters on Frequency Response Analysis Diagnosis of Oil-Immersed Transformer," Electrical Engineering in Japan, vol. 186, pp. 18-25, 2014.
40. A. A. Reykherdt and V. Davydov, "Case studies of factors influencing frequency response analysis measurements and power transformer diagnostics," IEEE Electrical Insulation Magazine, vol. 27, no. 1, pp. 22-30, Jan.-Feb. 2011.
41. Manojmohan Subramanian. Detection of winding inter-turn faults. Detection based on frequency response analysis - Part I TRANSFORMERS MAGAZINE | Volume 7, Issue 1 | 2020
42. S. M. Islam and G. Ledwich, "Locating transformer faults through sensitivity analysis of high-frequency modelling using transfer function approach," in Conference Record

of the 1996 IEEE International Symposium on Electrical Insulation, 1996, pp. 38-41 vol.1.

43. https://electrical-engineering-portal.com/measurement-of-insulation-resistance-2.
44. Hipot Testing of Magnetic Components. Coil craft. Document 1226-2 Revised 10/02/17.
45. https://electrical-engineering-portal.com/what-is-hipot-testing-dielectric-strength-test.
46. Alex Rojas, Power Factor Testing in Transformer Condition Assessment - Is There a Better Way? 1-4244-0288-3/06/$20.00 (©2006 IEEE.
47. Brandon Dupuis. An Introduction to Electrical Diagnostic Testing of Power Transformers. OMICRON electronics.
48. Dr. P K Maiti. Significance of Transformer Oil Testing. Central Power Research Institute, Sector V, Salt Lake, Kolkata 700 091.
49. M.K. Gradnik. Physical-chemical oil tests, monitoring and diagnostics of oil-filled transformers. Published in: Proceedings of 2002 IEEE 14th International Conference on Dielectric Liquids. ICDL 2002 (Cat. No.02CH37319). DOI: 10.1109/ICDL.2002.1022739.
50. The Megger guide to insulating oil dielectric breakdown testing. The word ‘Megger’ is a registered trademark.
51. Engr. Inigo v. Escopete, jr. Dissolved gas analysis in transformer maintenance. Reliability supervisor, ap renewables, inc. Itc level 2 certified thermographer phil. National certifying body: certified ndt-ut level 2.
52. N.A. Muhamad, B.T. Phung, and T.R. Blackburn. Dissolved Gas Analysis (DGA) of Partial Discharge Fault in Bio-degradable Transformer Insulation Oil.
53. Doina Elena GAVRILĂ, Ilies Ciprian and Horia Catalin GAVRILĂ. Applying the Recovery Voltage Method (RVM) to Study the Degradation of High-Power Transformer Insulation. Advanced Materials Research Vol. 911 (2014) pp 260-265 © (2014) Trans Tech Publications, Switzerland.
54. https://electricaleverywhere.com/transformer-core-ground-test/
55. https://wiki.testguy.net/t/transformer-winding-resistance-testing-explained/81.
56. Frequency Response Analysis for Transformer Winding Condition Monitoring Mohd Fairouz bin Mohd Yousof.
57. Moustafa Sahnoune Chaouche, Hamza Houassine, Samir Moulahoum, Ilhami Colak. BA to construction of an equivalent circuit of a transformer winding from frequency response analysis measurement. IET Electric Power Applications.

List of References

58. Moustafa Sahnoune Chaouche, Hamza Houassine, Samir Moulahoum, Ilhami Colak. Finite element method to construct a lumped parameter ladder network of the transformer winding. 2017 IEEE 6th International Conference on Renewable Energy Research and Applications (ICRERA).
59. Frequency Response Analysis Interpretation for Winding Deformation of Power Transformers.
60. M. F. M. Yousof, C. Ekanayake, and T. K. Saha. Locating Inter-disc Faults in Transformer Winding Using Frequency Response Analysis. School of Information Technology and Electrical Engineering. The University of Queensland St. Lucia, Queensland, Australia.
61. S. Al-Ameri, M. F. M. Yousof, M. R. Ramly and H. Ahmad. Investigating the Capacitive Inter-Winding Response of Power Transformer. Journal of Physics: Conference Series, Volume 1049, International Post Graduate Conference on Applied Science & Physics 2017 7 December 2017, Johor, Malaysia. DOI 10.1088/1742-6596/1049/1/012008.
62. Kamdin Shafiepour. Diagnostics of Distribution Transformers.
63. Transformer Engineering Design and Practice S.V. Kulkarni. S.A. Khaparde Indian Institute of Technology, Bombay Mumbai, India.
64. Carlos González, Jorge Pleite. Transformer Modeling Approaches for Frequency Response Analysis XIX International Conference on Electrical Machines - ICEM 2010, Rome.
65. Xianzhi Zhaoa , Chenguo Yaoa , Ahmed Abu-Siadab, Ruijin Liaoa. High frequency electric circuit modeling for transformer frequency response analysis studies.
66. Abderrazak Amara. Gacemi Abderrazak .Contribution à la conception d'une plateforme embarquée sans fils pour la détection de défauts dans les transformateurs. http://dspace.univ-medea.dz/handle/123456789/9296.
67. Moustafa Sahnoune Chaouche, Hamza Houassine, Samir Moulahoum, Ilhami Colak. Faults Investigation of Transformer Windings Using the Frequency Response Analysis FRA. 2016 15th IEEE International Conference on Machine Learning and Applications (ICMLA).
68. Ghanim M. Alwan. optimization techniques. Madenat Al-Elem University College (MAUC).
69. H. Mataifa; S. Krishnamurthy; C. Kriger. Volt/VAR Optimization: A Survey of Classical and Heuristic Optimization Methods. DOI: 10.1109/ACCESS.2022.3146366.

List of References

70. Yogita D. Shahakar; Deepak A. Shahakar. Introduction and Classification of Classical and Advanced Optimization Methods for Electric Power System. Published in: 2019 International Conference on Innovative Trends and Advances in Engineering and Technology (ICITAET). DOI: 10.1109/ICITAET47105.2019.9170241.
71. Miriam Esteve; Jesús Javier Rodríguez-Sala; José Juan López-Espín; Juan Aparicio. Heuristic and Backtracking Algorithms for Improving the Performance of Efficiency Analysis Trees. DOI: 10.1109/ACCESS.2021.3054006.
72. George Papageorgiou; Pantelis Bouboulis; Sergios Theodoridis. Robust Linear Regression Analysis— A Greedy Approach. Published in: IEEE Transactions on Signal Processing (Volume: 63, Issue: 15, August 2015). DOI : 10.1109/TSP.2015.2430840.
73. https://www.javatpoint.com/hill-climbing-algorithm-in-ai
74. Dongshu Wang. Dapei Tan. Lei Liu. Particle swarm optimization algorithm: an overview. DOI 10.1007/s00500-016-2474-6.
75. Ahmed G. Gad. Particle Swarm Optimization Algorithm and Its Applications: A Systematic Review. Archives of Computational Methods in Engineering.
76. Dongshu Wang, Dapei Tan & Lei Liu. Particle swarm optimization algorithm: an overview.
77. K. Ragavan and L. Satish, Senior Member, IEEE. Localization of Changes in a Model Winding Based on Terminal Measurements: Experimental Study. IEEE TRANSACTIONS ON POWER DELIVERY, VOL. 22, NO. 3, JULY 2007.
78. Pramanik, S., Satish, L.: Estimation of series capacitance for a three-phase transformer winding from its measured frequency response. IEEE Trans. Power Deliv. 28(4), 2437–2444 (2013).
79. Huan, L., Ziwei, Z.: Equivalent gradient area-based fault interpretation for transformer winding using binary morphology. IEEE Trans. Dielectr. Electr. Insul. 24(3) (2017).
80. Chaouche, M.S., Houassine, H.: BA to construction of equivalent circuit of a transformer winding from frequency response analysis measurement. IET Electr. Power Appl. 12, 728–36 (2018).
81. Shah, K.R., Ragavan, K.: Assessing mechanical deformations in two winding transformer unit using reduced-order circuit model. Electr. Power Energy Syst. 79, 235–244 (2016).
82. Mukherjee, P., Satish, L.: Construction of equivalent circuit of a transformer winding from driving-point impedance function – analytical approach. IET Electr. Power Appl. 6, 172–180 (2012).

List of References

83. Shah, K., Ragavan, K.: Estimation of transformer winding capacitances through frequency response analysis – an experimental investigation. Int. J. Emerg. Elec. Power Syst. 14(6), 549–559 (2013).
84. J.A.S.B. Jayasinghe, Z.D. Wang. P.N. Jarman. A.W. Darwin. Winding Movement in Power Transformers: A Comparison of FRA Measurement Connection Methods. J.A.S.B. Jayasinghe et al.: Winding Movement in Power Transformers.
85. Brian D.O. Anderson network analysis and synthesis a modern system theory approach.
86. Jin Gou Yu-Xiang Lei Wang-Ping Guo Cheng Wang Yi-Qiao Cai Wei Luo. A novel improved particle swarm optimization algorithm based on individual difference evolution. https://doi.org/10.1016/j.asoc.2017.04.025.
87. Jafar Nosratian, A., Saeed, S.: On the accuracy of detailed model inductance matrix estimation for air core winding. Arch. Elect. Eng. 66(4), 787–799 (2017).
88. S.V. Kulkarni. S.A. Khaparde. Transformer Engineering Design and Practice. Indian Institute of Technology, Bombay Mumbai, India.
89. Yi Li ; Qiuyuan Xu ; Yanfeng Lu. Electromagnetic Force Analysis of a Power Transformer Under the Short-Circuit Condition. Published in: IEEE Transactions on Applied Superconductivity (Volume: 31, Issue: 8, November 2021). DOI: 10.1109/TASC.2021.3107799.
90. Mehdi Bagheri; Mohammad Salay Naderi; Trevor Blackburn; Toan Phung. Frequency response analysis and short-circuit impedance measurement in detection of winding deformation within power transformers. Published in: IEEE Electrical Insulation Magazine (Volume: 29, Issue: 3, May-June 2013). DOI: 10.1109/MEI.2013.6507412.
91. Leonard L. Grigsby. Electric Power Engineering Handbook Second Edition.
92. https://studyelectrical.com/2018/05/percentage-impedance-of-transformer-and.html.
93. Sarzhanova. A.B. Simulation models of power engineering objects in theory and practice.
94. Pritam Mukherjee; L. Satish. Diagnosing axial displacement in an actual, single, isolated transformer winding: Experimental results. Published in: IEEE Transactions on Dielectrics and Electrical Insulation (Volume: 24, Issue: 2, April 2017). DOI: 10.1109/TDEI.2017.006211.
95. Pritam Mukherjee; L. Satish. Localization of Radial Displacement in an Actual Isolated Transformer Winding—An Analytical Approach. IEEE TRANSACTIONS ON POWER DELIVERY, VOL. 31, NO. 6, DECEMBER 2016.

List of References

96. E. Billig. Mechanical stresses in transformer windings. DOI: 10.1049/ji-2.1946.0057, Print ISSN 0367-7567, Online ISSN 2054-0590.
97. Steven D. Mitchell, James S. Welsh. Methodology to locate and quantify radial winding deformation in power transformers.
98. Amit Bakshi; S. V. Kulkarni. Coupled Electromagnetic-Structural Analysis of the Spiraling Phenomenon in a Helical Winding of a Power Transformer. IEEE Transactions on Power Delivery (Volume: 29, Issue: 1, February 2014). DOI: 10.1109/TPWRD.2013.2276047.
99. Amit Bakshi and S. V. Kulkarni, Senior Member, IEEE. Coupled Electromagnetic-Structural Analysis of the Spiraling Phenomenon in a Helical Winding of a Power Transformer. IEEE Transactions on Power Delivery, Vol. 29, No. 1, February 2014.
100. Data Acquisition Techniques Using PCs Second Edition Howard Austerlitz Parker Hannifin Corporation Parker Aerospace Electronic Systems Division Smithtown, New York.
101. K. Ragavan and L. Satish, An Efficient Method to Compute Transfer Function of a Transformer From its Equivalent Circuit. IEEE TRANSACTIONS ON POWER DELIVERY, VOL. 20, NO. 2, APRIL 2005.
102. B. de Metz-Noblat. F. Dumas. C. Poulain. Cahier technique no. 158 Calculation of short-circuit currents.
103. Zhijun YE, Wang YU, Julong GOU, Kaijia TAN1, Wenhui ZENG, Bonan AN, and Yong LI.A Calculation Method to Adjust the ShortCircuit Impedance of a Transformer.DOI 10.1109/ACCESS.2020.3042983, IEEE Access.